Isoform-specific knockout of the *Neuregulin-1* gene

I n a u g u r a l - D i s s e r t a t i o n

zur

Erlangung des Doktorgrades

der Mathematisch-Naturwissenschaftlichen Fakultät

der Universität zu Köln

vorgelegt von

Li Li

aus Guizhou, China

2003

Berichterstatter:	Prof. Dr. Walter Doerfler
	Prof. Dr. Carmen Birchmeier
Tag der Disputation:	29.11.2002

Contents

1. Introduction

1.1. Neuregulin-1

Neuregulins are a family of Epidermal Growth Factor (EGF)-like ligands that signal via receptor tyrosine kinases of the ErbB family. First identified as an activity able to promote the proliferation of glial cells (Glial Growth Factor, GGF; Raff et al., 1978; Brockes et al., 1980; Lemke and Brockes, 1984), Neuregulin was independently characterized as a factor that induces expression of acetylcholine receptors in cultured myotubes (Acetylcholine-Receptor-Inducing Activity, ARIA) and promotes the differentiation of developing muscle cells in vitro (Jessell et al., 1979; Falls et al., 1990). Later, in other independent studies, the factor was characterized as an activity that stimulates the phosphorylation of the ErbB receptor neu/HER2/ErbB2, and named Neu Differentiation Factor (NDF; Peles et al., 1992) or Heregulin (HRG; Holmes et al., 1992). The cloning of the cDNAs encoding NDF (Wen et al., 1992), HRG (Holmes et al., 1992), ARIA (Falls et al., 1993) and GGF (Marchionni et al., 1993) finally revealed that these proteins are encoded by a single gene. The presence of multiple promoters and extensive alternative splicing of mRNAs account for the diversity of isoforms encoded. The consensus name used today for the various isoforms is Neuregulin-1 (NRG1) (Marchionni et al., 1993).

In vertebrates, three additional *Neuregulin* genes, *Neuregulin-2* (Busfield et al., 1997; Carraway et al., 1997), *Neuregulin-3* (Chang et al., 1997; Zhang et al., 1997) and *Neuregulin-4* (Harari et al., 1999) have been identified (Fig. 1a). The encoded proteins share high sequence homology with Neuregulin-1 in their EGF-like domains (Fig. 1b). The EGF-like domain that contains about 50-60 amino acids is characterized by three pairs of cysteines, which are important for tertiary structure and biological function. In Neuregulin-1s, the EGF-like domain is essential to elicit receptor binding, and can on its own cause receptor heteromerization, tyrosine phosphorylation and downstream signal activation (Holmes et al., 1992). In addition to EGF and the Neuregulins, the family of EGF-like factors also includes Transforming Growth Factor-α (Kumar et al., 1995), Amphiregulin (Shoyab et al., 1989), Heparin-binding EGF-like Growth Factor (Higashiyama et al., 1991), Betacellulin (Shing et al., 1993) and Epiregulin (Toyoda et al., 1995).

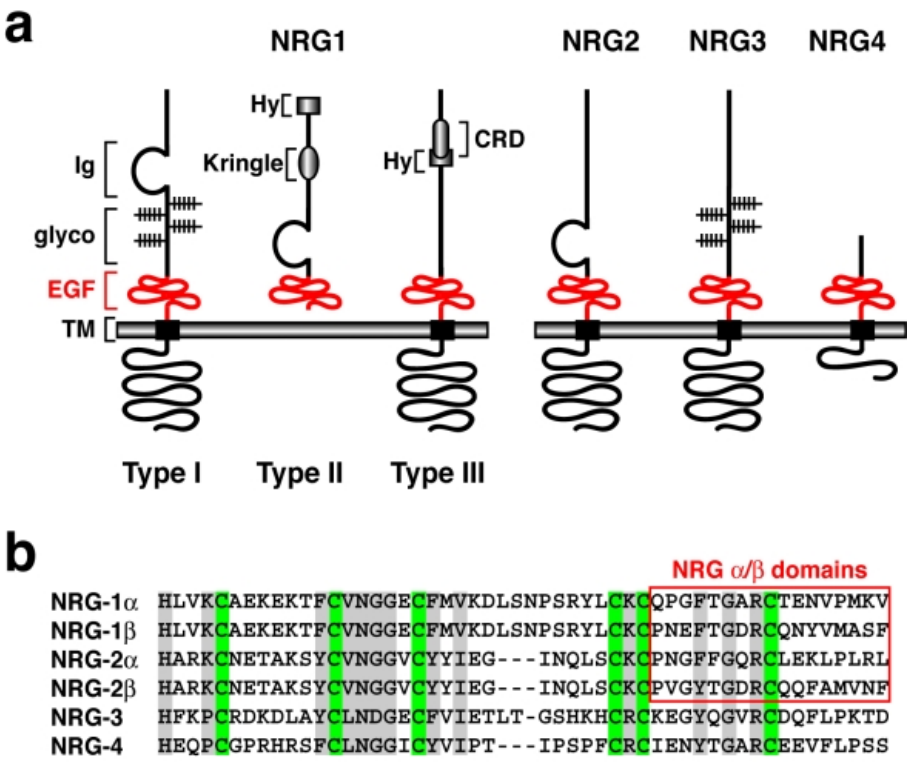

Figure 1. Schematic structures of the four Neuregulin ligands and alignment of their EGF-like domains
(a) All Neuregulins (NRG1-4) possess an EGF-like domain (red, EGF) that is essential for receptor binding and function. α- and β-variants of the EGF domain have been characterized for NRG1 and NRG2. Three major isoforms (types I-III) of NRG1 are produced by the usage of different promoters and alternative splicing. Other domains present in Neuregulins include Ig-like domains (Ig), domains rich in potential glycosylation sites (glyco), transmembrane domains (TM, black box) and cytoplasmic domains (wavy lines). Kringle-like (kringle) and cysteine-rich domains (CRD) are found in types II and III NRG1, respectively. Signal peptides or internal hydrophobic sequences are indicated as gray shaded boxes (Hy). **(b)** All Neuregulins share high sequence homology in their EGF-like domains, which are characterized by three pairs of cysteines (green). Amino acids identical or which are conservatively substituted in all Neuregulins are marked in gray. The α- and β-spliced variants of the EGF-like domain that have been characterized for NRG1 and NRG2 are boxed. (Adapted from Garratt et al., 2000; Buonanno and Fischbach, 2001).

1.2. Receptors of Neuregulin-1

Neuregulins signal through ErbBs, a family of receptor protein tyrosine kinases related to the receptor for Epidermal Growth Factor (EGFR). Four ErbB receptors, ErbB1/HER1/EGFR, ErbB2/HER2/neu, ErbB3/HER3 and ErbB4/HER4 (170-185 kDa), are encoded by the mammalian genome. They all contain two cysteine-rich domains in their extracellular parts, a single transmembrane domain and a relatively large cytoplasmic portion containing 8-18 tyrosine residues at the C-terminal tails (Fig. 2). While the extracellular parts of the receptors function in ligand binding, their cytoplasmic portions are responsible for their tyrosine kinase activities. Ligand binding activates the catalytic function of the ErbBs by promoting receptor

heteromerization and the phosphorylation of tyrosine residues in their cytoplasmic portions. The phosphorylated tyrosine residues serve as docking sites for various adapter proteins and other signaling molecules, which constitute a molecular signaling cascade and mediate further propagation of the signal.

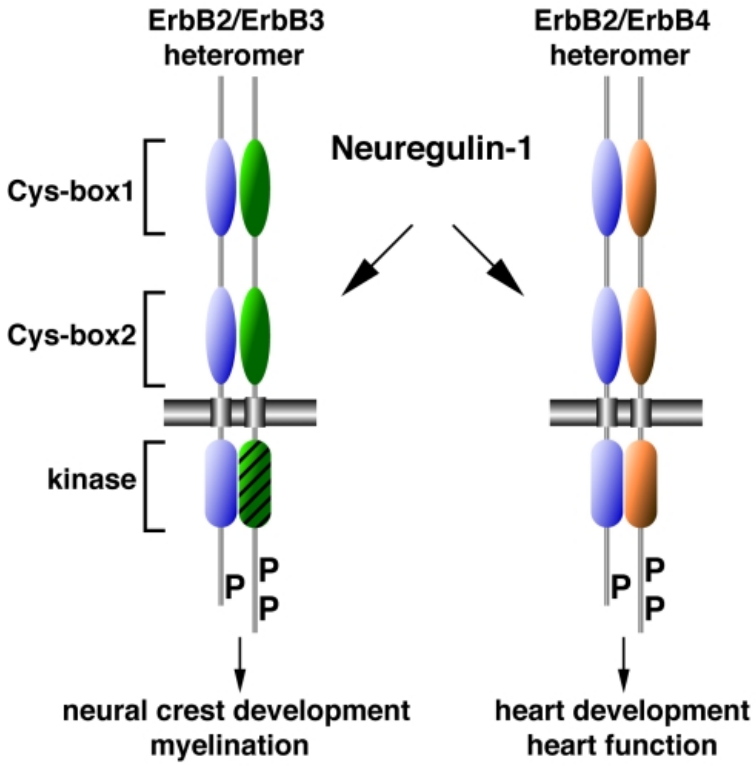

Figure 2. Schematic structures of the Neuregulin-1 receptors ErbB2, ErbB3 and ErbB4
The ErbB receptors contain two cysteine-rich domains, located extracellularly (ovals), a transmembrane domain and a cytoplasmically located tyrosine kinase domain (oblongs). Ligand binding stimulates heteromerization of the receptors and phosphorylation of tyrosine residues, located principally in the tails of the molecules. Whereas ErbB2 (blue) and ErbB4 (brown) have catalytically active tyrosine kinase domains, the corresponding domain in ErbB3 (green) possesses no or very little activity (hatched). ErbB2 acts as a co-receptor in transduction of Neuregulin-1 signals, in neural crest tissues through heteromerization with ErbB3, and in the heart, with ErbB4. (Adapted from a drawing of Stefan Britsch, C. Birchmeier laboratory).

Neuregulin-1 binds the ErbB3 and ErbB4 receptors directly. In contrast to the other ErbBs, ErbB3 exhibits no catalytic activity, as it lacks specific amino acid residues that are conserved in all other protein tyrosine kinases (Guy et al., 1994). ErbB2, on the other hand, is a receptor without any known direct ligand (Klapper et al., 1999), and is activated by Neuregulin-1 through heteromerization with ErbB3 or ErbB4 (Carraway and Cantley, 1994; Plowman et al., 1993; Sliwkowski et al., 1994; Tzahar et al., 1994). Genetic evidence has demonstrated that two

Neuregulin-1 receptor heteromers are essential for Neuregulin-1 signaling, the ErbB2/ErbB3 and the ErbB2/ErbB4 heteromers. The presence of ErbB2 in the receptors changes receptor affinities and signaling properties. ErbB2 stabilizes ligand-bound ErbB3 and ErbB4 receptors by reducing the rate of ligand dissociation, as well as increasing by 100-fold the ligand binding affinity (Fitzpatrick et al., 1998; Jones et al., 1999). ErbB2 is also a strong activator of the MAP kinase pathway. Thus, ErbB2-containing heteromers are stable, and have potent signaling properties (Graus-Porta et al., 1995; Graus-Porta et al., 1997; Karunagaran et al., 1996; Tzahar et al., 1996; Pinkas-Kramarski et al., 1996; Riese et al., 1995; Riese et al., 1996a; Riese et al., 1996b; Kokai et al., 1989).

1.3. Isoforms of Neuregulin-1

The *Neuregulin-1* gene has been extensively characterized. Usage of different promoters and alternative RNA splicing of exons give rise to at least 15 different isoforms (reviewed by Lemke, 1996). The various isoforms of Neuregulin-1 were originally named based on the distinct biological assays used for their identification. These isoforms include NDF, HRG, GGF, ARIA (mentioned above) and also SMDF (Sensory and Motoneuron-Derived Factor), which was identified later (Ho et al., 1995; Yang et al., 1998). The isoforms can be classified into three major types that are produced from three distinct promoters and contain distinct N-terminal sequences (Fig. 1a) (Meyer et al., 1997; Fischbach and Rosen, 1997). Type I Neuregulin-1 (NDF, HRG, and ARIA) contains an immunoglobulin (Ig)-like domain, a sequence stretch that contains many glycosylation sites, a transmembrane domain and a cytoplasmic portion. Type II Neuregulin-1 (GGF) contains a signal peptide, a GGF-specific (kringle-like) domain and an Ig-like domain. Type III Neuregulin-1 (SMDF) contains a cysteine-rich domain or SMDF domain, as well as the transmembrane domain and C-terminal part present in type I Neuregulin-1. Alternative splicing at the C-terminal region of the EGF-like domain gives rise to α- and β-variant isoforms of Neuregulin-1 (Holmes et al., 1992). Type I Neuregulin-1 contains either the α- or β-variant of the EGF-like domain, denoted as type Iα and type Iβ isoforms. Types II and III Neuregulin-1 contain only the β-variant of the EGF-like domain (Meyer et al., 1997). In tissues that express type I Neuregulin-1, frequently both isoforms, type Iα and

type Iβ are produced, with the exception of the mammary gland that produces only type Iα Neuregulin-1 (Yang et al., 1995).

All isoforms of Neuregulin-1 bind directly to both ErbB3 and ErbB4 receptors and can induce the formation of ErbB2/ErbB3 or ErbB2/ErbB4 receptor heteromers (Crovello et al., 1998; Pinkas-Kramarski et al., 1998; Tzahar et al., 1997; Harris et al., 1998). However, the α- and β-isoforms distinguished by their C-termini of the EGF-like domains differ each other dramatically in their receptor binding affinities. The isoforms containing the β-variant EGF-like domain have a much higher binding affinity for ErbB3 or ErbB4 homodimers than α-variant isoforms in a cell free system (Jones et al., 1999). The β-isoforms are also superior to the α-isoforms in eliciting responses in cellular systems that express different combinations of ErbB receptors (Pinkas-Kramarski et al., 1998). Although signaling by both α- and β-isoforms is funneled through MAP kinase, their distinct affinities for the receptors cause differential activation of the MAP kinase pathway, resulting in discrete biological effects (Pinkas-Kramarski et al., 1998). β-isoforms have significantly higher potency and elicit longer lasting cellular responses than α-isoforms.

In vivo, the different major isoforms of Neuregulin-1 have distinct spatial and temporal expression patterns and take over different biological functions (Meyer et al., 1997). During development, type I Neuregulin-1 is the earliest detectable isoform and is expressed in the endocardium. Type II Neuregulin-1 is expressed late and produced mainly in the nervous system. Type III Neuregulin-1 is the major Neuregulin-1 isoform produced by sensory and motoneurons, and is also expressed in the brain (Wen et al., 1994; Meyer and Birchmeier, 1994).

1.4. Functions of Neuregulin-1 in the heart

Mouse mutants homozygous for null mutations in *NRG1* (Meyer and Birchmeier, 1995), *ErbB2* (Lee et al., 1995; Erickson et al., 1997; Britsch et al., 1998) and *ErbB4* (Gassmann et al., 1995) died at embryonic day 10.5 (E10.5) with defects in heart trabeculation. The trabecules of the

developing heart form a sponge-like network of projections of myocardial tissue that protrude from the ventricle wall into the chamber. The formation of trabecules is associated with proliferation and morphogenesis of the cardiac myocardium. Neuregulin-1 is produced in the endocardium, the endothelial lining of the heart that directly apposes the myocardium, which expresses ErbB2 and ErbB4. The similar heart phenotypes of the mutants shows that Neuregulin-1 signaling through the ErbB2/ErbB4 heteromer is required for normal heart development at mid-gestation. Expression analyses, as well as the presence of the same heart defect in Ig-isoform mutants indicated that it is the type I Neuregulin-1 isoform that functions at this mid-gestation stage of heart development (Kramer et al., 1996; Meyer et al., 1997).

1.5. Functions of Neuregulin-1 in the neural crest and glial cell lineages

Neural crest cells constitute a transient and migratory cell population that detaches from the dorsal neural tube by an epithelial-mesenchymal transition. These pluripotent cells migrate along defined paths to their target sites, where they differentiate to form various types of tissue (Anderson, 1997; Le Douarin and Kalcheim, 1999). Almost the entire peripheral nervous system is formed by neural crest cells, including all neurons and glia of the dorsal root ganglia, the sympathetic nervous systems and the enteric nervous systems. Moreover, neural crest cells also contribute to cranial sensory ganglia, forming glia and subsets of neurons. Neural crest cells express a characteristic set of genes including *ErbB3*, whose expression is initiated in neural crest cells upon their dissociation from the neural tube. *ErbB3* expression continues during neural crest cell migration, is maintained in the glial lineage, particularly in Schwann cells, but is turned off in other neural crest cell derivatives.

Neuregulin-1 signaling is essential for the migration of at least a subpopulation of neural crest cells. During the early development of the sympathetic nervous system, neural crest cells migrate to the mesenchyme lateral of the dorsal aorta. There, they receive a signal that instructs their differentiation into sympathetic neurons and satellite (glial) cells, forming the primary sympathetic ganglion chain. In *Neuregulin-1*, *ErbB2* and *ErbB3* null mutants, the numbers of sympathogenic neural crest cells were severely decreased along their characteristic migratory

route and at their target (Britsch et al., 1998). This defect is not caused by cell death but rather by defective migration. Type I Neuregulin-1, which is expressed by the mesenchyme along the route towards the dorsal aorta, is required as a pro-migratory signal for the neural crest cells, which use the ErbB2/ErbB3 heteromer as the receptor (Britsch et al., 1998).

During peripheral glial cell development, type III Neuregulin-1, which is presented by the axon membranes of sensory and motoneurons, provides one of the principal axon signals to Schwann cells and their precursors, which are in axon contact and express the ErbB2/ErbB3 heteromeric receptors (Morrissey et al., 1995). In vitro culture studies indicate that this factor may facilitate migration of neural crest cells and Schwann cell precursors along the axons (Mahanthappa et al., 1996; Morris et al., 1999). Type III Neuregulin-1 also provides a growth and survival signal, which is thought to adjust the cell numbers in the Schwann cell precursor pool *in vivo* (Mahanthappa et al., 1996; Grinspan et al., 1996; Syroid et al., 1996; Dong et al., 1995; Jessen and Mirsky, 1997). *NRG1*, *ErbB2* and *ErbB3* null mutant embryos displayed a severe reduction in the number of neural crest cells that migrate along the developing axon tracts (Meyer and Birchmeier, 1995; Lee et al., 1995; Riethmacher et al., 1997; Morris et al., 1999; Woldeyesus et al., 1999). At subsequent developmental stages, these mutations resulted in a lack of Schwann cell and Schwann cell precursors along peripheral nerves. Analysis of isoform-specific mouse mutants of *NRG1* revealed that the type III Neuregulin-1 isoform indeed drives Schwann cell development *in vivo*, consistent with the high expression of this isoform in sensory and motoneurons (Wolpowitz et al., 2000; Yang et al., 1998; Bermingham-McDonogh et al., 1997; Kramer et al., 1996; Meyer et al., 1997). Interestingly, a severe degeneration of sensory neurons and subclasses of motoneurons was observed in *ErbB3* and rescued *ErbB2* (*ErbB2R*-/-, in which *ErbB2* expression in heart was specifically rescued) mutants, which is caused by indirect mechanisms, i.e. by the absence of Schwann cells (Riethmacher et al., 1997; Woldeyesus et al., 1999). This is similar to what is seen in *Sox10* mouse mutants, which lack all peripheral glia. (Britsch et al., 2001). Conditional mutagenesis of *ErbB2* in late stages of Schwann cell development revealed that upon maturation, Schwann cells no longer require the Neuregulin signaling system for survival. These conditional mutations also revealed a function for

NRG1/ErbB signaling in regulating Schwann cell myelination (Garratt et al., 2000).

1.6. Sox 10 and its functions in the development of glial cells

Sox10 is a member of a transcription factor family that contains a high-mobility-group (HMG) box in the DNA binding domain (Kuhlbrodt et al., 1998a; Wegner, 1999). Similar to *ErbB3*, *Sox10* expression is initiated in the emerging neural crest cells after dissociation from the neural tube. Expression of *Sox10* continues during neural crest cell migration and is subsequently maintained in the glial, but not neuronal derivatives (Kuhlbrodt et al., 1998a; Kuhlbrodt et al., 1998b). A spontaneous mutation of *Sox10* in mice has been described ($Sox10^{Dom}$ allele), which introduces a frameshift into the coding sequence, and results in the formation of a truncated protein lacking the transactivation domain. Similar mutations have also been identified in human. In the heterozygous state, they cause megacolon or Waardenburg-Hirschsprung disease in mice and human, respectively, i.e. defects in the development of melanocytes and the enteric nervous system (Herbarth et al., 1998; Kuhlbrodt et al., 1998b; Pingault et al., 1998; Southard-Smith et al., 1998; Southard-Smith et al., 1999). Homozygous $Sox10^{Dom}$ mutants lacked enteric ganglia, a portion of the sympathetic ganglion chain, and their peripheral glial cells did not differentiate from neural crest cells (Herbarth et al., 1998; Southard-Smith et al., 1998; Kapur, 1999; Britsch et al., 2001). Thus, Sox10 plays important roles in the development of neural crest cells.

An important target gene of Sox10 is *ErbB3*, and the expression of *ErbB3* in neural crest cells, but not in other tissue types is controlled by Sox10 (Britsch et al., 2001). In accordance, all phenotypes that were observed in *ErbB3* mutants were also present in homozygous *Sox10* mutants. Both mutants lacked the neural crest cell contribution to cranial ganglia, displayed severe hypoplasia of the primary sympathetic ganglion chain and a severe reduction in the number of neural crest cells that migrate along the developing axon tracts (Britsch et al., 2001). Moreover, as in *NRG1/ErbB* mutants, severe degeneration of sensory and motoneurons was also observed in *Sox10* mutants (Britsch et al., 2001). This result provides independent evidence for the essential role of Schwann cells in survival of sensory and motoneurons.

1.7. The olfactory system and the development of the primary olfactory path

Mammals recognize odorants through stimulation of olfactory sensory neurons, whose sensory endings and cell bodies are located in the olfactory epithelium of the nasal cavity. These bipolar neurons relay the stimulus of odor perception along their unmyelinated axons to the olfactory bulb in the forebrain (Fig. 3a, b). The axons of olfactory neurons are accompanied by glial cells along their entire path to the synaptic termini, the glomeruli of the olfactory bulb. There, they make synapses with the dendrites of mitral, tufted and periglomerular neurons. These neurons serve to relay the stimulus to the olfactory cortex, where the odorant information is further processed and transmitted to other brain centers (Farbman, 1992; Shepherd, 1994) (Fig. 3b).

The olfactory bulb is a laminated cortical structure located in the most rostral part of the forebrain (Fig. 3a). The outermost, the olfactory nerve layer, is formed mainly by axons of olfactory sensory neurons and olfactory glial cells. The second, the olfactory glomerular layer, is the location for anatomically specialized structures, glomeruli, where the olfactory sensory axons make synaptic connections with their central targets (Fig. 3b). Moving further inwards are the external plexiform layer, the mitral cell layer, the internal plexiform layer and the granule cell layer. The cells that contribute to these deeper olfactory layers originate from the central nervous system.

The early development of the primary olfactory path begins around E9 in the mouse. The olfactory placode first appears as a localized ectodermal thickening, that is recognizable as the olfactory pit at E10.5, and gives rise to the olfactory epithelium about one day later. The outgrowing axons of the olfactory neurons are accompanied by migratory cells, corresponding to neuronal and glial precursors, which also originate from the olfactory placode. The olfactory axons and migrating precursor cells migrate through the frontonasal mesenchyme surrounding the olfactory pit, and reach the telencephalic vesicle around E11.5, when the morphogenesis of the olfactory bulb is initiated. Soon after the arrival of the first olfactory axons, the rostral wall of the telencephalic vesicle evaginates to form the olfactory bulb primodium (Marin-Padilla and Amieva, 1989; Doucette, 1989; Valverde et al., 1992). On reaching the rostral part of the

telencephalic vesicle, the olfactory axons and glial progenitor cells begin to form the presumptive olfactory nerve layer, which extends along the surface of the developing olfactory bulb. The olfactory axons then synapse with their central target cells to create the glomerular layer later (Hinds, 1968a; Hinds, 1968b; Marin-Padilla and Amieva, 1989; Doucette, 1989; Valverde et al., 1992).

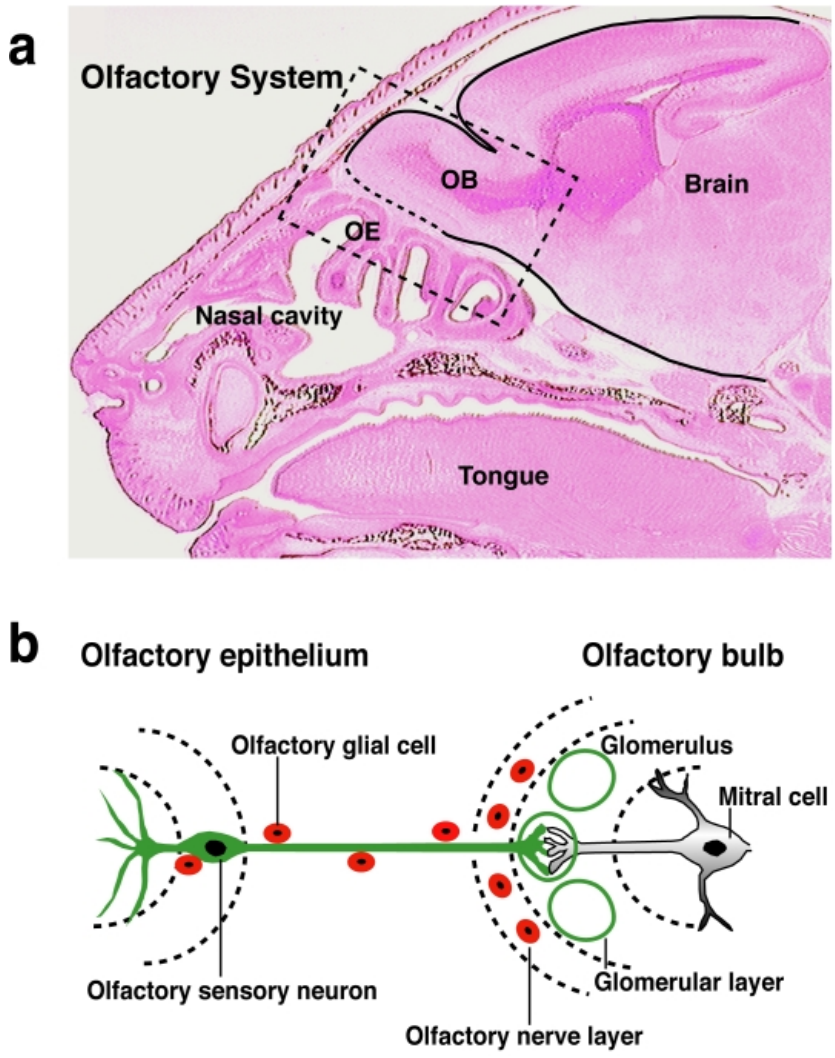

Figure 3. Schematic anatomical outline of the olfactory system
(a) Hematoxylin/eosin-stained parasagittal section of the head of an E18 mouse embryo showing the gross anatomy of the olfactory system. The boxed area highlights the main structures constituting this system: the olfactory bulb (OB), the axon entry zone of olfactory sensory neurons (dashed line), and the olfactory epithelium (OE) lining the nasal cavity. **(b)** Schematic outline, highlighting the olfactory glial cells (red ellipsoids) which accompany the axon projections of olfactory sensory neurons (green) along their path from the olfactory epithelium to the olfactory bulb. Upon reaching the olfactory bulb, the olfactory axons form the olfactory nerve layer together with olfactory glial cells, and then terminate in the glomeruli (green circles) of the olfactory glomerular layer, where they synapse with dendrites of mitral and tufted neurons (gray).

1.8. Odorant receptors and olfactory signal recognition

The cloning of the multigene family that encodes rat odorant receptors (Buck and Axel, 1991) marks the beginning of molecular studies of the olfactory system. The odorant receptors that mediate the initial detection of odorant stimuli are G protein-coupled seven-transmembrane domain proteins. They are encoded by the largest gene family in the mammalian genome, containing about 1000 genes, or more than 1% of genome in mouse and rat (Buck and Axel, 1991; Levy et al., 1991; Lancet et al., 1993; Ngai et al., 1993; Mombaerts, 1999). Odorant receptors are extremely diverse in sequence, which enables them to distinguish odorants that vary in size, shape, functional group, and charge (Beets, 1970).

Several million olfactory sensory neurons reside in the olfactory epithelium of a mammal, each expressing only a single of the thousand odorant receptor genes (Nef et al., 1992; Strotmann et al., 1992; Ngai et al., 1993; Ressler et al., 1993; Vassar et al., 1993; Chess et al., 1994; Malnic et al., 1999). A given odorant receptor is however expressed in many individual olfactory neurons, and neurons that express different receptors are intermingled (Buck and Axel, 1991; Ressler et al., 1993; Vassar et al., 1993; Sullivan et al., 1996). Remarkably, the axons of all olfactory neurons expressing a particular odorant receptor converge onto two or a few specific glomeruli among the 1800 ones present in the olfactory bulb (Ressler et al., 1994; Vassar et al., 1994; Mombaerts et al., 1996). Between individuals, the position and number of the glomeruli that respond to a given odorant receptor are more or less consistent, although small variations do exist (Royal and Key, 1999; Strotmann et al., 2000; Schaefer et al., 2001).

1.9. The olfactory topographic map and olfactory axon guidance

The olfactory neurons activated by a given odorant converge their axons to glomeruli in a spatially-defined pattern. A series of genetic studies has been performed to explore the roles of odorant receptors in the axon guidance process that results in the organized formation of glomeruli (Mombaerts et al., 1996; Wang et al., 1998). For example, insertion of *IRES-tau-lacZ*, a gene cassette encoding the microtubule-associated protein tau fused with ß-galactosidase (Callahan and Thomas, 1994), into specific odorant receptor coding sequences allows both their

disruption, and tracking of the odorant receptor axons by histochemical staining. Mutation of the *P2* receptor gene causes the axons of *P2*-expressing neurons wandering in the olfactory bulb rather than converging to specific glomeruli. Thus, the P2 receptor is essential for the convergence of axons of *P2*-expressing neurons to discrete glomeruli (Wang et al., 1998). In addition, substitution of receptor coding sequences indicates also that the odorant receptors play instructive roles in olfactory axon guidance and topographic map formation, although they can not be the exclusive determinants and additional molecules must be involved (Mombaerts et al., 1996; Wang et al., 1998; O'Leary et al., 1999).

Guidance cues which might be provided by the major neuronal cell types in the olfactory bulb, the projection neurons (mitral and tufted cells) and the GABAergic interneurons (periglomerular and granular cells) could contribute to correct projections of olfactory sensory neurons. However, in mouse embryos deficient for the transcription factors Tbr-1, or Dlx1/Dlx2, which lack mitral and tufted cells, or periglomerular and granular cells, respectively, olfactory axons converge (Bulfone et al., 1998). Another potential source of guidance cues for olfactory sensory neuron axons during development are glial cells. However, despite demonstrated roles for glial cells in neuronal development in the central nervous system of *Drosophila* (Granderath and Klambt, 1999; Rangarajan et al., 1999; Hidalgo and Booth, 2000), their potential roles in the development of the mammalian olfactory system has not yet been investigated.

1.10. Olfactory glial cells

While the glial cells that ensheath sensory and motoneurons derive from the neural crest, glial cells that ensheath the olfactory nerve originate from the olfactory placode (Couly and Le Douarin, 1985; Marin-Padilla and Amieva, 1989; Doucette, 1989; Chuah and Au, 1991). Olfactory glial cells are a unique type of glia present only in the olfactory system, albeit with some characteristics which are reminiscent of non-myelinating Schwann cells of peripheral nerves. Olfactory glia wrap entire bundles of unsorted axons, in contrast to non-myelinating Schwann cells, which surround each individual small diameter axon with a collar of plasma membrane (Barber and Lindsay, 1982; Fraher, 1982). Olfactory glial progenitor cells migrate

along the developing olfactory axon tracts, enveloping the bundles of axons with cytoplasmic processes, and undergoing numerous mitotic divisions. In the olfactory bulb, they form the olfactory nerve layer together with the olfactory axons.

1.11. The purposes of the project

The Neuregulin-1 signaling system and the transcription factor Sox10 are essential for the development of Schwann cells. Like Schwann cells, olfactory glial cells express *ErbB3* and *Sox10* (Meyer et al., 1997; Perroteau et al., 1998; Perroteau et al., 1999; this study). Olfactory glial cells also respond to Neuregulin-1 by increased proliferation and survival in culture, in a similar manner as cultured Schwann cell precursors (Pollock et al., 1999). In this thesis, I analyzed whether the Neuregulin-1 signaling system and Sox10 also control the development of olfactory glial cells. For this, I generated a new mutant mouse strain (*NRG1β)* and also used other strains, which were already available (*ErbB3*, rescued *ErbB2* and $Sox10^{Dom}$). The newly established mouse strain carries an alteration in the coding sequence of *Neuregulin-1*, which interferes with the synthesis of β-isoforms, allowing only α-isoforms of Neuregulin-1 to be produced. Similar to what was observed previously in the Schwann cell lineage, I found that olfactory glial cells depend on the Neuregulin-1 signaling system for their development. However, the role of Sox10 in the development of these two glial lineages is distinct. In particular, Sox10 controls *ErbB3* expression in Schwann cell precursors, but not in olfactory glial cells. Olfactory glial cells can be generated in *Sox10* mutant mice, although these glial cells do not accompany the olfactory nerve over its entire length, and do not enter the olfactory bulb. Furthermore, I observed severe alterations in the axon projections of olfactory sensory neurons in *NRG1β*, *ErbB3*, rescued *ErbB2* and $Sox10^{Dom}$ mutants, which appear to be caused indirectly by the developmental changes in olfactory glial cells.

2. Materials and Methods

2.1. Abbreviations

ATP	adenosine triphosphate
BrdU	bromodeoxyuridine
bp	base-pair
cDNA	complementary DNA
cpm	counts per minute
CTP	cytosine triphosphate
DEPC	diethylpyrocarbonate
DIG	digoxigenin
DiI	1,1'-dioctadecyl-3,3,3',3'-tetramethyl indocarbocyanine perchlorate
dNTP	deoxyribonucleoside triphosphate
DNase	deoxyribonuclease
DTT	dithiothreitol
ES cell	embryonic stem cell
EtOH	ethanol
FCS	fetal calf serum
G418	geneticin
GS	heat inactivated goat serum
GTP	guanosine triphosphate
HAc	acetic acid
hr	hour
HS	heat inactivated horse serum
kb	kilobasepairs
LIF	leukemia inhibitory factor
min	minute
mRNA	messenger RNA
NaAc	sodium acetate

neo	neomycin resistance gene
PBS	phosphate-buffered saline
PBT	PBS containing 0.01% Tween-20
PCR	polymerase chain reaction
PFA	paraformaldehyde
RNase	ribonuclease
rpm	rotations per minute
RT	room temperature
RT-PCR	reverse transcription-polymerase chain reaction
SDS	sodium dodecyl sulphate
SSC	standard saline citrate
O/N	over night
TTP	thymidine triphosphate
UTP	uridine triphosphate
X-gal	5-bromo-4-chloro-3-indolyl-beta-D-galactopyranoside
Bluo-gal	5-bromo-3-indolyl-beta-D-galactopyranoside

2.2. Materials

Chemicals, enzymes and kits for molecular biology, oligonucleotides, or antibodies were purchased from the following companies, unless indicated otherwise:
Amersham-Pharmacia (Freiburg); Biotez (Berlin); Biozym (Hess. Oldendorf); Dianova (Hamburg); Gibco/BRL (Karlsruhe); Heraeus-Kulzer (Wehrheim); Invitek (Berlin); MBI-Fermentas (St.Leon-Rot); Merck (Darmstadt); MWG-Biotech (Ebersberg); New England Biolabs (Frankfurt); Pan-Biotech (Aidenbach); Promega (Mannheim); Qiagen (Hilden); Roche (Mannheim); Roth (Karlsruhe); Serva (Heidelberg); Shandon (Frankfurt); Sigma (Deisenhofen).

2.2.1. Bacterial strains

Escherichia coli XL1-Blue MRF ' Jerpseth et al., 1992

2.2.2. Vectors/plasmids

pBluescript II SK$^+$	Sorge, 1988
pGEM-T	Promega
pL2-neo (contains *loxP*-neo-*loxP* cassette)	H. Gu/K. Rajewsky laboratory
pGEM-30 (contains *loxP* site)	H. Gu/K. Rajewsky laboratory
pIC (Cre expression plasmid)	H. Gu/K. Rajewsky laboratory

Genomic clones of *Neuregulin-1* (in pBluescript II SK$^+$):

Clone 3.5	D. Meyer/C. Birchmeier laboratory
Clone 6	D. Meyer/C. Birchmeier laboratory
Clone 7	D. Meyer/C. Birchmeier laboratory

2.2.3. ES cell line

Embryonic stem (ES) cells from the line E14.1, derived from the 129/Ola mouse strain (Hooper et al., 1987; Kühn et al., 1991) were used for introducing targeted mutations into the mouse germline.

2.2.4. Primary antibodies

Antigen	Host animal*	Dilution	Source
BFABP	Rabbit	1:5000	T. Müller
BrdU	mo IgG	1:200	Sigma
GABA	Rabbit	1:1000	Sigma
GAP-43	mo IgG	1:100	Chemicon
Laminin	Rabbit	1:200	ICN/Cappel
Nestin	Rabbit	1:100	T. Müller
NF160	mo IgG	1:500	Sigma
OMP	Goat	1:1000	F. Margolis
P75	Rabbit	1:100	Promega
Peripherin	Rabbit	1:100	Chemicon
S100	Rabbit	1:400	Dako

Sox10	Rabbit	1:100	Sigma
TH	Rabbit	1:1000	Sigma
TuJ1	mo IgG	1:1000	T. Müller
β-galactosidase	Rabbit	1:2000	ICN/Cappel

*Antibodies were polyclonal, except mouse monoclonals (mo).

2.2.5. cDNA probes for *in situ* hybridization

BFABP	T. Müller, Berlin, Germany
ErbB3	D. Meyer/C. Birchmeier laboratory
ErbB4	D. Meyer/C. Birchmeier laboratory
mOR37A	H. Breer laboratory, Stuttgart, Germany
P75	Palko laboratory, Frederic, USA.
PDGFαR	Chiayeng Wang, Chicago, USA
Reelin	T. Curran laboratory, Memphis, USA
SMDF	D. Meyer/C. Birchmeier laboratory
Sox10	M. Wegner laboratory, Erlangen, Germany
Tbr-1	J. Rubinstein laboratory, San Francisco, USA
TH	H. Baker laboratory, New York, USA

2.2.6. Mouse strains

C57Bl/6J:	Charles River
CB6F1/CrlBR	Charles River
NRG1-null	D. Meyer/C. Birchmeier laboratory
ErbB2R	M. Woldeyesus/C. Birchmeier laboratory
ErbB3	D. Riethmacher/C. Birchmeier laboratory
Sox10^{Dom}	M. Wegner laboratory, Erlangen, Germany
mOR37A-IRES-tau-lacZ	H. Breer laboratory, Stuttgart, Germany
P2-IRES-tau-lacZ	P. Mombaerts, New York, USA

2.3. Methods: Generation of the knockout mouse strain

2.3.1. Molecular biological techniques

Apart from the special techniques detailed in the following part of this section, standard procedures for molecular cloning, sequencing and targeting vector construction were carried out according to "Molecular Cloning" (Sambrook and Russell, 2001) or manufacturers' instructions in the case of kits.

2.3.2. Site specific mutagenesis with PCR

Adapted from "PCR technology: Principles and applications for DNA amplification" (Erlich, 1989).

To generate specific point mutations in corresponding exon7 (for the *NRG*α allele) and exon8 (for the *NRG*β allele) of *Neuregulin-1*, two pairs of internal primers, E7MS and E7MA for exon7, E8MS and E8MA for exon8 were designed, containing mismatches at two or three bases (highlighted bold, below). Each pair of primers anneals to the antisense and sense strands of the same segment of the target DNA (genomic clone 3.5 of *Neuregulin-1*), respectively. The mismatches lead to the same sequence alteration in two primary PCR products in the first round PCRs, which were performed using single pairs of primers, consisting of an external primer and its corresponding mutant antisense or sense primer. For example, for the mutation in exon 7, 5'-external primer (sense) and E7MA (antisense) were used to generate the product P71, 3'-external primer (antisense) and E7MS (sense) to generate the product P72. PCR products were then purified, and pairs of corresponding PCR products (e.g. P71 and P72 for *NRG*α) were mixed together, denatured and allowed to reanneal. Second-round PCRs were performed with the external primers in order to amplify the hybrid mutant DNAs, in which point mutations were present on both strands. Final mutated products were 751 bp in size for both fragments containing mutated exons 7 or 8. These mutant products were cloned into the pGEM-T vector, sequenced and used for generation of the final targeting vectors.

Primer:

5'-external primer (sense): 5'-TCC TTT TGT GTG TGT TCA GCA CCG G-3'

E7MS (mutant exon7, sense): 5'-TCT AGG TG**A** CAA CCT G**A**A TTC ACT GGA-3'

E7MA (mutant exon7, antisense): 5'-TCC AGT GAA T**T**C AGG TTG **T**CA CCT AGA-3'

E8MS (mutant exon8, sense): 5'-T CTC AGG TG**A** CCA AAT GA**A** TT**C** ACT GGT-3'

E8MA (mutant exon8, antisense): 5'-ACC AGT **G**AA **T**TC ATT TGG **T**CA CCT GAG A-3'

3'-external primer (antisense): 5'-AGG CTC TAG CTC TAG GTG ACT CTG A-3'

2.3.3. ES cell culture, electroporation and neomycin-resistant selection

All cell culture procedures were based on protocols according to “Gene Targeting: A Practical Approach” (Joyner, 1999).

Dulbecco's modified Eagle's medium (DMEM) with high glucose (4500 mg/l) and stabilized glutamine (glutamax-I) was generally used, with 10% heat inactivated (55°C 30min) fetal calf serum (FCS) for Feeder cell culture, and 15% FCS plus LIF (f.c. 500-1000 U/ml) for ES cells. LIF-containing supernatant was routinely prepared from COS cells stably transfected with a LIF-expression plasmid (Genetics Institute Inc., Cambridge, MA, USA).

ES cells were cultured on layers of growth-arrested embryonic fibroblasts 'Feeder cells', which provide an ideal environment for growth of ES cells. Feeder cells were routinely prepared from embryos derived from mouse strains homozygous for a transgene containing a neomycin resistance cassette (*neo*^{R}). *neo*^{R} feeder cells survive during positive selection of ES cells with G418. Stocks of primary neomycin-resistant feeder cells were prepared from E14-16 embryos, passaged up to three times, and treated with mitomycin C for growth arrest prior to culture with ES cells.

As a standard procedure, 1x10^7 ES cells were electroporated in 0.8 ml PBS with 20 µg of linearised targeting vector (240 V, 500 µF, BioRad Gene Pulser). Selection with 400 µg/ml G418 (geneticin) was started 48 hours later. After a further 7-8 days culture in selective medium, single ES cell colonies were picked and cultured for additional 1-2 days in 96 well plates.

2.3.4. Identification of homologous recombinant clones

Adapted from (Ramirez-Solis et al., 1992).

-Trypsinize the G418 resistant colonies cultured on 96 well plates.

-Freeze one half of cell suspension and store at -70°C.

-Grow other half on a gelatin-coated 96 well replica plate until confluency.

-Lyse the cells with 50 µl/well lysis buffer.

-Incubate the plate O/N at 60°C in a humid chamber.

-Add 125 µl/well EtOH/NaAc (100:5) and precipitate DNA for 60min at RT.

-Discard supernatant and wash with 70% EtOH for 5 times, dry the plate at RT.

-Digest with 50 µl/well restriction enzyme digestion cocktail O/N at 37°C with shaking.

-Load 25 µl samples on a 1.0% agarose gel and proceed with Southern blot analysis (see 2.3.7).

ES cell lysis buffer:

10 mM Tris, pH 7.5

10 mM EDTA

10 mM NaCl

0.5% Sarcosyl (N-Lauroylsarcosin)

200 µg/µl Proteinase K

Restriction enzyme digestion cocktail:

1 x buffer

0.5 U/µl Enzyme

50 µg/ml RNase

2.3.5. Cre transient expression

After identification of recombinant clones by Southern blot analysis, 5 x 10^6 ES cells from a *NRG1αneo* or *NRG1βneo* clone was electroporated in 0.4 ml PBS with 10 µg Cre transient expression plasmid, pIC-Cre. The ES cell suspension was diluted with ES cell medium, and up to 1 x 10^3 cells were placed in each 100 mm cell culture dish. Colonies were picked after 8-9 days in culture and processed as above (see 2.3.4) to identify *NRG1α* or *NRG1β* clones.

2.3.6. Microinjection of blastocysts

Two independent heterozygous ES cell clones were injected to establish mouse strains that carry the α- or β-isoform specific mutation of *NRG1*.

For microinjection, 10-15 ES cells were injected into each blastocysts, which were harvested from uteruses of C57Bl/6J mice on day 3.5 post-coitum. These blastocysts were transferred into the uterus of pseudo-pregnant CB6F1 foster mice (day 2.5, post-coitum). The resulting chimeric male offspring were crossed with C57Bl/6J females, and the offspring with brown coat color were analyzed for genotype.

2.3.7. Genotyping of mice by PCR or Southern hybridization

Mice were genotyped routinely by PCR. Southern blot analysis was used during the establishment of the F1 generation and occasionally for verification of genotypes derived by PCR. Mouse tissue was digested in Proteinase K-containing lysis buffer at 55°C with shaking. For Southern blot analysis, genomic DNA was isolated according to standard methods. Otherwise, tissue lysates were heat inactivated at 95°C for 10 min, diluted with 200 µl H_2O; 1-2 µl was used per 30 µl PCR reaction.

Tail or ear hole lysis buffer:	**Yolksac or tissue lysis buffer:**
100 mM Tris, pH8.5	10 mM Tris, pH8.9
5 mM EDTA	50 mM KCl
200 mM NaCl	200 mM $MgCl_2$
0.2% SDS	0.01% gelatin
100 µg/µl Proteinase K	0.45% Nonidet-P40
	0.45% Tween-20
	100 µg/µl Proteinase K

2.3.7.1. Genotyping of Nrg1α and Nrg1β mutants by PCR

Primers:

NRG1S (sense): 5'-TCC TTT TGT GTG TGT TCA GCA CCG G-3'

NRG1A (antisense): 5'-GCA CCA AGT GGT TGC GAT TGT TGC T-3'

Reaction mix:

DNA (~100 ng)	1.0 µl
10 x PCR buf.	3.0 µl
50 mM $MgCl_2$	3.0 µl
2.5 mM dNTP	3.0 µl
5.0 U/µl Taq Polymerase	0.3 µl
5 µM Primer1	2.0 µl
5 µM Primer2	2.0 µl
H_2O	15.7 µl
	30.0 µl

Program:			**Products:**			
95°C	3.00 min		Wildtype:	260 bp		
95°C	45 s		Mutant:	380 bp		
68°C	30 s	40 x	**After EcoRI digestion:**			
72°C	50 s (+1s/cycle)		α mutant:	170 bp	125 bp	85 bp
72°C	5.00 min		β mutant:	210 bp	170 bp	
4°C	∞					

2.3.7.2. Southern analysis

-Precipitate 5-10 µg DNA in a 1.5 ml Eppendorf tube (or in gelatin coated 96 well plates).

-Add 50 µl digestion cocktail and digest O/N at 37°C with shaking.

-Separate 25 µl of samples on a 1.0% agarose gel, for 6hrs at 80 V or 12 hrs at 40 V.

-Denature in 0.5 M NaOH, 1.5 M NaCl for 30-45 min (depending on the gel size).

-Transfer to nylon membrane (Hybond-N, Amersham-Pharmacia) O/N in 20 x SSC.

-Rinse the membrane in 6 x SSC for 3 min at RT and crosslink with UV light.

-Prehybridize for 2 hrs and hybridize O/N at 65°C.

-Wash with 2 x SSC, 0.1% SDS, 5-10 min x 3 at 65°C.

-Wash with 0.2 x SSC, 0.1% SDS, 5-10 min x 3 at 65°C.

-Expose to X-ray film or phosphorimager screen.

Hybridization buffer:

6 x SSC

5 x Denhardt's solution

0.5% SDS

100 µg/ml denatured salmon sperm DNA

α-^{32}P-dCTP-labelled DNA probes were prepared by random-labeling and purified with Qiagen nucleotide removal kit.

2.3.8. RT-PCR

RT-PCR analysis was performed on E12.5 embryos to confirm that the introduced point mutations interfered specifically with the production of the expected isoform and left the expression level of the other one unchanged.

-Extract total RNA with TRIzol reagent (Gibco/BRL)

-Synthesize cDNA with single strand cDNA synthesis kit (Amersham-Pharmacia)

Primers:

E6S (common exon6, sense): 5'-CCA CAT CTA CAT CCA CGA CT-3'

E7A (α-specific, antisense): 5'-TTT GGA CTT TCA TGG GCA CAT TCT C-3'

E8A (β-specific, antisense): 5'-GTA GAA GCT GGC CAT TAC GTA-3'

Programm:			**Products:**		
95°C	3.00 min		E6-7 (α):	198bp	
95°C	45 s		E6-8 (β):	188bp	
64°C	30 s	40 x	**After EcoRI digestion:**		
72°C	30 s		α mutant:	141bp	57bp
72°C	5.00 min		β mutant:	141bp	47bp
4°C	∞				

2.3.9. Establishment of strain and mouse breeding

F1 heterozygous mutant mice with targeted alleles were back-crossed to C57/Bl6 mice. The phenotype analysis of the NRG1α and NRG1β mutants was carried out on a mixed genetic background (129/Ola and C57/Bl6).

2.4. Methods: Analysis of phenotype

2.4.1. Histology and staining

Embryos were dissected in PBS (cranium and the body walls were opened in embryos of E14 and older), fixed with 4% PFA at 4°C, dehydrated in an ethanol series and embedded in Technovit 7100 (Heraeus Kulzer GmbH). 4-5 µm semi thin sections were stained with hematoxylin/eosin or toluidine-blue/Nissl.

Staining procedures were adapted from “Staining Procedures” (Clark, 1981).

2.4.1.1. Hematoxylin/Eosin staining

Delafield's hematoxylin solution:

-Dissolve 4 g hematoxylin (Merck, No. 4305) in 25 ml 100% ethanol.

-Add 400 ml 10% $NH_4Al(SO_4)_2.12H_2O$.

-Expose to air and light for one week.

-Filtrate and add 100 ml each glycerol/methanol.

-Store for 4-6 weeks and filtrate before use.

Eosin solution:

Stock solution: 1.0% eosin Y in dH_2O

Working solution: 0.25% eosin Y in 0.1 M HAc

Staining procedure:

-Stain slides in Delafield's hematoxylin solution for 15-20 min.

-Wash slides with running tap water for 15 min and then with dH_2O, twice, 1 min each.

-Stain slides in eosin solution for 10 min.

-Wash slides with dH_2O twice, 1 min each.

-Reduce background shortly with 70% EtOH for 20 seconds.

-Wash slides immediately with dH_2O three times, 2 min each.

-Air dry slides and cover with 'Corbit Balsam' or 'Entellan® new' embedding agent (Merck).

2.4.1.2. Nissl staining

Toluidine blue-O solution:

Stock solution: 0.5% in dH_2O

Working solution: 1:10 dilute stock solution in 0.2 M Walpole buffer

Walpole buffer: 0.2 M acetic acid/0.2 M sodium acetate (3:2), pH 4.45

Staining procedure:

-Stain slides into toluidine blue-O solution for 15-20 min (depending on thickness of sections).

-Wash slides with running tap water for 15 min.

-Wash slides with dH_2O twice, 2 min each.

-Reduce background shortly with 70% EtOH for 20 seconds.

-Wash slides immediately with dH_2O, 3 x 2 min.

-Air dry slides and cover with 'Corbit Balsam' or 'Entellan® new' embedding agent (Merck).

2.4.2. Immunohistochemistry

2.4.2.1. Whole mount

-Dissect E9-11 embryos in PBS.

-Fix the embryos in ice cold 4% PFA for 1-2 hrs.

-Wash with PBT three times, 5 min each.

-Dehydrate in 25%, 50%, 75%, 100% methanol/PBS, 10 min each on ice.

-Bleach in 3:1 methanol (100%) : H_2O_2 (33%) for 1 hr at RT.

-Wash with 100% methanol twice, 10 min each.

-Store in 100% methanol at -20°C until use.

-Rehydrate in 75%, 50%, 25% methanol/PBS, 10 min each on ice.

-Wash with PBT three times, 10 min each.

-Treat with 20 µg/ml proteinase K/PBT, 5 min at RT.

-Wash with PBT, 3 x 10 min.

-Refix in 4% PFA/PBS, 1hr on ice.

-Wash with PBT 5 times, 1 hr each.

-Incubate with 10% inactivated goat serum/PBT for 1-2 hrs.

-Incubate with primary antibody diluted in 1% GS/PBT, O/N at 4°C.

-Wash with PBT 5 times, 1 hr each.

-Incubate with peroxidase-conjugated secondary antibody (in 1% GS/PBT), O/N at 4°C.

-Wash with PBT 5 times, 1 hr each.

-Incubate with 0.3 mg/ml DAB, 0.04% $NiCl_2$ in PBT, 1-2 hrs at RT.

-Develop with 0.3 mg/ml DAB, 0.04% $NiCl_2$ and 0.0075% H_2O_2, 10-20 min at RT.

-Wash with PBT, O/N at 4°C, clear with 25%, 50%, 75% glyceol/PBS.

2.4.2.2. On sections

Immunohistological analysis on sections was performed on tissue prefixed with 2%-4% PFA and cryoprotected with 20% sucrose.

-Refix the sections in ice cold 4% PFA/PBS, 2 min.

-Wash with PBT, 5 x 5 min.

-Incubate with 10% inactivated horse serum/PBT (HS/PBT) for 1-2 hrs.

-Incubate with primary antibody diluted in 10% HS/PBT, O/N at 4°C.

-Wash with PBT, 5 x 5 min.

-Incubate with Cy2 or Cy3-conjugated secondary antibody (in 10% HS/PBT), O/N at 4°C.

-Wash with PBT, 5 x 5 min.

-Cover with “Immumount” (Shandon, Frankfurt).

2.4.3. *In situ* hybridization

2.4.3.1. Whole mount

Tissue samples and embryos for whole mount *in situ* hybridization were pre-fixed with 4% PFA. The probes were labeled with a DIG RNA labeling Kit (Roche).

Preparation of probes:

-Mix 1.0 µl linearized plasmid-DNA (1 µg/µl)
2.0 µl 10x Transcription buffer
2.0 µl 10mM/GTP/ATP/CTP, 6.5mM/UTP, 3.5mM/DIG-UTP
0.5 µl RNase-Inhibitor (20U/µl)
12.5 µl DEPC-H_2O
2.0 µl RNA-Polymerase (20U/µl)

-Incubate 1 hr at 37°C.

-Add 2 µl DNase (10U/µl), 20 min at 37°C.

-Mix with 2µl tRNA (50µg/µl), 76 µl H_2O, 50 µl 7.5 M CH_3COONH_4, 375 µl EtOH.

-Precipitate in liquid nitrogen for 3 min and centrifuge at 13,500 rpm for 5 min.

-Dissolve the precipitated probe in 50 µl H_2O.

-Mix with 50 µl formamide, 1 µl 1 M DTT, store at -20°C until use.

-Check 5 µl probe by agarose gel electrophoresis.

Hybridization:

-Dissect E9-11 embryos in PBS.

-Fix the embryos in 4% PFA, O/N at 4°C.

-Wash with PBT, 3 x 5 min.

-Dehydrate in 25%, 50%, 75%, 100% methanol / PBS, 10 min each on ice.

-Bleach in 3:1 methanol (100%) : H_2O_2 (33%) for 1 hr at RT.

-Wash with 100% methanol, 2 x 10 min on ice.

-store in 100% methanol at -20°C until use.

-Rehydrate in 75%, 50%, 25% methanol / PBS, 10 min each on ice.

-Wash with PBT, 3 x 10 min.

-Treat with 20 µg/ml proteinase K / PBT, 10-30 min at RT.

-Wash with PBT, 3 x 10 min.

-Refix in 4% PFA, 0.2% glutaraldehyde, 60 min on ice.

-Wash with PBT, 3 x 10 min.

-Incubate with hybridization buffer, 1-3 hrs at 70°C.

-Incubate with hybridization mix (100-500ng denatured probe in 2 ml buffer), O/N at 70°C.

-Wash with prewarmed 5 x SSC, 50% formamide, 0.1% Tween-20, 2 x 30 min at 70°C.

-Wash with 10 mM Tris pH 7.5, 0.5 M NaCl, 0.1% Tween -20, 3 x 10 min at 37°C.

-Incubate with 20 µg/ml RNase A in the same buffer for 60 min at 37°C.

-Wash with prewarmed 2 x SSC, 50% formamide, 0.1% Tween-20, 3 x 60 min at 65°C.

-Wash with TBST, 3 x 10 min at RT.

-Block with 10% inactivated goat serum/TBST for 60 min at RT.

-Incubate with anti-DIG antibody solution O/N at 4°C.

-Wash with TBST for whole day at RT, change TBST every 60 min.

-Wash with alkaline phosphatase (AP) buffer, 3 x 10 min at RT.

-Develop color in filtrated color solution (9 µl NBT, 7 µl BCIP in 2 ml AP buffer) in the dark.

-Stop the reaction with 3 x 10 min wash in PBT/1 mM EDTA.

-Postfix embryos and clear with 25%, 50%, 75% glycerol/PBS.

Hybridization buffer:	**10 x TBST:**	**AP buffer:**
50% deionized formamide	25 mM Tris pH 7.4	100 mM Tris pH 9.5
5 x SSC	8.0% NaCl	100 mM NaCl
40 µg/ml Heparin	0.2% KCl	50 mM $MgCl_2$
100 µg/ml denatured salmon sperm DNA	1% Tween-20	0.1% Tween-20
50 µg/ml yeast tRNA		
0.1% Tween-20		
store at -20°C		

Anti-DIG antibody solution:

-Incubate about 50 µg embryo powder in 2 ml TBST for 30 min at 70°C.

-Centrifuge at 5,000 rpm for 10 min, discard supernatant.

-Resuspend the pellet in 0.5 ml anti-DIG antibody mix (1:500 diluted in 1% goat serum/TBST).

-Incubate 60 min at 4°C, centrifuge at 5,000 rpm for 10 min.

-Dilute supernatant 1:4 with 1% goat serum/TBST.

2.4.3.2. On sections

In situ hybridization on sections was performed on unfixed tissue directly embedded in Tissue-Tek® O.C.T. Compound (Sakura). 10 µm sections were cut and stored at -70°C until hybridized with ^{35}S- labeled probes (Amersham).

Preparation of probe:

-Mix 1.0 µl linearized template (0.5-1 µg/µl)
2.0 µl 10 x Transcription buffer
2.0 µl 10 mM GTP/ATP
0.5 µl RNAse-inhibitor (20 U/µl)
2.5 µl α-^{35}S-UTP (12.5 µCi/µl)
2.5 µl α-^{35}S-CTP (12.5 µCi/µl)
8.5 µl DEPC-H_2O
1.0 µl RNA-Polymerase (20 U/µl)

-Incubate 1 hr at 37°C.

-Add 2 µl DNase (10 U/µl), 20 min at 37°C.

-Clean the probe with RNeasy Kit (Qiagen).

-Elute the probe with 30 µl d H_2O.

-Mix with 30 µl formamide, 1 µl 1 M DTT, store at -20°C until use.

-Dilute 1 µl probe in 100 µl d H_2O, and mix with 2 ml scintillation solution.

-Check the labeling efficiency by measuring radioactivity in a scintillation counter
(A good probe yields between 5.0 x 10^5-1.0 x 10^6 cpm/µl).

Section pretreatment:

-Move the boxes with sections from -70°C to RT and warm up for at least 2 hrs before open.

-Fix sections in 4% PFA, 20 min at RT.

-Wash with PBS twice, 5 min each.

-Acetylate for 10 min in Triethanolamin solution.

-Wash with PBS twice, 5 min each.

-Dehydrate in aqueous series of 30%, 50%, 70%, 85%, 96%, 100% EtOH, 1min each.

-Dry the slides 1-2 hrs at RT.

Triethanolamine solution:

-250 ml ddH_2O

-3.12 ml triethanolamine

-675 µl acetic anhydride

-Prepare freshly

Hybridization:

-Dilute probe with hybridization buffer to 5.0 x 10^4- 1.0 x 10^5 cpm/µl.

-Denature at 95°C for 5 min and transfer to ice.

-Add 1/10 volume of 1 M DTT and mix thoroughly.

-Apply 50-60 µl of hybridization mix to each slides and cover with Sigmacote coated cover slip.

-Incubate O/N at 60°C in a chamber humidified with 50% formamide, 5 x SSC.

Hybridization buffer:

-50% deionized formamide

-10 mM Tris pH 7.5

-10 mM sodium phosphate, pH 6.8

-5 mM EDTA

-2 x SSC

-150 µg/µl denatured salmon sperm DNA

-150 µg/µl yeast tRNA

-10% dextrane sulphate

store at -20°C

Posthybridization wash:

-Wash with 5 x SSC, 1 mM DTT for 20 min at 65°C.

-Wash with 2 x SSC, 1 mM DTT for 20 min at 65°C.

-Wash with 2 x SSC, 1 mM DTT for 5 min at 37°C.

-Digestion with 20 µg/ml RNase, 2 x SSC, 1 mM DTT for 30 min at 37°C.

-Wash with 2 x SSC, 1 mM DTT twice, 5 min each at 37°C.

-Wash with 2 x SSC, 50% formamide, 1 mM DTT twice, 60 min each at 65°C.

-Wash with 2 x SSC for 15 min at 65°C.

-Wash with 0.1 x SSC three times, 15 min each at 65°C.

-Dehydrate in 30%, 50%, 70%, 85%, 96%, 100% EtOH, 1min each.

-Dry the slides for 1-2 hrs at RT.

-Expose O/N on X-ray film (Kodak Biomax MR) to check the signal intensity.

Autoradiography: (In darkness)

-Melt Kodak NTB2 autoradiography emulsion (Cat. No. 1654433) at 42°C.

-Dilute emulsion 1:1 with dH_2O.

-Dip slides in emulsion solution and dry them at RT for 2 hrs.

-Put slides in a light-safe box.

-Store at 4°C for 3-14 days, depending on signal intensity.

Developing slides:

-Warm up the box with slides for 2-3 hrs at RT.

-Develop in Kodak D-19 develop solution for 3 min.

-Tansfer to 2% HAc for 1min.

-Fix in 30% $Na_2O_3S_2 \cdot 5H_2O$ solution for 3 min.

-Wash with dH_2O twice, 2 min each.

-Wash with running tap water for 20 min.

-Wash with dH_2O twice, 2 min each, dry at RT.

2.4.4. X-gal/Bluo-gal staining

2.4.4.1. Whole mount

In order to prevent parturition, Perlutex (Medroxyprogesteronacetat, Boehringer Ingelheim) was injected to pregnant female at day 17 of pregnancy.

-E18-20 embryos were dissected and the region containing olfactory system was isolated.

-Fix in 2% PFA, 5mM $MgCl_2$/PBS, 1-3 hrs at 4°C.

-Wash with 5 mM $MgCl_2$/PBT three times, 30 min each at 4°C.

-Incubate with staining solution O/N at RT.

-Wash with 5 mM $MgCl_2$/PBT three times, 30 min each at 4°C.

-Clear after a methanol series in 1:2 benzyl alcohol/benzyl benzoate.

Staining solution (filter before use):

1 mg/ml Bluo-Gal (Sigma)

5 mM $K_3Fe(CN)_6$

5 mM $K_4Fe(CN)_6$

5 mM $MgCl_2$

PBT

2.4.4.2. On sections

-Dissect the embryos in PBS.

-Fix in 2% PFA, 5 mM $MgCl_2$/PBS, 4-8 hrs at 4°C.

-Wash with 5 mM $MgCl_2$/PBS, 2 hrs x 2 at 4°C.

-Cryoprotect with 20% sucrose, 5 mM $MgCl_2$/PBS.

-Embed in Tissue-Tek® O.C.T. Compound (Sakura) and cut 10 µm sections.

-Postfix the sections in 2% PFA, 5 mM $MgCl_2$/PBS, 2 min on ice.

-Wash with 5 mM $MgCl_2$/PBT 5 times, 5 min each at 4°C.

-Incubate with staining solution 3-6 hrs at 37°C.

-Wash with 5 mM $MgCl_2$/PBT 5 times, 5 min each at RT.

-Counterstain in neutral red solution.

2.4.5. DiI injection

-Dissect the embryos in PBS.

-Fix with 4% PFA.

-Insert a small crystal of DiI (Molecular Probes, Eugene, USA)

-Return the sample to 4% PFA.

-Incubate 2-4 days at 37°C.

-Cut 30-50 µm vibratome sections in PBS.

-Mount and photograph in PBS.

2.4.6. TUNEL assay

After staining with 1st and 2nd antibodies, a TUNEL assay was carried out using the Apop Taq Plus kit (a fluorescein-based *in situ* apoptosis detection kit, Intergen, Gaithersburg, MD, USA)

2.4.7. Detection of cell proliferation

-Inject pregnant females with 75 µg/g body weight BrdU (5-Bromo-2'-deoxy-uridine).

-Dissect the embryos in PBS after 2 hrs.

-Fix, cryoprotect, embed, section embryos as for standard immunohistological analysis.

-Postfix the sections after 1st and 2nd antibody staining.

-Treat the sections with 2.4 M HCl for 30 min at 37°C.

-Wash with PBT and block with 10% HS.

-Detect proliferating cells with anti-BrdU antibodies and secondary antibodies.

2.4.8. Chimeric analysis

ErbB3-/- ES cells (Riethmacher et al., 1997) were electroporated with a targeting vector containing genomic sequences of the *mOR37A* odorant receptor gene, an *IRES-tau-lacZ* cassette inserted in the 3' non-coding portion of the *mOR37A* gene, and a hygromycin cassette for selection. Colonies that had inserted the targeting vector by homologous recombination were identified by Southern hybridization following hygromycin selection. The extent of chimerism of E18.5 mice generated by injections of *ErbB3-/-; mOR37A-IRES-tau-lacZ* ES cells (which express the glucose phosphate isomerase type a, GPI^{α}) into C57/Bl6 blastocysts (which express GPI^{β}) was determined by measuring GPI isoenzyme ratios in tail tissue. Chimeras with more than 50% ES cell contribution were further analyzed.

3. Results

3.1. Generation of *NRG1α* and *NRG1β* mutant alleles

The EGF-like domain of Neuregulin-1 encoded by exons 6, 7 and 8 is essential for receptor binding and function (Fig. 1). The N-terminal portion of the EGF-like domain shared by all isoforms of Neuregulin-1 is encoded by exon 6. The C-terminal portion of the EGF-like domain exists as two variants, α and β, which are encoded by the alternatively spliced exons 7 and 8, respectively. In the mouse, targeted mutations that disrupt exon 6, or delete exons 7 and 8, abolish all Neuregulin-1 functions and correspond to null mutations (Meyer and Birchmeier, 1995). *NRG1*-null mutant embryos die at mid-gestation (E10.5), which precluded the functional analysis of *NRG1* in late development or in the adult. I generated two novel mutant alleles of *NRG1*, which disrupt specifically Neuregulin-1 isoforms containing the α- or β-variant EGF-like domain, respectively, and which, in addition, contain *loxP* sequences for conditional inactivation of the gene by the use of Cre-recombinase (Figs. 4, 5).

A similar strategy was used for the construction of both targeting vectors, enabling the introduction of α- or β-isoform-specific mutations into the *NRG1* gene (*NRG1α* and *NRG1β*, respectively; Figs. 4a and 5a). Small sequence alterations, consisting of a stop codon and a novel *Eco*RI restriction site, were introduced into either exon 7 (Figs. 4b) or 8 (Figs. 5b). Thus, the coding sequence of one of these two exons that encode the C-terminal portion of the EGF-like domain was disrupted, whereas the other remained intact. In addition, the targeting vectors contained three *loxP* sites. One was located 3' of the altered exons. Two more were located 5' of exon 7, flanking a *neomycin*-resistance cassette, which was introduced to serve as a selectable marker. The presence of these mutations in the targeting vectors was confirmed by sequencing. The targeting vectors were then electroporated into ES cells, which were selected for the presence of the *neo* cassette by the use of the antibiotic G418 (Geneticin). Southern hybridizations analysis of genomic ES cell DNA were employed to identify those ES cells that had incorporated the targeting vector correctly into the *Neuregulin-1* locus by homologous recombination (*NRG1αneo* and *NRG1βneo* alleles, Figs. 4a and 5a).

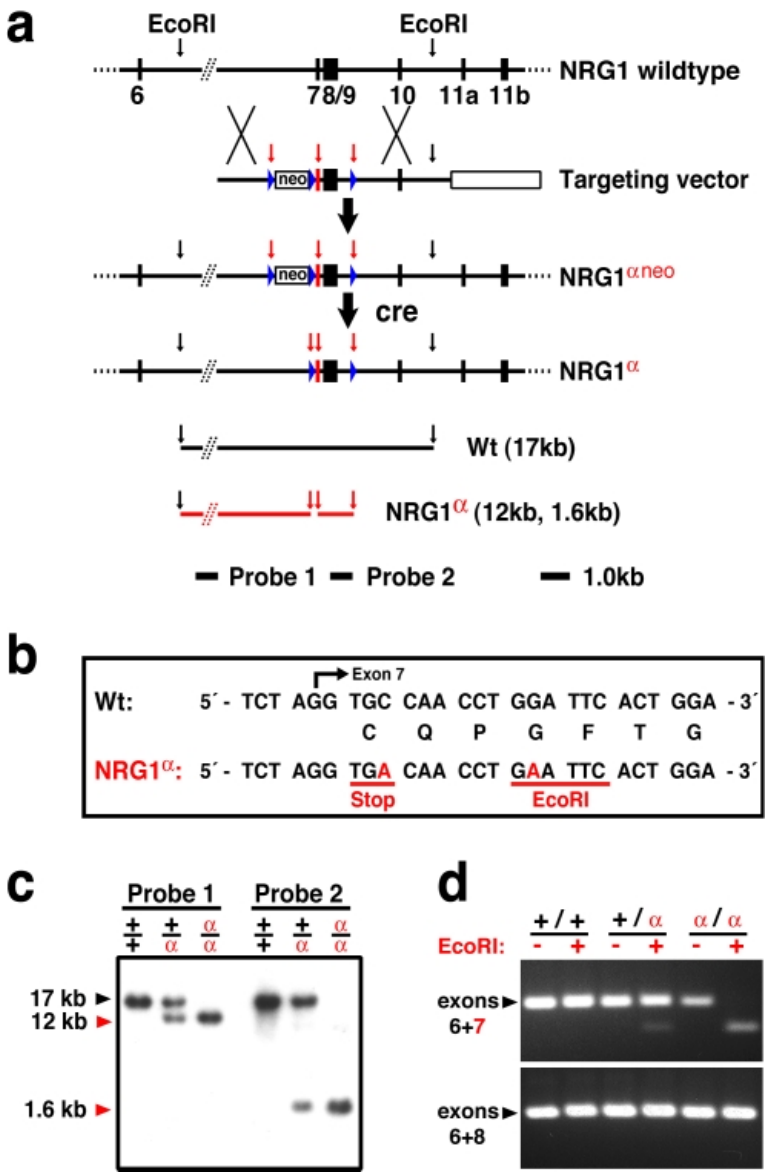

Figure 4. Strategy employed to mutate specifically the α-isoform of Neuregulin-1
(a) The structure of the wildtype *NRG1* locus is shown at the top. The *NRG1α* mutant allele was generated in two steps. First, the targeting vector containing the sequence alterations in exon 7 (indicated in red, see also b) and a neomycin-resistance cassette flanked by *loxP* sites was introduced into the mouse genome by homologous recombination in ES cells, generating the *NRG1α neo* allele. Second, the neomycin-resistance cassette of this *NRG1α neo* allele was removed by transient transfection of a Cre-expression plasmid (pIC-cre), resulting in the *NRG1α* allele. Exons in the *NRG1* gene are shown as black boxes and numbered; *loxP* sites are indicated as blue triangles. Black arrows mark the position of two *Eco*RI sites present in the wildtype allele. In contrast, three additional *Eco*RI sites that were introduced into the mutant allele are indicated by red arrows; one is located in the mutant exon 7 (see also b) and the others at the borders of two *loxP* sites. The probes used for Southern hybridization in (c) are shown, as are the sizes and positions of expected fragments generated by *Eco*RI digestion of genomic DNA containing wildtype and *NRG1α* mutant alleles. **(b)** Partial sequences of wildtype and mutant *NRG1α* exon 7; two point mutations (red) in the mutant *NRG1α* allele introduce a stop codon into the sequence encoding the α-isoform-specific EGF-like domain, and generate a novel *Eco*RI site. **(c)** Southern hybridization of genomic DNA from wildtype, *NRG1α/+* and *NRG1α/α* embryos after *Eco*RI digestion. The fragments used as probes are indicated in (a). **(d)** RT-PCR analysis on total RNA from E12.5 wildtype, *NRG1α/+* and *NRG1α/α* embryos. The primers used in PCR amplification hybridize to exon 8 (β-specific) or 7 (α-specific) and exon 6 (shared by α- and β-isoforms). The amplified products were digested with *Eco*RI as indicated, to detect the novel *Eco*RI restriction site present in transcripts of the mutant *NRG1α* allele.

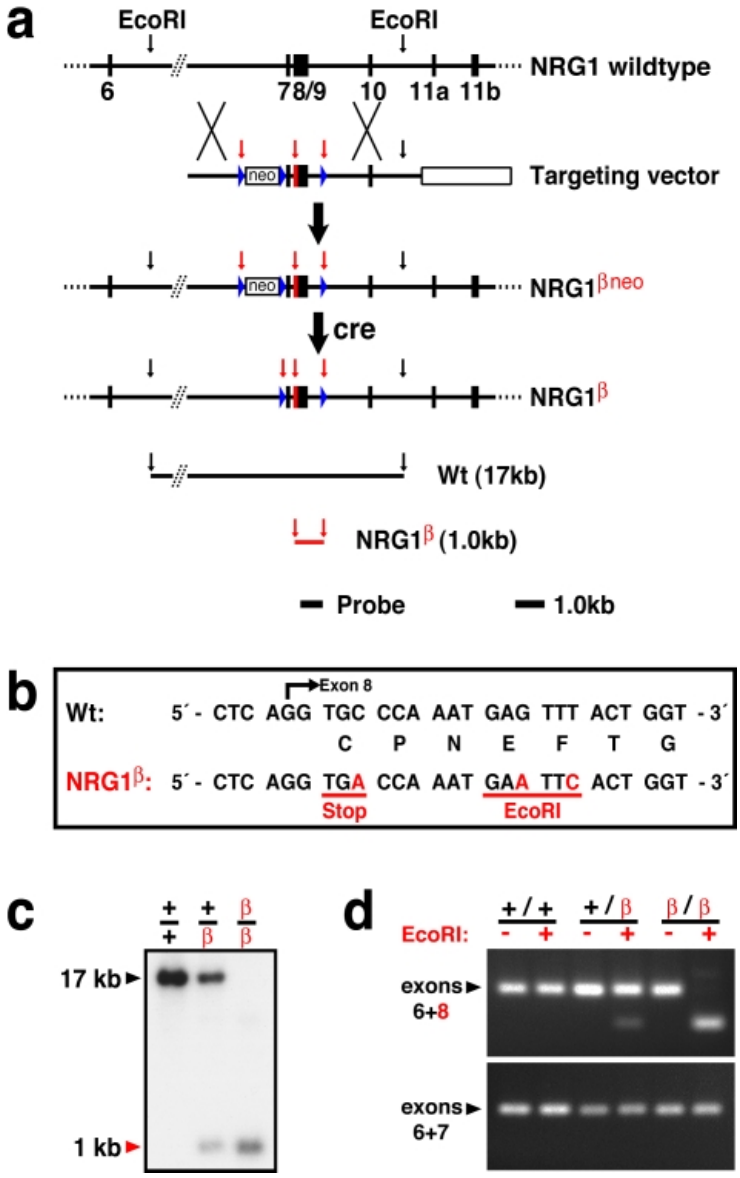

Figure 5. Strategy employed to mutate specifically the β-isoform of Neuregulin-1
(a) The structure of the wildtype *NRG1* locus is shown at the top. The *NRG1β* mutant allele was generated in two steps. First, the targeting vector containing the sequence alterations in exon 8 (indicated in red, see also b) and a neomycin-resistance cassette flanked by *loxP* sites was introduced into the mouse genome by homologous recombination in ES cells, generating the *NRG1β neo* allele. Second, the neomycin-resistance cassette of this *NRG1β neo* mutant allele was removed by transient transfection of a Cre-expression plasmid (pIC-cre), resulting in the *NRG1β* allele. Exons in the *NRG1* gene are shown as black boxes and numbered; *loxP* sites are indicated as blue triangles. Black arrows mark the position of two *Eco*RI sites present in the wildtype allele. In contrast, three additional *Eco*RI sites that were introduced into the mutant allele are indicated by red arrows; one is located in the mutant exon 8 (see also b) and the others at the borders of two *loxP* sites. The probe used for Southern hybridization in (c) is shown, as are the sizes and positions of expected fragments generated by *Eco*RI digestion of genomic DNA containing wildtype and *NRG1β* mutant alleles. **(b)** Partial sequences of wildtype and mutant *NRG1β* exon8; three point mutations (red) in the mutant *NRG1β* allele introduce a stop codon into the sequence encoding the β-isoform-specific EGF-like domain, and generate a novel *Eco*RI site. **(c)** Southern hybridization of genomic DNA from wildtype, *NRG1β*/+ and *NRG1β/β* embryos after *Eco*RI digestion. The fragment used as probe is indicated in (a). **(d)** RT-PCR analysis on total RNA from E12.5 wildtype, *NRG1β*/+ and *NRG1β/β* embryos. The primers used in PCR amplification hybridize to exon 8 (β-specific) or 7 (α-specific) and exon 6 (shared by α- and β-isoforms). The amplified product were digested with *Eco*RI as indicated, to detect the novel *Eco*RI restriction site present in transcripts from the mutant *NRG1β* allele.

The presence of a single insertion event by homologous recombination was verified by Southern hybridization using various probes derived from the *NRG1* locus. In a subsequent step, the *neo*-cassette was removed by transient expression of Cre-recombinase in ES cells (cf. Torres and Kühn, 1997), resulting in the ES cell clones that contain *NRG1α* or *NRG1β* mutant alleles. Each mutant allele contained the corresponding mutant exon (7 or 8) and the two *loxP* sites, which flank the exons encoding the C-terminal portion of EGF-like domain (Figs. 4a and 5a). The removal of the *neo*-cassette was also controlled by Southern blot analysis of genomic ES cell DNA (Figs. 4c and 5c). The mutant ES cells were injected into blastocysts and transferred into foster mothers. From such blastocysts, chimeric mice developed. Chimeras that transmitted the mutant allele through their germline were identified, and used to establish mouse strains that contain the *NRG1α*- or *NRG1β*-specific mutations. The novel *Eco*RI restriction site introduced in the mutant exon allowed an unambiguous identification of the mutant allele in ES cells and mice, and was useful for the analysis of mutant transcripts (Figs. 4c, d and 5c, d).

3.2. Abnormal development of the mammary gland in *NRG1α* mutant mice

Homozygous *NRG1α* (*NRG1α/α*) mice appeared healthy and fertile and no overt phenotype has been noted throughout their life span. RT-PCR analysis (Fig. 4d) on RNA isolated from *NRG1α/α* embryos confirmed that transcripts containing exon 7 carried the expected sequence alteration, i.e. the *Eco*RI restriction site that is linked to the stop codon, which interferes with the production of NRG1 α-isoforms. I observed reproducibly in heterozygous or homozygous mutant mice a decreased amount of the PCR product from the mutant allele. This might reflect a destabilization of the mutant mRNA by nonsense-mediated decay, a mechanism used for the elimination of mRNAs that carry premature termination codons (reviewed by Culbertson, 1999; Hentze and Kulozik, 1999). In contrast, amounts of transcripts containing exon 8 that encode the β-isoforms were unaffected.

The α-isoforms of NRG1 are expressed mainly in mesenchymal cells (Wen et al., 1994; Meyer and Birchmeier, 1994). In the mammary gland mesenchyme, α-isoforms constitute the sole expressed Neuregulin-1 (Yang et al., 1995). In collaboration with Frank Jones (Tulane

University, USA), the development of the mammary gland was analyzed in mice that carry a homozygous *NRG1α* mutation.

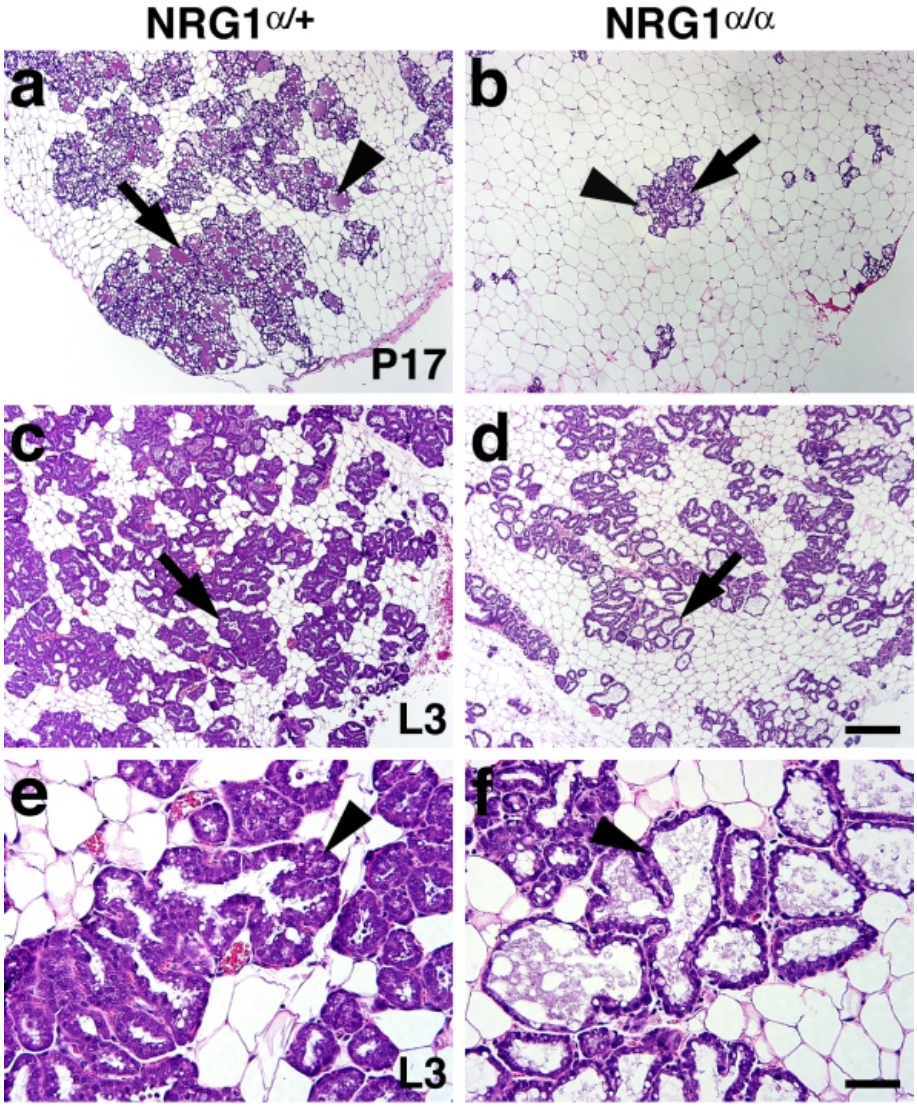

Figure 6. Aberrant morphology of the mammary gland of *NRG1α/α* mice during pregnancy and lactation
A portion of the number four inguinal mammary gland from wildtype (a, c, e) and *NRG1α/α* (b, d, f) mice at day 17 of pregnancy (P17, a, b) and day 3 of lactation (L3, c-f) was fixed in paraformaldehyde, paraffin embedded, and stained with hematoxylin/eosin. **(a)** At P17, large lobuloalveolar clusters are detected in control mammary glands (arrow). The lobuloalveolar lumens are distended with lipids and early lactation products (arrowhead). **(b)** In *NRG1α/α* mice at P17, the development of lobuloalveolar clusters is less extensive. Each lobuloalveolar cluster consists of fewer lobuloalveoli (arrow) and the lobuloalveoli remain condensed (arrowhead). **(c)** At L3, dense aggregates of lobuloalveoli (arrow) composed of secretory active cuboidal lumenal epithelium are seen in control mice (arrowhead in e). **(d)** In contrast, lobuloalveolar accumulation is impaired in *NRG1α/α* mice at L3 resulting in a fatpad that is sparsely populated with abnormally distended lobuloalveoli (arrow). **(e)** Higher magnification of (c), indicating the cuboidal epithelium observed in wildtype lobuloalveoli (arrowhead). **(f)** Higher magnification of (d), showing that the majority of the lumenal epithelium appears flat in the mutants (arrowhead). Bars: (a-d) 200µm; (e, f) 50µm.

Consistent with earlier organ culture and *in vitro* experiments, the α-isoforms of Neuregulin-1 were found to be a mitogen critical for development of mammary gland (Fig. 6 and Li et al., 2002). Two phases of mammary gland morphogenesis can be distinguished in normal animals. The first involves branching and elongation of epithelial ducts during puberty and results in the formation of a ductal tree. During the second phase, which occurs during pregnancy, milk-producing lobuloalveolar structures are generated. The α-isoform of Neuregulin-1, whose expression peaks on pregnancy day 15, regulates the second phase of morphogenesis. In *NRG1α* mutant mice, transient impairment of lobuloalveolar budding was observed at two temporally and functionally distinct stages of development, mid-pregnancy (P12.5-17) and early post-partum (lactation day 3) (Fig. 6).

3.3 Conditional mutagenesis of the *NRG1* gene

Since the *NRG1α* mutant strain carries also two *loxP* sites that flank exons 7, 8 and 9, this strain can be used to induce mutations with Cre-recombinase, enabling a tissue-specific ablation of *NRG1*. In collaboration with the laboratory of Steve Burden (Skirball Institute, New York University Medical School, USA), this conditional *NRG1* mutant allele was used to analyze the role of neuronally produced Neuregulin-1 in the establishment of the neuromuscular synapse. In cultured skeletal muscle cells, Neuregulin-1 stimulates the expression of AChR (acetylcholine receptor). It has been postulated that neuronally produced Neuregulin-1 is an important determinant of synapse formation (Fischbach and Rosen, 1997). Using an *Isl1-Cre* allele, *NRG1* mutations were specifically introduced in motoneurons and sensory neurons. However, the formation and maturation of neuromuscular synapses were not affected (Yang et al., 2001).

3.4. NRG1 α-isoform rescues *NRG1β* mutants from the heart trabeculation defect

Heterozygous *NRG1β* mice were healthy and fertile. However, homozygous *NRG1β* mutant embryos (*NRG1β/β*) were not viable. About 20% of *NRG1β/β* mutants developed to term, but died shortly after birth. Upon external inspection, it was noted that the mutant pups displayed drooped heads and forelimbs, they could not move and displayed a cyanotic body color. These mutants resembled in external appearance *ErbB3, ErbB2R* and type III-specific *NRG1* mutants

(Riethmacher et al., 1997; Woldeyesus et al., 1999; Morris et al., 1999; Wolpowitz et al., 2000). Histological analyses demonstrated that the lung alveoli of *NRG1β/β* newborns did not expand, i.e. they did not breathe, with the lack of oxygen accounting for the cyanotic body color.

RT-PCR (Fig. 5d) performed on RNA isolated from *NRG1β/β* embryos demonstrated that the transcripts containing exon 8 carried the expected sequence alteration, i.e. an *Eco*RI restriction site, which is linked to the stop codon that interferes with the production of the NRG1 β-isoforms. In heterozygous or homozygous mutant embryos a decreased amount of the PCR product that contains such an *Eco*RI site was observed, i.e. reduced amounts of mRNA of the mutant NRG1 β-isoforms (Fig. 5d, see also above for the reduction in amount of the mRNA of the mutant NRG1 α-isoforms). This might again reflect a destabilization of the mutant transcripts by nonsense-mediated decay (reviewed by Culbertson, 1999; Hentze and Kulozik, 1999). In contrast, transcripts containing exon 7 that encode the α-isoforms were observed at normal levels in *NRG1β/β* mutant embryos. Therefore, only the isoforms that contain the β-variant of the EGF-like domain (type Iβ, type II and type III Neuregulin-1) are lacking in these mutant embryos.

NRG1-null mutants died at E10.5 due to a heart defect. In such embryos, the trabecules of the heart ventricle did not form and the walls of the ventricles were thinned (Fig. 7c, compare to control in 7a). In contrast, *NRG1β/β* mutants survived longer. Histological analysis demonstrated that the heart ventricles of *NRG1β/β* mutants at E10.5 contained trabecules, although they were less well developed than those of control embryos. In addition, the thickness of the ventricular wall was comparable to that of control embryos (Fig. 7b). At E18.5, the heart of *NRG1β/β* embryos appeared normal in histological appearance, and the ventricle and ventricular trabecules were well developed (Fig. 7e; compare to control in 7d). Previous work demonstrated that type I Neuregulin-1 is expressed in the endocardium, and signals to the myocardium that expresses the ErbB2/ErbB4 receptor heteromer (Lemke, 1996). The expression of type Iα NRG1 in the endocardium was therefore able to rescue in part the heart defect observed in the *NRG1-null* mutant embryos, enabling *NRG1β/β* mutants to survive to

birth. Furthermore, embryos with *NRG1β/NRG1-null* genotype died at E10.5 showing that the amount of α-isoform produced by the developing heart can be limiting for development. Thus, the expression of the α-isoform from a single gene copy is not sufficient for a rescue.

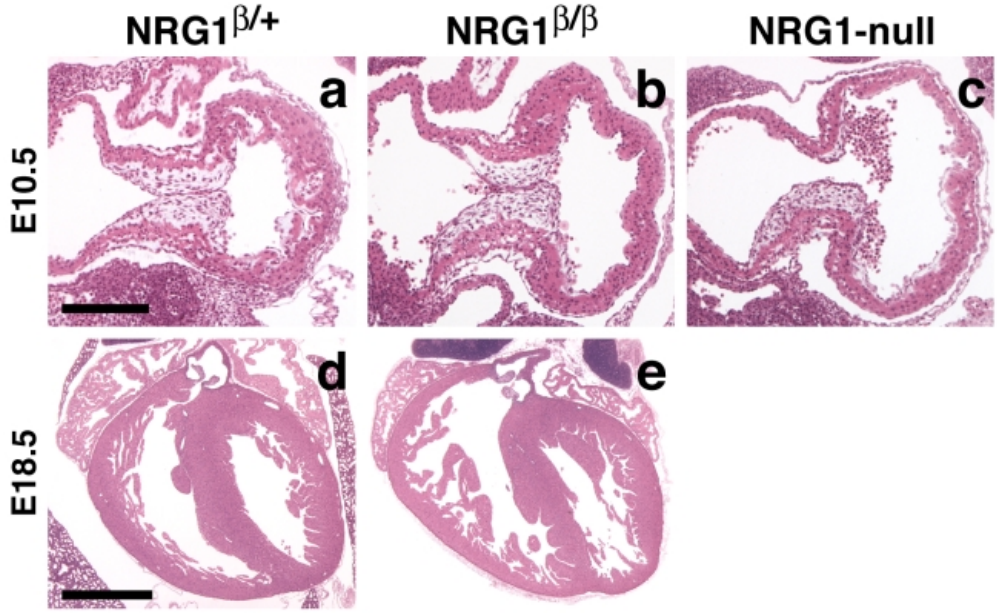

Figure 7. NRG1 α-isoform rescues *NRG1β/β* mutants from the heart trabeculation defect seen in *NRG1-null* mutants
(a-c) Hematoxylin/eosin stained heart sections of control (a), *NRG1β/β* (b) and *NRG1-null* (c) embryos at E10.5. Note the presence of compact trabecules in the ventricle of the *NRG1β/β* mutants, compared with the *NRG1-null* mutants, which entirely lacks trabecules. **(d, e)** Hematoxylin/eosin stained sections of control (d) and *NRG1β/β* mutant (e) embryo hearts at E18.5, indicate that the ventricle and trabecules are well developed in *NRG1β/β* mutants. *NRG1-null* mutants die at E10.5 and are therefore not available for analysis at later stages. Bars: (a-c) 250μm; (d, e) 1mm.

3.5. The functions of the NRG1β isoforms in the neural crest and glial cell lineages

Neuregulin-1 signals are essential for migration and growth of neural crest and glial cells of the peripheral nervous system, respectively. These cells respond to NRG1 signals with heteromeric ErbB2/ErbB3 receptors. The histological analysis of *NRG1β/β* mutants revealed that they displayed the same neural crest phenotypes as null mutants of *NRG1*, *ErbB2* or *ErbB3*. Thus, Neuregulin-1 isoforms containing the α-variant of the EGF-domain, which were present in *NRG1β/β* mutants, are not sufficient for the normal development of neural crest and glial cells of the peripheral nervous system.

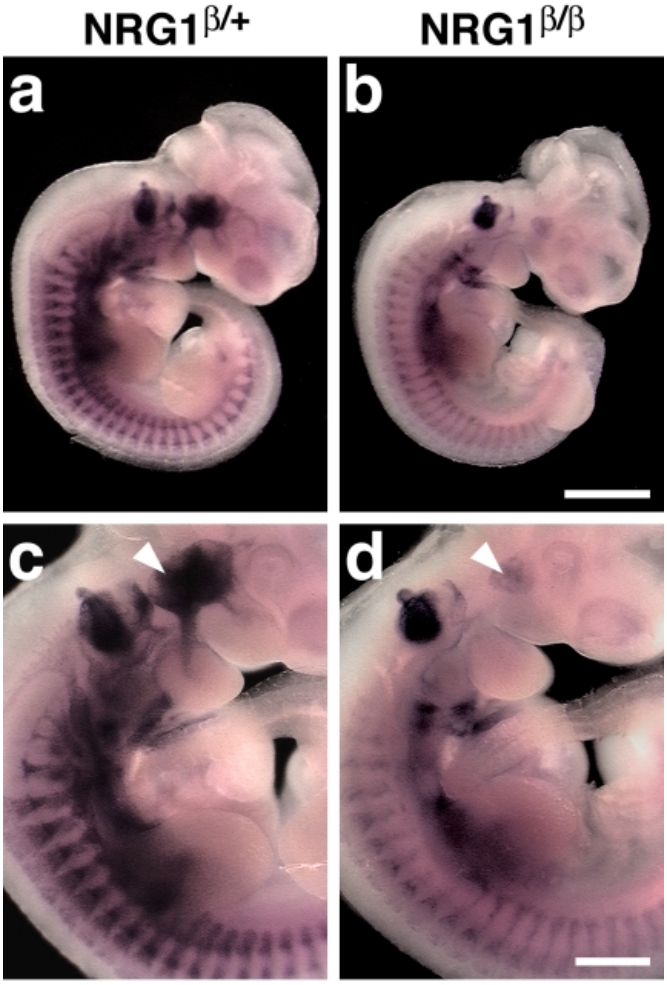

Figure 8. Defective development of neural crest cells in *NRG1β/β* mutants
Whole mount *in situ* hybridization of control (a, c) and *NRG1β/β* (b, d) E10.5 embryos using an *ErbB3*-specific probe to visualize neural crest cells and their derivatives. Note that the numbers of *ErbB3*-expressing neural crest cells in the mutant embryos are dramatically reduced in cranial ganglia, e.g. the trigeminal ganglion (arrowheads), and also along the axon projections in the trunk. Bars: (a, b) 1mm; (c, d) 500µm.

Cranial sensory ganglia derive from neural crest cells that migrate from the hindbrain. In addition, the ectodermal placodes contribute also to these ganglia. While both placodal and neural crest cells generate sensory neurons in cranial ganglia, all glial cells associated with these ganglia derive from the neural crest (Le Douarin and Kalcheim, 1999). As revealed by whole mount *in situ* hybridization, at E10.5 the numbers of *ErbB3*-expressing neural crest cells in cranial ganglia of *NRG1β/β* mutants were dramatically reduced compared to control embryos (Fig. 8). Furthermore, immunohistochemical analysis with anti-NF160 antibodies, that recognize

specifically neurofilament protein, revealed a severely altered morphology of cranial ganglia in *NRG1β/β* mutants (Fig. 9). In particular, those neurons generated by the neural crest were lacking (cf. Meyer and Birchmeier, 1995). Thus, both neural crest derived neurons and glia of cranial ganglia were affected in *NRG1β/β* mutants. This is similar, if not identical to the phenotype previously observed in *NRG1*, *ErbB3* and *ErbB2R* mutant embryos.

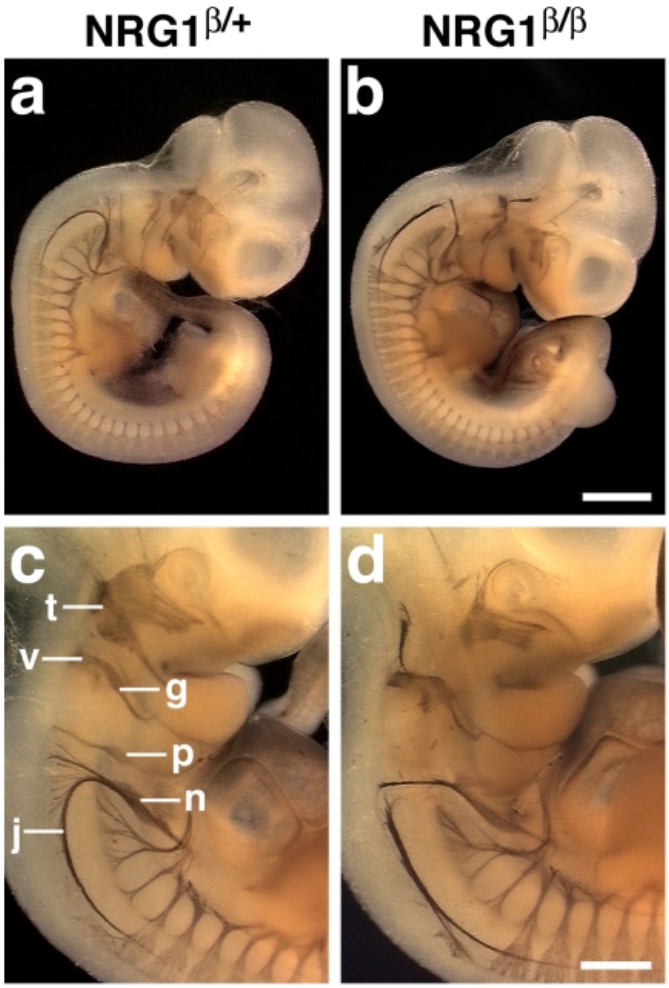

Figure 9. Aberrant morphology of cranial ganglia in *NRG1β/β* mutants
Whole mount immunohistological staining of control (a, c) and *NRG1β/β* mutant (b, d) E10.5 embryos using anti-neurofilament (NF160) antibodies. Note the severe alterations in morphology of cranial nerves in *NRG1β/β* mutants. Cranial ganglia sensory neurons derived from neural crest cells are lacking in these mutants, resulting in a reduction in size of some cranial ganglia, which is particularly pronounced in the trigeminal ganglion (t) that contains a large proportion of neural crest derived neurons. Other cranial ganglia (v, vestibulocochlear; g, geniculate; p, petrosal; n, nodose; j, jugular) are also indicated. Bars: (a, b) 1mm; (c, d) 500µm.

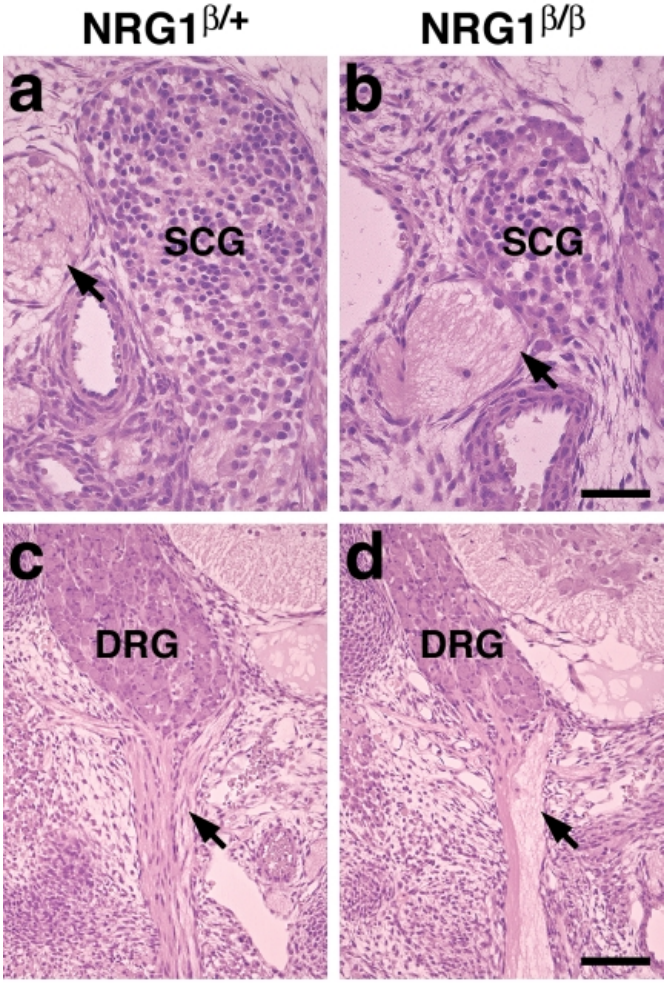

Figure 10. Lack of neural crest contribution to sympathetic ganglia and absence of Schwann cell precursors in the spinal nerves of *NRG1β/β* mutants
Histological analysis of control (a, c) and *NRG1β/β* (b, d) embryos at E14.5. **(a, b)** Hematoxylin/eosin stained section of the superior cervical ganglion (SCG), a sympathetic ganglion produced by neural crest cells from the hindbrain. Note the reduced size of the SCG in the mutants. In addition, the vagus nerve (arrow) contains fewer Schwann cell precursors in the mutants. **(c, d)** Transverse sections through the trunk, showing dorsal root ganglia (DRG), spinal nerves, and ventral spinal cord. Note the reduced size of the dorsal root ganglia, and the reduced numbers of nuclei of Schwann cell precursors in the spinal nerves (arrow) in *NRG1β/β* mutants. Bars: (a, b) 50µm; (c, d) 100µm.

The sympathetic nervous system develops from neural crest cells. Sympathogenic neural crest cells migrate from the neural tube along the medial pathway to the mesenchyme lateral of the dorsal aorta. There they form the primary sympathetic ganglion chain, i.e. neurons and glia of the sympathetic nervous system of the trunk. *In situ* hybridization with *ErbB3* as a probe showed that the numbers of neural crest cells along this path and in the mesenchyme lateral of

the aorta were strongly reduced in *NRG1β/β* mutants (data not shown). Histological analysis indicated that the primary sympathetic ganglion chain in the trunk and the chromaffin cells of the adrenal medulla that derive from the primary ganglion chain were absent in *NRG1β/β* mutants at E14.5 (data not shown). More anterior sympathetic ganglia that derive from hindbrain neural crest cells, for instance the superior cervical ganglion (SCG), were present but reduced in size (indicated in Fig. 10a, b). The β-isoform of Neuregulin-1, which has high affinity for the ErbB2/ErbB3 heteromer, is therefore essential for the development of the sympathetic nervous system (c.f. Britsch et al., 1998).

The type III isoform of NRG1 is expressed by sensory and motor neurons (Yang et al., 1998; Bermingham-McDonogh et al., 1997). The protein product is incorporated into the axon membrane and provides a crucial signal for the development of the Schwann cell lineage (Meyer and Birchmeier, 1995; Meyer et al., 1997; Wolpowitz et al., 2000). In *NRG1β/β* embryos at E10.5, the numbers of neural crest cells that migrate along the developing axon tracts were severely reduced. At subsequent stages (E14.5), histological analyses demonstrated a lack of Schwann cell precursors along the spinal nerves in *NRG1β/β* mutant mice (arrows in Fig. 10). In addition, a degeneration of the sensory neurons was apparent at late developmental stages in the mutant embryos. Dorsal root ganglia (DRG), which appeared normal in size at E10.5, were significantly smaller at E14.5 (indicated in Fig. 10c, d). A similar degeneration of sensory neurons, the consequence of the absence of Schwann cell precursors, was observed previously in *ErbB3* and *ErbB2R* mutant embryos (Riethmacher et al., 1997; Woldeyesus et al., 1999).

3.6. NRG1β is important for the development of the olfactory system

The type III isoform of NRG1 is also expressed in the olfactory system, as assessed by *in situ* hybridization using a type III isoform-specific probe, *SMDF*, on a sagittal section (Fig. 11a). The hybridization signal is associated with cells that line the base of the olfactory epithelium, where olfactory sensory neurons are located (Fig. 11c). On the other hand, the NRG1 receptor, ErbB3 is also expressed in the olfactory system (Fig. 11b). These *ErbB3*-expressing cells localize to the surface of the epithelium, and correspond therefore to the support cells (Fig. 11d).

Furthermore, the olfactory glial cells that ensheath the olfactory axons and accompany the olfactory nerve, express *ErbB3*. These *ErbB3*-expressing cells can be observed along the entire tracts of olfactory axons from the olfactory epithelium to the olfactory bulb (arrow in Fig. 11b) and in the olfactory nerve layer, the outermost layer of the olfactory bulb (arrowhead in Fig. 11b).

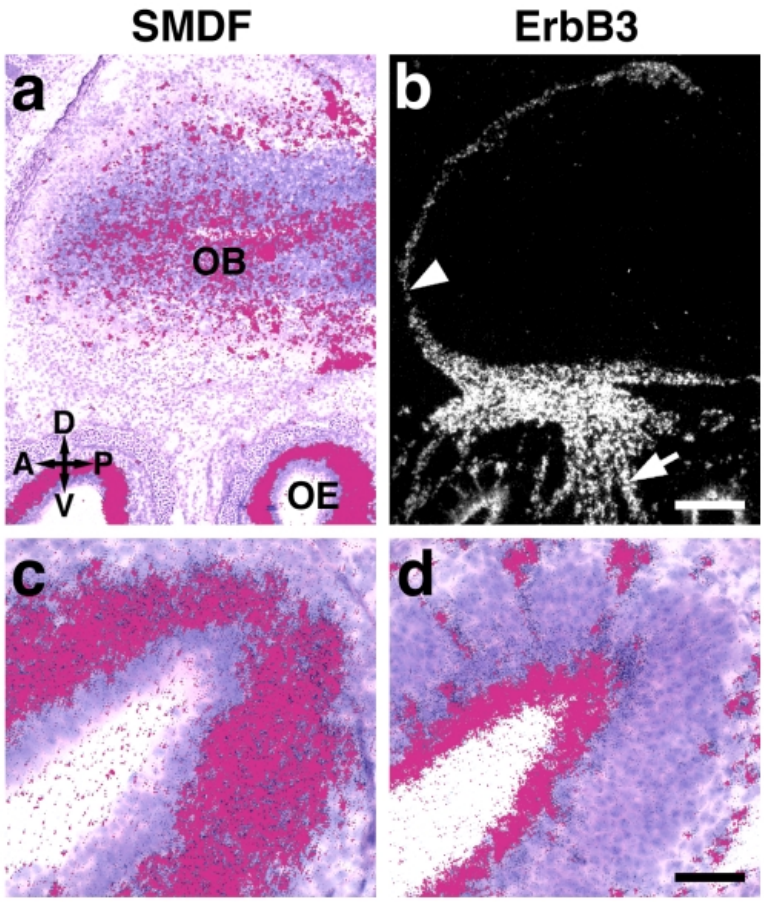

Figure 11. Expression of *type III NRG1* and *ErbB3* in the developing olfactory system
In situ hybridization using *type III NRG1* (*SMDF*) (a, c) and *ErbB3* (b, d) specific probes on sagittal sections of E18.5 embryos. **(a)** Overlay picture of an *in situ* hybridization (false color, magenta, to visualize the silver grains) and the corresponding bright-field section stained with hematoxylin/eosin, showing the presence of *type III NRG1* transcripts in the olfactory epithelium (OE) and in the olfactory bulb (OB). **(b)** Dark-field *in situ* image shows that *ErbB3* transcripts are present in the olfactory epithelium and the olfactory bulb. Cells that express *ErbB3* also accompany the axon projections of olfactory sensory neurons from the olfactory epithelium to the olfactory bulb (arrow) and are present in the outermost layer, the olfactory nerve layer of the olfactory bulb (arrowhead). **(c)** Higher magnification of the olfactory epithelium in (a). T*ype III NRG1* transcripts are present in the base of the olfactory epithelium, where olfactory sensory neurons are located. **(d)** In contrast, *ErbB3* transcripts locate to the surface of the olfactory epithelium, where support cells are present. Bars: (a, b) 200µm; (c, d) 50µm.

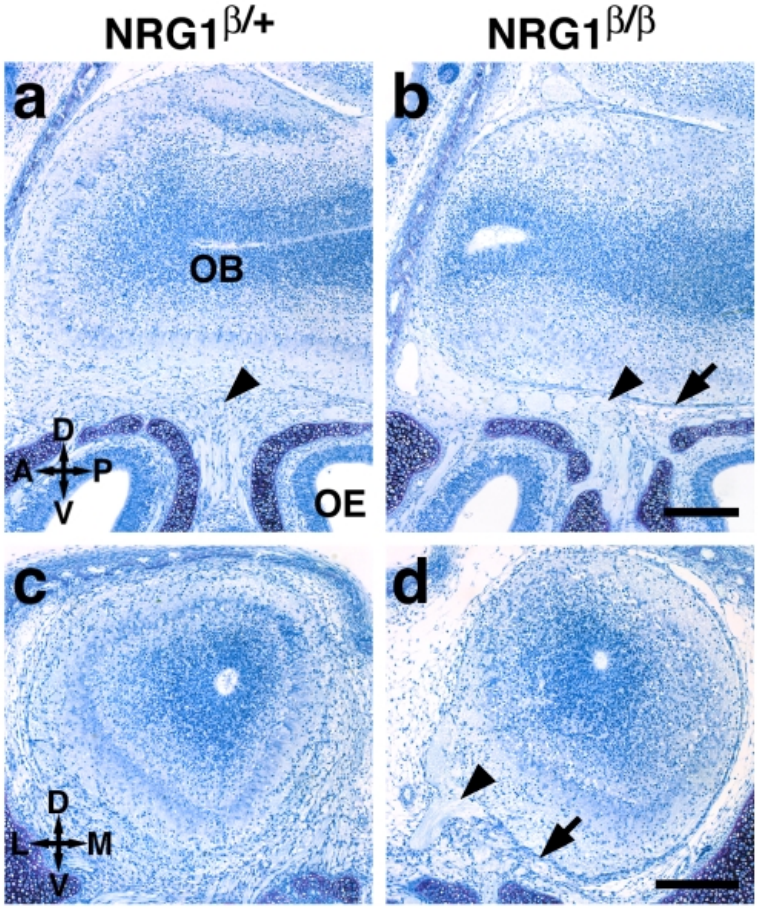

Figure 12. Histological analysis of the olfactory system of *NRG1β/β* mutants
Nissl-stained semi thin sections through the olfactory system of *NRG1β/+* (a, c) and *NRG1β/β* (b, d) embryos at E18.5. **(a, b)** Sagittal sections are shown with anterior to the left and posterior to the right (A, anterior; P, posterior; D, dorsal; V, ventral). **(c, d)** Mirror images of coronal sections present the control (c) and mutant (d) olfactory bulbs, respectively (L, lateral; M, medial; D, dorsal; V, ventral). Olfactory nerves of the *NRG1β/β* mutants contained fewer nuclei than controls (arrowheads), indicating that the development of olfactory glial cells is impaired. In addition, the outermost layer of the olfactory bulb is aberrant and the meningeal membrane is prominent (i.e. not fragmented) in the ventrolateral aspect of the olfactory bulb in *NRG1β/β* mutants (arrows). Bars: (a-d) 250µm.

Analysis of *NRG1β/β* mutants demonstrated that Neuregulin-1 is important for the development of the olfactory system, a phenotype compatible with the expression pattern. Histological analysis at E18.5 embryos of *NRG1β/β* mutant revealed an abnormal olfactory system (Fig. 12b for sagittal view and Fig. 12d for coronal view). Compared to their heterozygous littermates, reduced numbers of olfactory glial cells along the olfactory axon tracts were apparent in homozygous *NRG1β/β* mutants (arrowheads in Fig. 12). Although the mitral cell layer and deeper layers of the olfactory bulb were present, the superficial olfactory nerve layer appeared

disturbed. Moreover, the meningeal membrane between the olfactory bulb and surrounding mesenchymal tissue was abnormal. During development, the meningeal membrane in the entry zone of olfactory axons starts to be fragmented as soon as olfactory axons and accompanying glial cells grow into the olfactory bulb, and is hardly distinguishable on histological sections at E18.5 in control embryos (Fig. 12a, c). However, the meningeal membrane in *NRG1β/β* mutants was clearly visible as a barrier that separates the olfactory bulb from the surrounding mesenchymal tissue, particularly in the ventrolateral aspect of the olfactory bulb where axons apparently failed to enter the olfactory bulb in these mutants (arrows in Fig. 12b, d). The entry zone of olfactory axons appears thus to be restricted to a ventromedial position of the bulb in *NRG1β/β* mutants.

3.7. NRG1β is essential for the development of olfactory glial cells

Olfactory glial cells develop from the olfactory placode, and have thus a distinct developmental origin from Schwann cells, that derive from the neural crest. However, the two cell types share many features, and express also a similar set of genes. During the course of this study, the expression of *ErbB3*, *Sox10* and also *BFABP* (Brain Fatty Acid Binding Protein) were found in developing olfactory glia. All three genes are also expressed in the developing Schwann cell lineage. These markers were used to assess further the effect of the *NRG1β/β* mutation on the development of olfactory glial cells.

In control embryos at E18.5, *ErbB3*- and *Sox10*-expressing olfactory glia accompany olfactory axons along their trajectories from the olfactory epithelium to the olfactory bulb (arrows in Fig. 13a, c) and fill the olfactory nerve layer (arrowheads in Fig. 13a, c; see also Fig. 11b for sagittal view). However, in *NRG1β/β* mutant embryos, the numbers of *ErbB3*- or *Sox10*-expressing cells were significantly reduced, and only few such cells could be observed between the olfactory epithelium and the olfactory bulb, or in the ventromedial aspect of the olfactory nerve layer (arrowheads in Fig. 13b, d). In control embryos at E12.5, olfactory axons reach the olfactory bulb primodium ventromedially (arrows in Fig. 14a) and extend dorsocaudally along the external surface of the developing bulb (arrowheads in Fig. 14a); the

axons are accompanied by BFABP-positive glial progenitors, which are present throughout the entire axon tract (arrows in Fig. 14a; 14c) and in superficial layer of the developing bulb (arrowheads in Fig. 14a; 14c). In contrast, in *NRG1β/β* mutant embryos, no BFABP-positive glial progenitors were present within the axon tracts (arrows in Fig. 14b; 14d) or in the superficial layer of developing bulb (arrowheads in Fig. 14b; 14d). A few remaining BFABP-positive cells located to the outside of the fascicles (arrows in Fig. 14b; 14d).

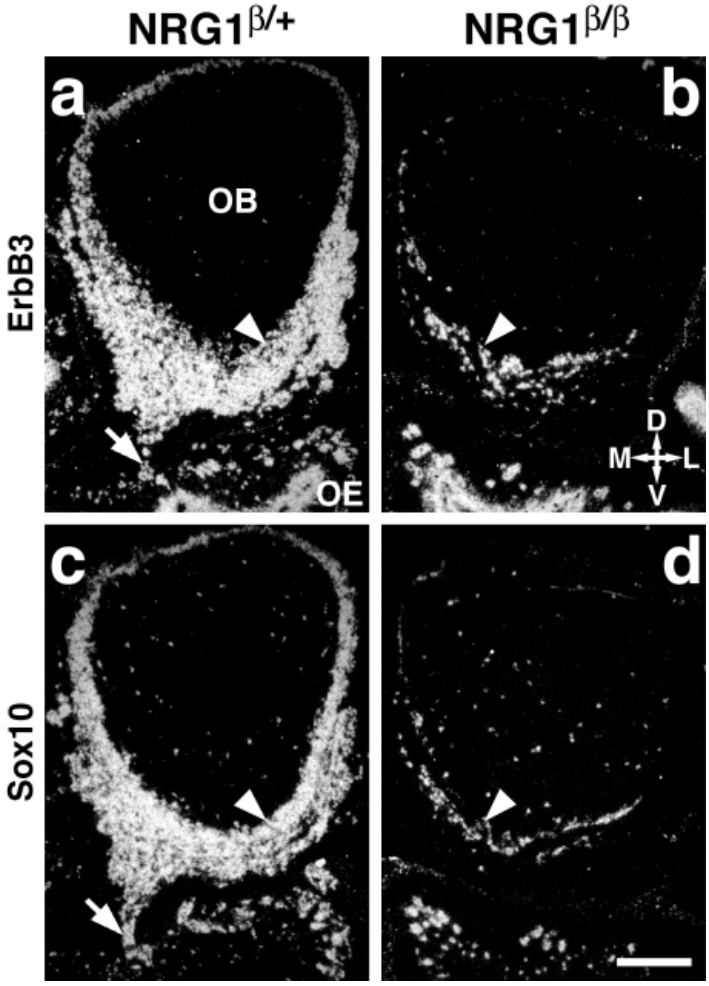

Figure 13. Impaired development of olfactory glia in *NRG1β/β* embryos at E18.5
Dark-field images of *in situ* hybridizations using *ErbB3* (a, b) and *Sox10* (c, d) specific probes on coronal sections of E18.5 *NRG1β/+* (a, c) and *NRG1β/β* embryos (b, d). In *NRG1β/β* mutant embryos, the numbers of *ErbB3*- or *Sox10*-expressing cells are significantly reduced along the axon tracts of olfactory sensory neurons from the olfactory epithelium to the olfactory bulb (arrow). This reduction is particularly pronounced in the olfactory nerve layer, the outermost layer of the olfactory bulb, where only few *ErbB3*- or *Sox10*-expressing cells remain in the ventromedial aspect of the olfactory bulb (arrowheads). (Mirror images, the orientation shown is for mutant column. L, lateral; M, medial; D, dorsal; V, ventral). Bar: (a-d) 250μm.

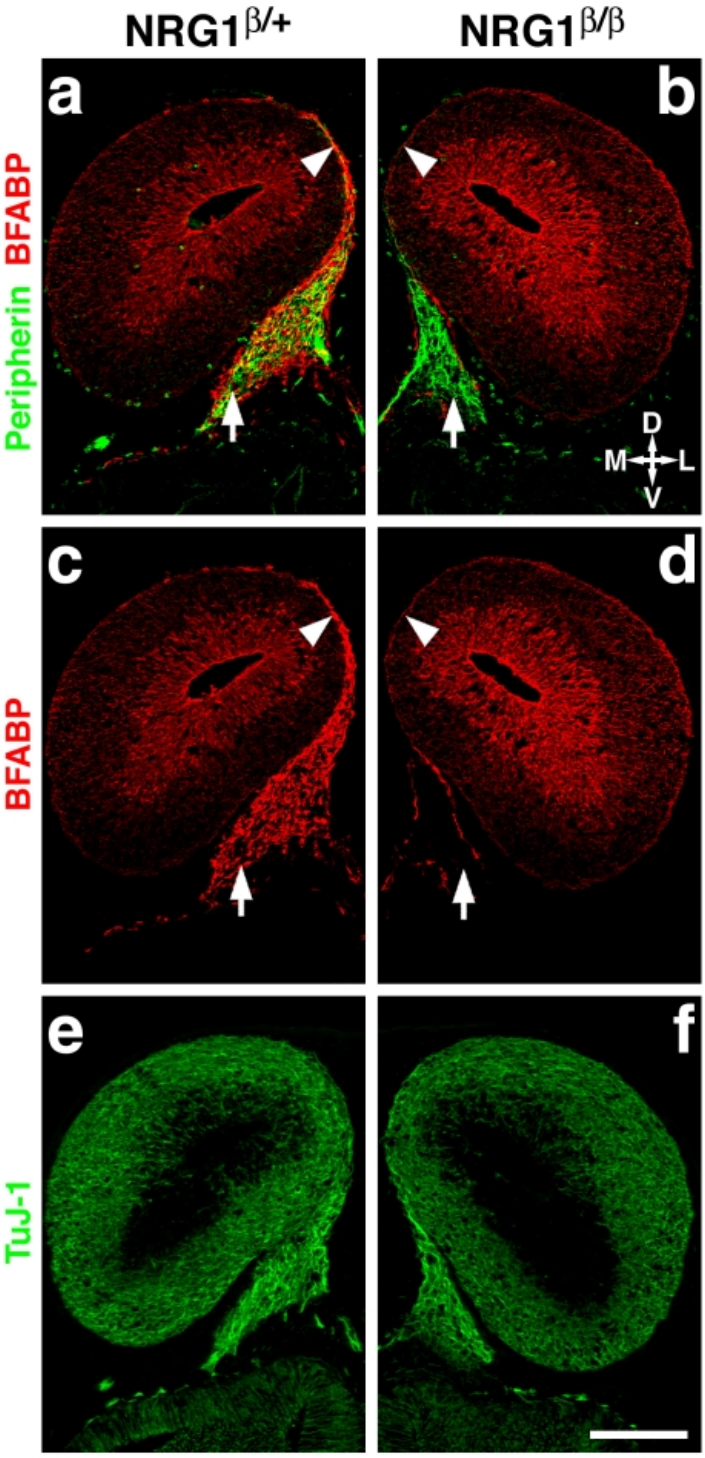

Figure 14. Impaired development of olfactory glia in *NRG1β/β* embryos at E12.5
Immunohistological analysis on transverse sections of *NRG1β/+* (a, c, e) and *NRG1β/β* (b, d, f) embryos at E12.5 using the following antibodies: (a, b) anti-peripherin (green) and anti-BFABP (red); (c, d) anti-BFABP (red); (c, d) TuJ-1 (anti-βIII tubulin) (green). At E12.5, olfactory axons and accompanying BFABP-positive glial progenitors reach the olfactory bulb primordium ventromedially (arrows in a, c) and extend dorsocaudally along the external surface of the developing bulb (arrowheads in a, c). In contrast, in *NRG1β/β* mutants, no BFABP-positive glial progenitors are present within the axon tract (arrows in b, d), nor in the superficial layer of the developing bulb (arrowheads in b, d). A few remaining BFABP-positive cells are located to the outside of the olfactory axon fascicles (arrows in b, d). However, in the *NRG1β/β* mutants, both olfactory sensory neurons in the olfactory epithelium and olfactory axon trajectories appear normal at this stage (f, and also anti-peripherin staining in b), although the region where olfactory axons contact the bulb primordium is narrowed. (Mirror images, the orientation shown is for mutant column.) Bar: (a-f) 200µm.

Similarly, *ErbB3*-, *Sox10*-expressing and BFABP-positive glial progenitors can already be detected along olfactory axon tracts at E11 in control embryos; their numbers were reduced in *NRG1β/β* mutant embryos, even at this early stage (not shown). In order to investigate the effect of the *NRG1β* mutation on proliferation and apoptosis rates of olfactory glia progenitors, BrdU was injected into pregnant mice, and the embryos were isolated 2hrs after injection. Anti-Sox10 antibodies were used to identify the progenitors, and anti-BrdU antibodies to assess the number of proliferating glial progenitors, i.e. cells that had incorporated BrdU into their DNA. In mutant embryos at E11, the proliferation rate of remaining glial progenitor cells was reduced by 31% compared to controls (BrdU incorporation in Sox10-positive cells: control, 40.8%; mutant, 28.0%). In addition, apoptotic glial progenitor cells were identified using TUNEL staining. Apoptosis was almost 5-fold increased in the glial cells along the axon tracts in the mutant embryos (TUNEL-positive nuclei coinciding with Sox10-immunofluorescence: control, 5.9%, mutant, 28.7%). Therefore, the severe effect on the development of olfactory glia in the *NRG1β/β* mutants results from reduced proliferation and increased apoptosis. Moreover, *ErbB2R* and *ErbB3* mutants also displayed a similarly severe reduction in the numbers of developing olfactory glial cells (c.f. Fig. 15 and data not shown), indicating that these cells use an ErbB2/ErbB3 heteromer to receive the Neuregulin-1β signal.

3.8 Olfactory axons project aberrantly in *NRG1β* mutant embryos

Olfactory neurons and their axon projections can be detected with TuJ1 (anti-βIII tubulin) antibodies at E12.5 (Fig. 14e, f). Normally, several small fascicles of olfactory axons coalesce in the mesenchyme near the ventral olfactory bulb and contact the olfactory bulb. In the *NRG1β/β* mutant, both olfactory sensory neurons in the olfactory epithelium and olfactory axon trajectories appeared normal at this stage. However, the region where olfactory axons contact the bulb primordium was narrowed in the *NRG1β/β* mutants (Fig. 14f; compare to control in 14e). This could also be observed when anti-Peripherin antibodies were used for visualizing the olfactory axons (Fig. 14a, b).

Olfactory marker protein (OMP) is an abundant cytoplasmic protein present in the cell bodies and the axons of maturing olfactory sensory neurons, which can be detected at E14.5 and later stages in mice (Baker et al., 1989; Farbman and Margolis, 1980). Using anti-OMP and anti-BFABP antibodies for a double staining, olfactory axons and olfactory glial cells can be visualized simultaneously (Fig. 15a-d). In control embryos, olfactory axons and glial cells penetrate the cribriform plate and the meningeal membrane, forming the olfactory nerve layer (arrowhead in Fig. 15a). In *NRG1β/β, ErbB3-/-* and *ErbB2R-/-* mutant embryos, the olfactory axon projections appeared disrupted (Fig. 15b-d). Again, the axon entry zone was observed to be narrower than in control embryos. Moreover, fewer axons were found in the dorsal olfactory bulb in these mutants, demonstrating that the olfactory nerve layer was not fully formed. In addition, olfactory axons appeared to enter deeper layers of the olfactory bulb in the mutants, which is not seen in control littermates (arrows in Fig. 15b-d).

Anti-GABA antibodies can be used to visualize the GABAergic interneurons of the olfactory bulb, the periglomerular cells and the granular cells, which are arranged in two distinct cell layers. With anti-OMP and anti-GABA double labeling, the defective olfactory axon projections inside the olfactory bulb could be visualized more clearly in *NRG1β/β* mutants. Olfactory axon projections in the *NRG1β/β* mutants reached the deep granular cell layer (arrow in Fig. 15f), whereas olfactory axons in control embryos are never detected in this cell layer (Fig. 15e).

3.9. Distributions of other major cell types in the olfactory bulb of *NRG1β* mutants.

To investigate the changes in the olfactory bulb further, other cell types present in this structure were also analyzed. The mitral cells that locate in the mitral cell layer represent the major targets of olfactory axons, and express *Reelin* (Fig. 16a, b). Periglomerular cells in the glomerular cell layer and granular cells in the granular cell layer express tyrosine hydroxylase (TH) (Fig. 16c, d). These major neuronal cell types of the olfactory bulb were present and arranged in characteristically ordered layers in *NRG1β/β* mutants. However, the layers appeared less organized and fewer *Reelin*- and *TH*-expressing cells were observed in the dorsolateral aspect of the olfactory bulb (arrows in Fig. 16).

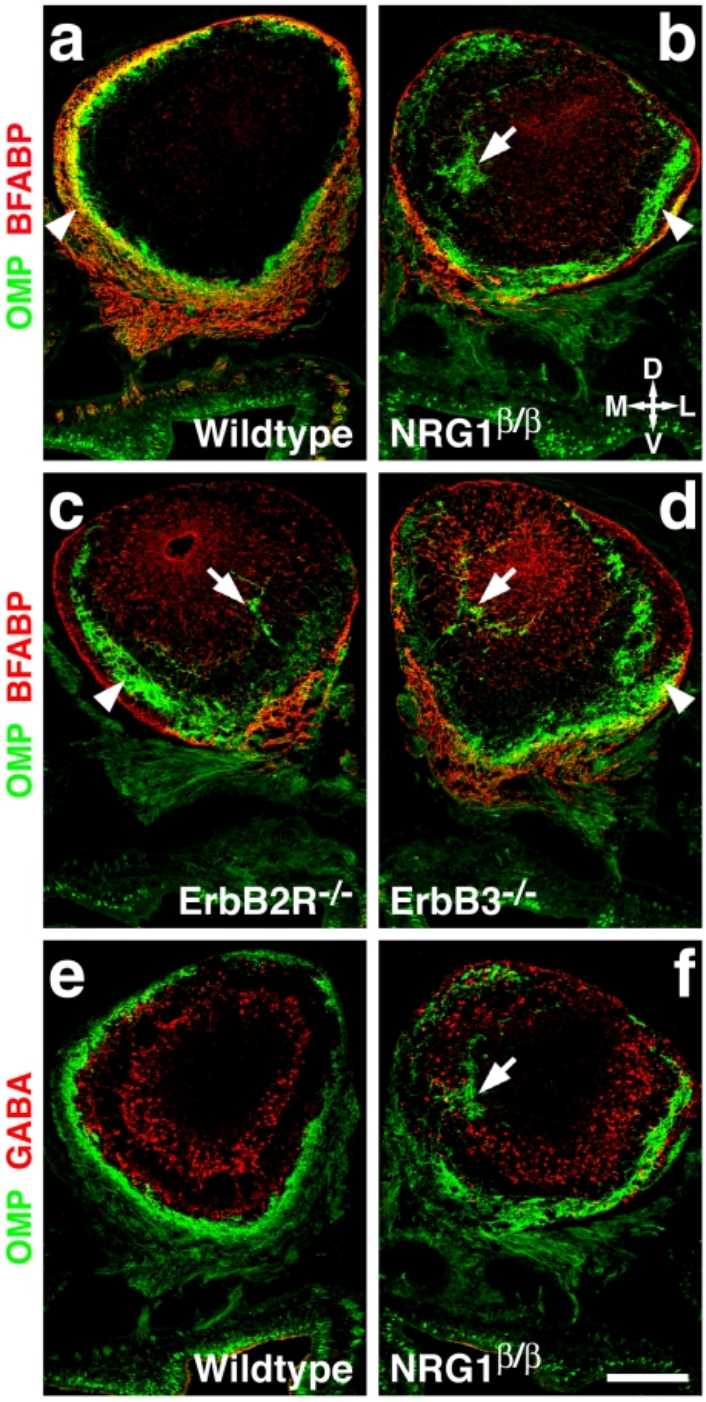

Figure 15. Aberrant olfactory axon projections in *NRG1β/β* mutants
(a-d) Immunohistological analysis on coronal sections of *NRG1β/+* (a), *NRG1β/β* (b), *ErbB2R-/-* (c) and *ErbB3-/-* (d) mutants at E18.5 using anti-OMP antibodies (green) to visualize olfactory sensory neurons and their axon projections, and anti-BFABP antibodies to detect the olfactory glial cells (red). The numbers of olfactory glial cells accompanying the axon tracts from the OE to the OB and in the olfactory nerve layer (arrowheads) are dramatically reduced. The olfactory axon projections are generally disorganized in these mutants and some project into deep layers of the olfactory bulb (arrow), where wildtype olfactory axons are never present. (e, f) Staining using anti-OMP antibodies (green), and anti-GABA antibodies (red) that detect GABAergic periglomerular and granular cells, demonstrates that some olfactory axon projections reach the GABA-expressing granular cell layer in the mutants. (Mirror images) Bar: (a-f) 250µm.

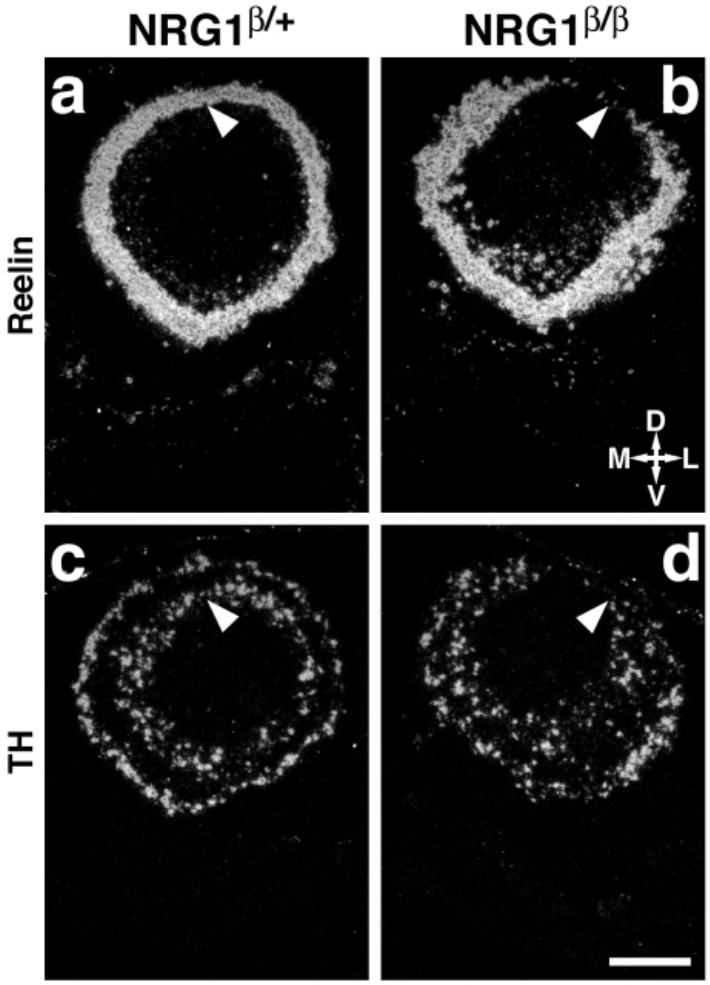

Figure 16. Neuronal cell types in the olfactory bulb of *NRG1β/β* mutants
In situ hybridization analysis on coronal sections of *NRG1β/+* (a, c) and *NRG1β/β* (b, d) embryos at E18.5 using *Reelin*- (a, b) and *TH*- (c, d) specific cDNA probes. *Reelin* marks projection neurons in the mitral cell layer, and *TH* labels GABAergic interneurons in the periglomerular and granular cell layers (see also 15e, f). The *Reelin*- and *TH*-expressing neurons are arranged in layers in controls and *NRG1β/β* mutants. However, the layers appear less organized in *NRG1β/β* mutants and are particularly disrupted in the dorsolateral aspect of the olfactory bulb (arrowheads). (Mirror images) Bar: (a-d) 250µm.

The major glial cell types in the developing olfactory bulb are radial glial cells/astrocytes and oligodendrocyte precursors. Immunohistology with Nestin-specific antibodies was used to visualize radial glia in the olfactory bulb of *NRG1β/β* mutant embryos (Fig. 17a, b). The intensity of Nestin staining is not homogeneous in control mice, and distinct layers can be discerned. In the *NRG1β/β* mutants, this layered arrangement appeared less organized, particularly in the dorsal part. *PDGFR-α* is expressed by oligodendrocyte precursors of the olfactory nervous system (Fig. 17c, d) and also by cells in the meningeal membrane and other

tissues. Compared to controls, no differences in the numbers or the distribution of oligodendrocyte precursors in the olfactory bulb of *NRG1β/β* mutants were detected. However, the meningeal membrane in the mutants was largely intact, reflecting the narrowed entry zone of olfactory axons. The distribution of *Reelin*- and *TH*-expressing neurons, Nestin-positive radial glia and *Sox10*-expressing oligodendrocytes in *ErbB3* mutant embryos resembled what had been observed in *NRG1β/β* mutants (not shown). Therefore, the various cell types in the olfactory bulb that originate from the central nervous system are present in *NRG1β* or *ErbB3* mutant animals, but appear less organized in their layered arrangement.

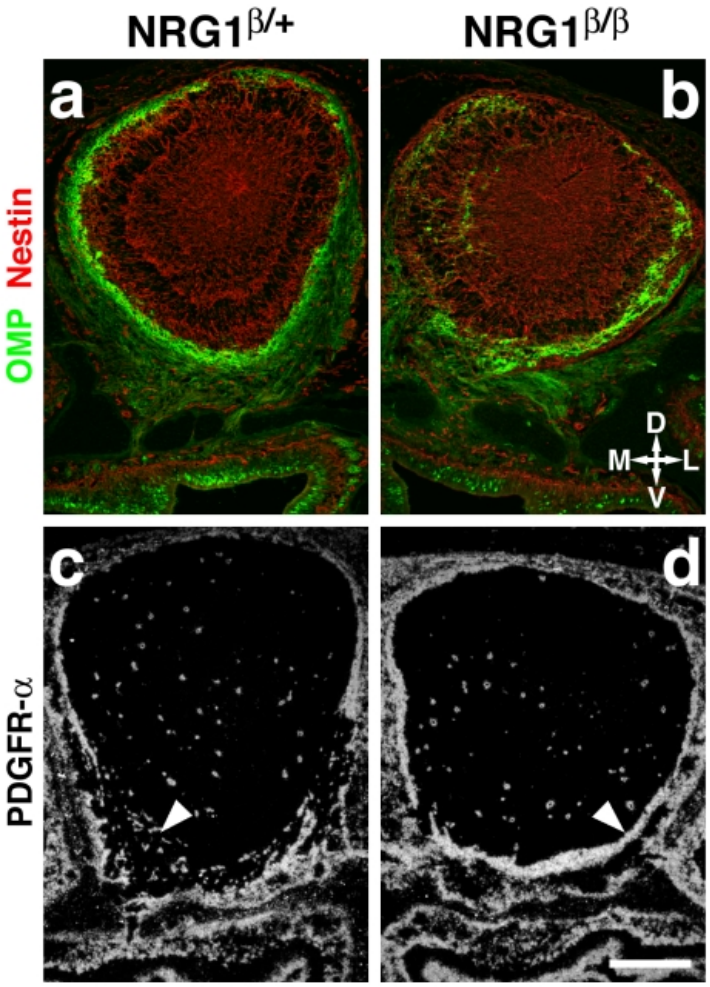

Figure 17. Glial cell types in the olfactory bulb of *NRG1β/β* mutants
Immunohistological analysis on coronal sections of *NRG1β/+* (a, c) and *NRG1β/β* (b, d) embryos at E18.5 using anti-Nestin antibodies (red) to detect radial glia cells (a, b), and *PDGFR-α*-specific *in situ* probe to detect oligodendrocyte precursors (c, d). Note the layered arrangement of Nestin-positive cells appears less organized in the mutants, particularly in the dorsal part of the olfactory bulb. In addition, the *PDGFR-α* positive meningeal membrane remains intact in the ventrolateral aspect of the mutant bulb (arrowheads) and only a small axon entry zone presents ventromedially. However, no changes are detected in the numbers or the distribution of *PDGFR-α* positive oligodendrocyte precursors within the olfactory bulb. (Mirror images) Bar: (a-d) 250µm.

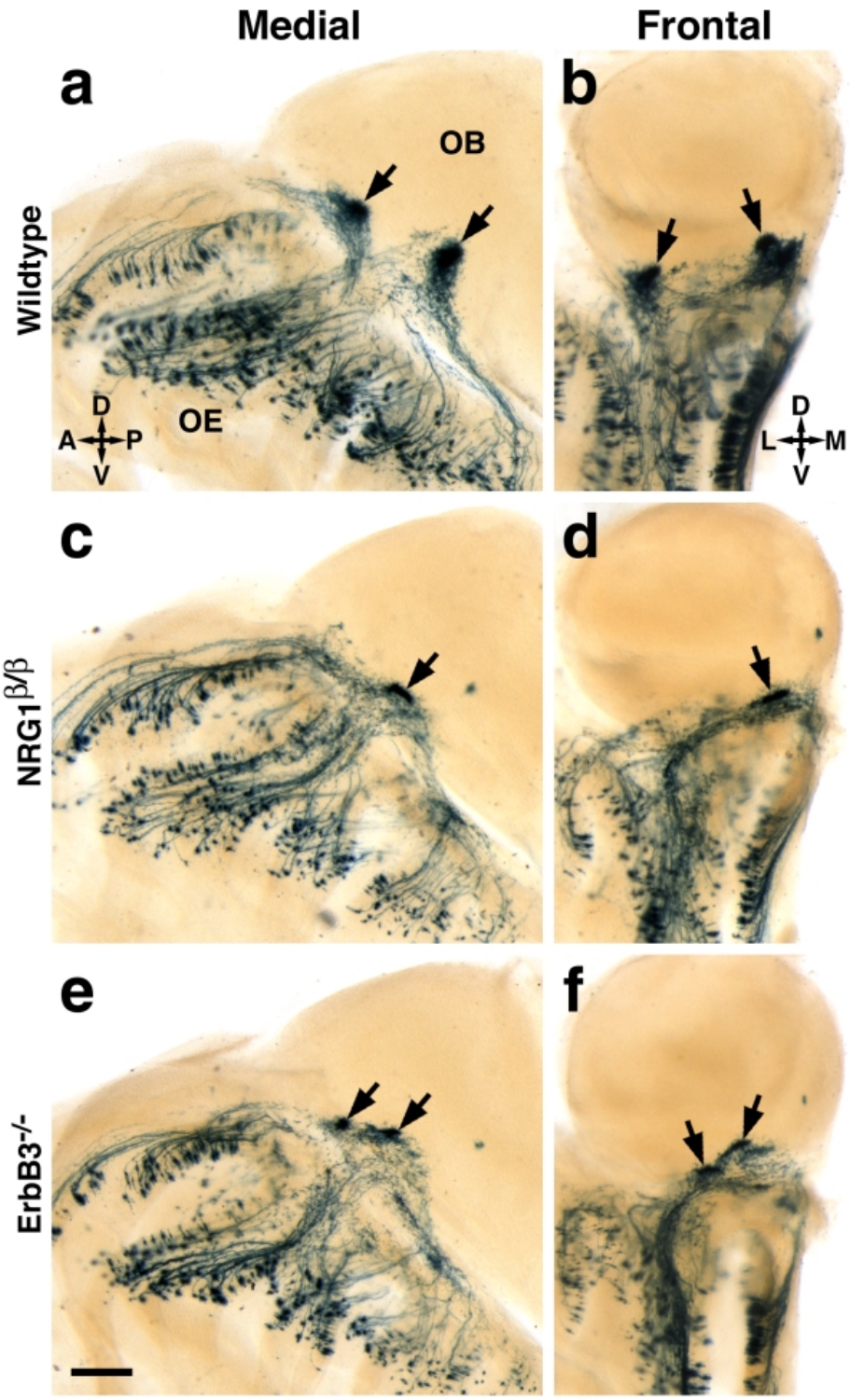

Figure 18. Aberrant axon projections of *P2*-expressing olfactory sensory neurons in *NRG1β/β* and *ErbB3*-/- mutants

The *P2-IRES-tau-lacZ* indicator allele was crossed into wildtype (a, b), *NRG1β/β* (c, d) and *ErbB3*-/- (e, f) embryos, and the whole mounts were stained with Bluo-Gal to visualize the axon projections of *P2*-expressing olfactory sensory neurons. *P2* axons converge onto two glomeruli in control embryos, one locate medially and the other laterally (arrows in a, b). However, in *NRG1β/β* and *ErbB3*-/- mutants, the glomeruli form aberrantly. The *P2*-glomeruli are frequently absent (e.g. only one glomerulus in c, d). Glomeruli that do form are small and located at aberrant positions (e.g. arrows in e, f). Orientations for medial and frontal views are indicated in (a) and (b), respectively (A, anterior, P, posterior, D, dorsal, V, ventral, L, lateral, M, medial). Bar: (a-f) 250µm.

3.10. *P2* and *mOR37A* axon projections are aberrant in *NRG1β* mutants

To investigate further the projections of olfactory axons in *NRG1β* and *ErbB3* mutants, two 'indicator' mouse strains were crossed into these mutant backgrounds. The first carries the *P2-IRES-tau-lacZ* allele (Mombaerts et al., 1996; Royal and Key, 1999), and the second harbors an *IRES-tau-lacZ* insertion in the odorant receptor *mOR37A* locus (Strotmann et al., 2000). These indicator strains permit the direct visualization of *P2*- and m*OR37A*-expressing neurons and their axon projections.

In control animals, the axons of *P2*-expressing neurons converge onto two to four glomeruli located at stereotypical positions in the ventromedial and caudolateral aspects of the olfactory bulb to form medial and lateral glomeruli (arrows in Fig. 18a, b). In *NRG1β* or *ErbB3* mutants, *P2* glomeruli formed in an aberrant manner and were frequently absent. 58% of the bulbs examined had no lateral glomerulus, and 29% had no medial one. The observed glomeruli were reduced in size, and their positions were variable and aberrant (arrows in Fig. 18c-f).

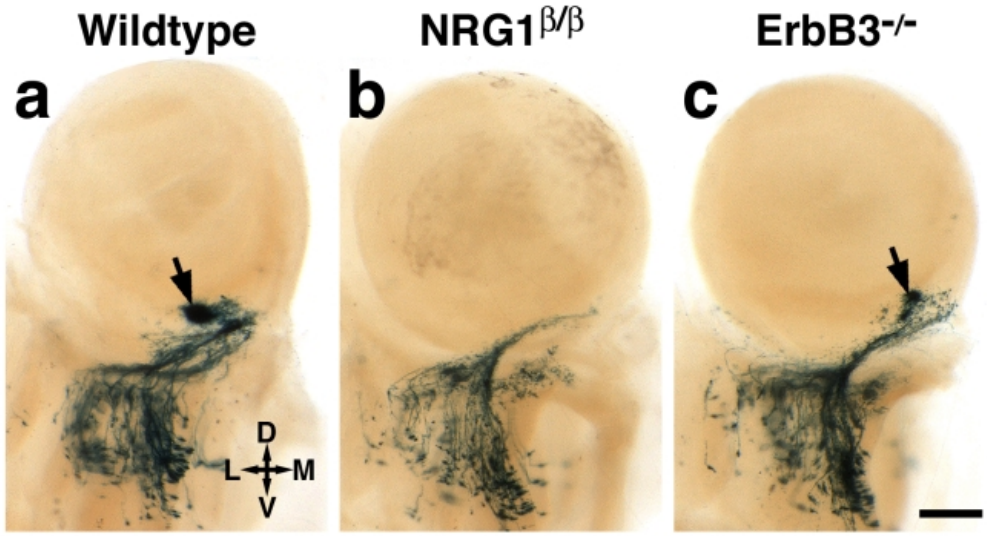

Figure 19. Aberrant axon projections of *mOR37A*-expressing olfactory sensory neurons in *NRG1β/β* and *ErbB3*-/- mutants
The *mOR37A-IRES-tau-lacZ* indicator allele was crossed into wildtype (a), *NRG1β/β* (b) and *ErbB3*-/- (c) embryos and the whole mounts were stained with Bluo-Gal to visualize the axon projections of *mOR37A*-expressing olfactory sensory neurons. Axons of *mOR37A*-expressing neurons converge onto one glomerulus located in the ventral olfactory bulb in controls (arrow in a). However, in *NRG1β/β* and *ErbB3*-/- mutants, *mOR37A*-expressing axons aberrantly wander at the entrance zone of the bulb and do not form discernable glomeruli (b). In some cases, they coalesce with each other in small aggregates that locate in incorrect positions (arrow in c). Bar: (a-c) 250µm.

In control embryos that carry a *mOR37A-IRES-tau-lacZ* allele, β-galactosidase positive *mOR37A* axons converge to one or two glomeruli in the ventral olfactory bulb at E18.5 (arrow in Fig. 19a). In the majority of the olfactory bulbs analyzed, no *mOR37A* glomeruli were observed in *NRG1β* or *ErbB3* mutant embryos (80%, n=10). *mOR37A*-expressing axons aberrantly wander at the entry zone of the bulb rather than forming discernible glomeruli (Fig. 19b). They occasionally coalesce with each other in small aggregates. However, these small aggregates were formed at aberrant positions, located more medially than the glomeruli seen in controls (arrow in Fig. 19c).

3.11. The *ErbB3* mutation affects axon projections in an indirect manner

Compared to control littermates at E18.5, in which *mOR37A*-expression axon projections converge to a glomerulus in the ventral olfactory bulb (arrow in Fig. 20a), the axon projections of both OMP-positive and *mOR37A*-expressing neurons were aberrant in *ErbB3*-/- mutants (arrow in Fig. 20b).

To test whether *ErbB3* is required in a cell-autonomous manner for appropriate axon projections of olfactory neurons, experiments utilizing chimeras were performed. *A mOR37A-IRES-tau-lacZ* allele was introduced into *ErbB3*-/- ES cells by gene targeting. The *ErbB3*-/-//*mOR37A-IRES-tau-lacZ* ES cell line was then used to generate chimeric embryos by injection into wildtype blastocysts. Thus, *mOR37A*-expressing neurons and their axon projections, which were generated by *ErbB3*-/- ES cells could be directly visualized and distinguished in these chimeras. In such chimeras, olfactory glia cells developed normally. A similar result was observed previously for Schwann cells in *ErbB3*-/- chimeric embryos, by which it was demonstrated that only wildtype cells present in the chimera contribute to the Schwann cell compartment (Riethmacher et al., 1997). In contrast to the defective axon projections of olfactory sensory neurons in *ErbB3-/-* mutants, OMP-positive axon projections appeared ordered in these chimeras, and axon projections of *mOR37A*-expressing olfactory sensory neurons converged correctly on 1-2 glomeruli in the ventral olfactory bulb (Fig. 20c). Thus, olfactory neurons do not require *ErbB3* in a cell autonomous manner for their correct

axon projection. The aberrant olfactory axon projections observed in *ErbB3-/-* mutants (Fig. 20b) are thus caused by indirect mechanisms, and presumably due to the absence of the olfactory glia.

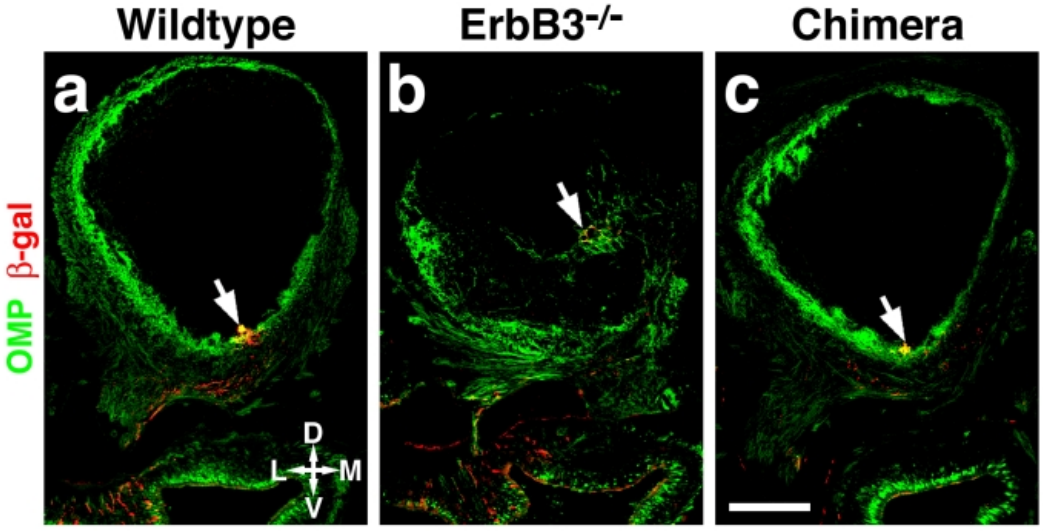

Figure 20. *ErbB3* is not required in a cell autonomous manner for appropriate axon projections of *mOR37A*-expressing olfactory sensory neurons
Coronal sections of E18.5 wildtype (a), *ErbB3*-/- (b), and *ErbB3*-/- : wildtype chimeric embryos (c), carrying a *mOR37A-IRES-tau-lacZ* indicator allele. Axon projections of olfactory sensory neurons were analyzed by immunohistochemistry using antibodies against β-galactosidase (red, marking projections of *mOR37A*-expressing neurons) and OMP (green, all mature olfactory sensory neurons and their axons). In control embryos, olfactory axons converge onto one glomerulus located in the ventral olfactory bulb in control litters (arrow in a). In *ErbB3*-/- mutants, however, the majority of the β-gal-positive axon projections are observed wandering at the medial aspect of axon entry zone and occasionally also penetrating into deeper layers of the olfactory bulb (arrow in b). In chimeric embryos produced by injecting *ErbB3*-/-//*mOR37A-IRES-tau-lacZ* ES cells into wildtype blastocysts, β-gal-positive *mOR37A* axons converge onto one well-developed *mOR37A*-glomerulus, and there are no aberrant OMP-positive axons locate in deep layers of the olfactory bulb. Bar: (a-c) 250μm.

3.12. Sox10 is essential for the development of olfactory glial cells

To investigate a potential role of olfactory glial cells in the projections of olfactory sensory neurons further, I also analyzed *Sox10* mutants that show defects in development of Schwann cell and oligodendrocytes (Britsch et al., 2001; Stolt et al., 2002). It should be noted that *Sox10* is also expressed in olfactory glial cells although the functions of *Sox10* in this type of glia had not been described previously.

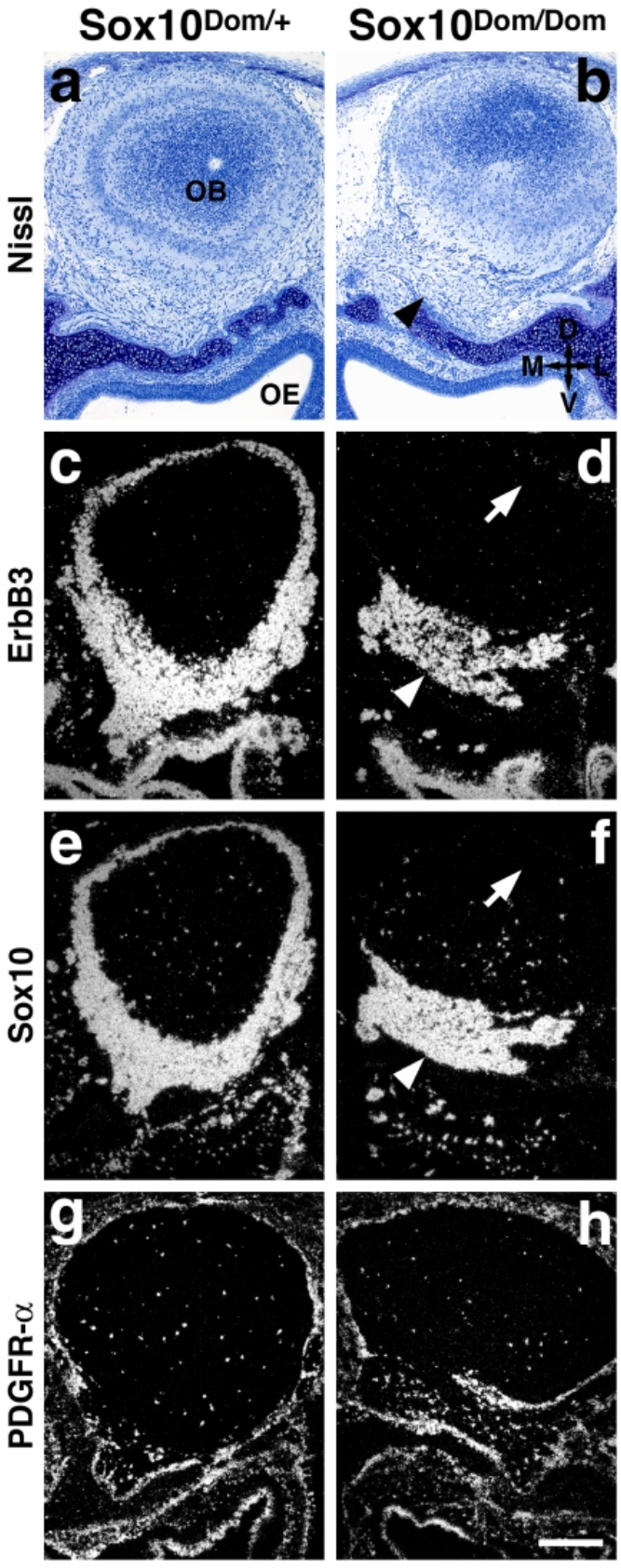

Figure 21. Functions of Sox10 in the development of olfactory glial cells
Analysis of the olfactory system on coronal sections of *Sox10*$^{Dom/+}$ (a, c, e, g) and *Sox10*$^{Dom/Dom}$ (b, d, f, h) embryos using histology (a, b) and *in situ* hybridization with *ErbB3* (c, d), *Sox10* (e, f) and *PDGFR-α* (g, h) specific probes at E18.5. In the *Sox10*$^{Dom/Dom}$ mutants, a large mass of olfactory glial cells is present ventromedially between the cribriform plate and the olfactory bulb, (arrowheads in b, d and f). However, olfactory glial cells along the peripheral olfactory axon trajectories between the olfactory epithelium and the cribriform plate and also in the olfactory nerve layer around the olfactory bulb are absent (arrows in d, f). While there are no changes detected in the numbers or the distribution of oligodendrocyte precursors in the olfactory bulb of *Sox10*$^{Dom/Dom}$ mutants, *PDGFR-α in situ* hybridization reveals an intact *PDGFR-α*-expressing membrane in the ventrolateral aspect of the olfactory bulb, and a narrowed ventromedial axon entry zone in these mutants. (Mirror images) Bar: (a-h) 250µm.

Histological analysis revealed an abnormal olfactory system in *Sox10*$^{Dom/Dom}$ mutants at E18.5 (Fig. 21b, compare to control in 21a). The olfactory bulb was misshaped, and moreover, a narrowed axon entry zone was observed. The outermost layer of the olfactory bulb, the olfactory nerve layer, appeared to be absent. However, olfactory glial cells were detectable in *Sox10* mutants at E18.5, but they were distributed in a highly abnormal manner. In particular, large agglomerations of cells were observed between the cribriform plate and the olfactory bulb (arrowhead in Fig. 21b). It should be noted that Sox10 transcripts are produced from the mutant *Sox10*^{Dom} locus, which however do not encode functional protein. *In situ* hybridizations with *ErbB3*- and *Sox10*-specific probes demonstrated that this large group of cells indeed corresponded to glia (arrowheads in Fig. 21d, f). However, olfactory glia that accompany the nerves between the olfactory epithelium and the cribriform plate were absent, as were olfactory glia in the outermost nerve layer of the olfactory bulb of the *Sox10* mutant mice (arrows in Fig. 21d, f). *Sox10* and *PDGFR-α* mark also oligodendrocytes that start to invade the olfactory bulb on E18.5 (Fig. 21e, g). In *Sox10* mutant embryos, *Sox10*- or *PDGFR-α*-expressing cells were present in the olfactory bulb (Fig. 21f, h). The mutations in *Sox10* and the genes of the Neuregulin-1 signaling system have therefore distinct effects on the development of the olfactory glia. In *Sox10* mutant animals, these cells were present but remain outside of the olfactory bulb. In contrast, in embryos with mutations in the genes of Neuregulin-1 signaling system, the numbers of these cells are severely reduced.

The development of olfactory glia at earlier stages was also investigated in the *Sox10* mutants (Fig. 22). In control litters at E12.5, BFABP-positive olfactory glial progenitors fill the large fascicles of olfactory axons (arrows in Fig. 22a, c) and extend dorsocaudally along the external surface of the developing bulb (arrowhead in Fig. 22a). In *Sox10* mutants, the numbers of BFABP-positive cells associated with the olfactory nerve appeared reduced and these cells appeared to produce less BFABP protein (Fig. 22b, d). Even at this early stage, BFABP-positive olfactory glial progenitors appeared to accumulate in the distal portion of the olfactory axons, and could not be observed in the proximal portion.

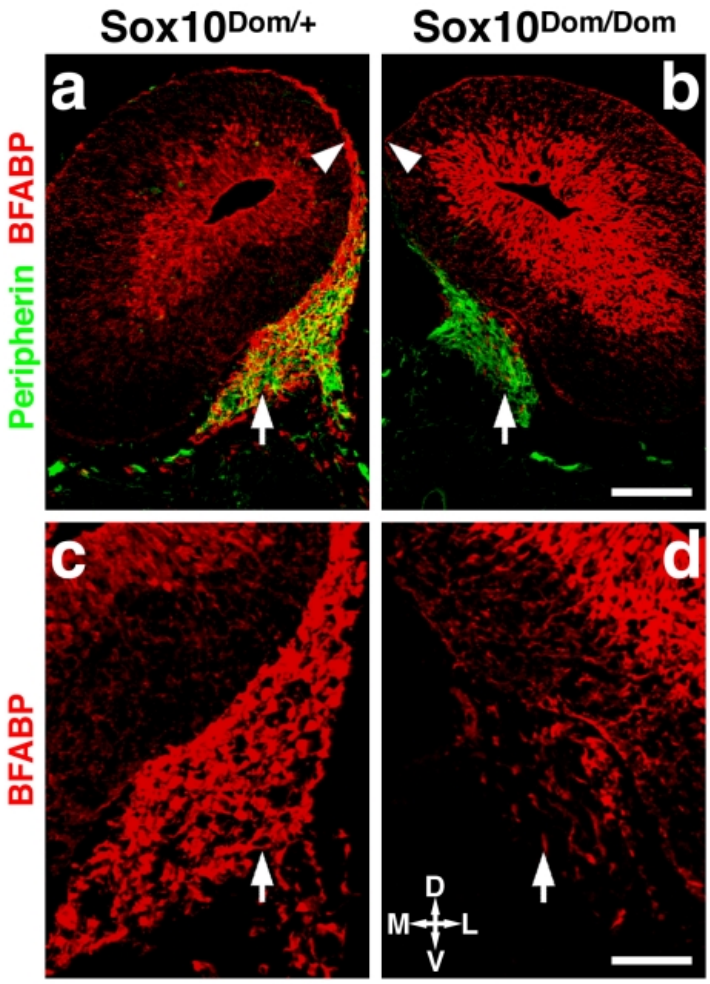

Figure 22. Defective development of olfactory glial cells in $Sox10^{DOM}$ mutants at E12.5
Immunohistological analysis on transverse sections of $Sox10^{Dom/+}$ (a, c) and $Sox10^{Dom/Dom}$ (b, d) embryos at E12.5 using antibodies against BFABP (red) and peripherin (green). At E12.5, olfactory axons and accompanying BFABP-positive glial progenitors reach the olfactory bulb primodium ventromedially (arrows in a, c) and extend dorsocaudally along the external surface of the developing bulb (arrowheads in a). In contrast, in $Sox10^{Dom/Dom}$ mutants, no BFABP-positive glial progenitors are present in the superficial layer of the developing bulb (arrowheads in b) or along the peripheral olfactory axon trajectories in the olfactory epithelium. However, some BFABP-positive glial progenitors are present in the olfactory axon fascicles in the frontonasal mesenchyme (arrows in b, d). (Mirror images) Bars: (a, d) 300µm; (c, d) 150µm.

3.13. Axon projections of olfactory sensory neurons are aberrant in *Sox10* mutants

Axon projections of olfactory sensory neurons were also abnormal in *Sox10* mutant embryos (Fig. 23). Staining of the olfactory axons with OMP-specific antibodies revealed a general disorganization of the axon projections. Some olfactory axons penetrated into deep layers of the olfactory bulb, and the axon projections in the dorsal olfactory bulb were absent (Fig. 23b, compare to control in 23a).

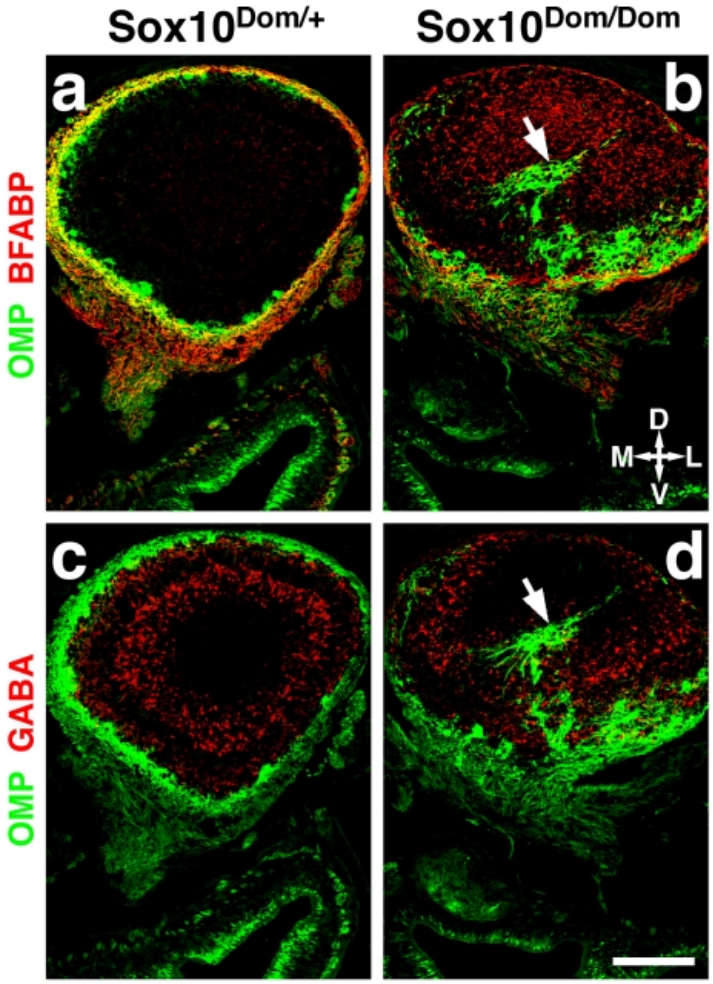

Figure 23. Aberrant olfactory axon projections in *Sox10* mutants
Immunohistological analysis on coronal sections of *Sox10*$^{Dom/+}$ (a, b) and *Sox10*$^{Dom/Dom}$ (b, d) embryos at E18.5 using antibodies against OMP (green), and BFABP (red, a, b) or GABA (red, c, d). While olfactory glial cells along the peripheral olfactory axon trajectories and in the olfactory nerve layer are absent in *Sox10*$^{Dom/Dom}$ mutants, BFABP-positive glial cells are present ventromedially between the cribriform plate and the olfactory bulb. However, the olfactory axon projections are generally disorganized in these mutants. They enter the bulb in a narrowed entry zone, restricted to the ventromedial aspect of the bulb, and only very few axons are able to reach the dorsal part of the olfactory bulb. Some axons in the mutant project into deep layers of the olfactory bulb (arrows in b, d), where wildtype axons are never present. The analysis using anti-GABA antibodies (red) demonstrates further that these aberrant olfactory axons projections reach the GABA-expressing granular cell layer in the mutants (c, d). (Mirror images) Bar: (a-d) 250µm.

The staining with anti-OMP (green) and anti-GABA (red) antibodies demonstrated that olfactory axons were present in the deep granular cell layer of the bulb (arrows in Fig. 23b, d), where olfactory axons in control littermates are never found. Similar to the phenotype seen in *NRGβ* mutants, the layered organization of the GABA-positive neurons was disrupted in *Sox10* mutants, particularly in the dorsal bulb. *In situ* hybridizations with TH- and Reelin-specific

probes demonstrated similar defects in the layered organization of mitral and periglomerular cells (not shown). In general, the defects in olfactory axon projections and in the layered organization of neurons observed in Sox10 mutants are reminiscent of those observed earlier in *NRG1* or *ErbB3* mutant animals.

4. Discussion

4.1. Distinct functions of NRG1α and NRG1β *in vivo*

The α- and β-isoforms of Neuregulin-1 differ in their affinities towards Neuregulin receptors. In general, the β-isoforms are high affinity ligands, that frequently elicit stronger and longer lasting cellular responses than α-isoforms. For instance, the β-isoforms stimulate growth and long-lasting MAP kinase activity, while the α-isoforms stimulate survival and transient MAP kinase activation (Pinkas-Kramarski et al., 1998). The analysis of isoform-specific *Neuregulin-1* mouse mutants revealed distinct functions for α- and β-isoforms in development. *NRG1α/α* mutant mice, which retained the β-isoforms but were unable to produce the α-isoforms, reached adulthood and appeared healthy and fertile. Thus, the α-isoforms of Neuregulin-1, which have low affinity for ErbB heteromers, appear to be dispensable for embryonic development and postnatal survival. In contrast, *NRG1β/β* mutants that retained α-isoforms but were unable to produce β-isoforms displayed severe developmental deficits. The β-isoforms of Neuregulin-1 provide thus important developmental functions.

It is noteworthy that the α-variant isoforms of type I NRG1 are the only NRG1 isoforms produced by the mammary gland mesenchyme (Yang et al., 1995). *NRG1α/α* mutant mice displayed deficits in lobuloalveolar morphogenesis of the mammary gland epithelium during mid-pregnancy and early post-partum, indicating an important role of NRG1α-isoforms in regulating lobuloalveolar development and lactogenesis.

The endocardial cells of the heart produce type I NRG1 during heart development. However, in contrast to the mammary gland mesenchyme, these endocardial cells produce both α- and β-isoforms. The presence of the α-isoforms in *NRG1β/β* mutants was able to rescue partially the defect in heart development and the mid-gestation lethality observed in *NRG1-null* mutants. In the heart, NRG1 signals are received by the ErbB2/ErbB4 heteromeric receptors produced in myocardial cells (Meyer and Birchmeier, 1995; Lemke, 1996). In comparison with the ErbB2/ErbB3 receptors, the ErbB2/ErbB4 receptors have a higher affinity towards NRG1s,

including the α-isoforms (Jones et al., 1999; Sliwkowski et al., 1994; Pinkas-Kramarski et al., 1998). Thus, binding of α-isoforms of NRG1 to the high affinity ErbB2/ErbB4 receptors elicits cellular responses that suffice for a partial rescue in the heart.

In addition, the changes observed in development of neural crest and glial cells were similar in severity in both *NRG1β/β* and *NRG1-null* mutants. Neural crest and glial cells receive NRG1 signals using ErbB2/ErbB3 receptor heteromers, which have low affinity towards the α-isoforms of NRG1. Therefore, when the α-isoforms of NRG1 are produced alone in *NRG1β/β* mutants, the low affinity ErbB2/ErbB3 receptors do not elicit cellular responses that suffice for a rescue of neural crest- related phenotypes.

4.2. NRG1/ErbB2/ErbB3 are essential for the development of olfactory glial cells

The analysis of *NRG1β/β* mutants revealed a novel function of Neuregulin-1 in the development of the olfactory system, and particularly in the development of olfactory glia. The type III isoform of NRG1 is produced by olfactory sensory neurons, and this isoform is known to be incorporated into axon membranes (Meyer et al., 1997; Buonanno and Fischbach, 2001). Olfactory glial cells and their precursors express the ErbB2/ErbB3 receptors, which receive the axonally-presented NRG1 signals (Meyer et al., 1997). In accordance, identical alterations in the development of olfactory glia in *NRG1β/β*, *ErbB3-/-* or *ErbB2R-/-* mutant embryos were observed.

Olfactory glial cells, also called olfactory ensheathing cells, ensheath and accompany the axons of olfactory sensory neurons from the olfactory epithelium to the glomeruli of the olfactory bulb (reviewed by Ramon-Cueto and Avila, 1998). This glial cell type is unique and has been described as a glial cell type with properties intermediary between non-myelinating Schwann cells and astrocytes. This type of glial cells originates from the olfactory placode and has thus a developmental origin distinct from Schwann cells that are generated from neural crest cells, and from astrocytes that are generated in the central nervous system. In mouse embryos carrying mutations in the Neuregulin-1 signaling system, the numbers of olfactory glial cells that line the

olfactory axon tracts were severely reduced. This applied also to the olfactory glial cells that locate to the olfactory nerve layer of the olfactory bulb. The reduction in the numbers of olfactory glial cells could be observed even at early stages of development, and was caused by a decrease in cell proliferation and an increase in apoptosis. These observations made *in vivo* are consistent with previous experiments in cell culture, where Neuregulin-1 was observed to promote growth and survival of olfactory glial cells (Pollock et al., 1999).

The essential role of the Neuregulin-1 signaling system in development of olfactory glia is similar to the function of this factor in the development of the Schwann cell lineage. Schwann cells and their precursors line the axon tracts of sensory and motoneurons, from which type III NRG1 is also produced (Meyer et al., 1997). Schwann cells and their precursors express the ErbB2/ErbB3 receptors. In *NRG1β/β, ErbB3-/-* or *ErbB2R -/-* mutants, although satellite cells in the sensory ganglia were formed, numbers of Schwann cell precursors were severely reduced at E10, and Schwann cells were absent at later developmental stages. Axonally-presented NRG1 is therefore essential for the development of both Schwann cells and olfactory glial cells.

4.3. The functions of Sox10 in the development of olfactory glial cells

Sox10, a transcription factor of the HMG-box family, is expressed in neural crest cells, Schwann cells and oligodendrocytes. Previous experiments using mutants that carry a spontaneous (*Sox10^{Dom}* allele) or targeted (*Sox10^{lacZ}* allele) mutation in the *Sox10* gene demonstrated that the gene is important in development of Schwann cells and oligodendrocytes (Britsch et al., 2001; Stolt et al., 2002). In both *Sox10^{Dom}* and *Sox10^{lacZ}* mutants, the expression of *ErbB3* in neural crest cells was initiated, but not maintained. Moreover, since neural crest cells did not differentiate into peripheral glial cell progenitors, these *Sox10* mutants lacked early Schwann cell progenitors as well as the glial cells associated with sensory ganglia, i.e. satellite cells. In the oligodendrocyte lineage, Sox10 controls terminal differentiation and the expression of myelin proteins in oligodendrocytes was not initiated in *Sox10* mutants (Stolt et al., 2002). Sox10 is thus known to take over important roles in the development of glia in the peripheral

and the central nervous system.

The results obtained in this thesis demonstrated that Sox10 is also essential for the development of olfactory glia. Olfactory glial cells were formed in the *Sox10* mutant embryos, but were distributed in an abnormal manner. In control embryos, olfactory glial cells accompany the olfactory axons along their entire trajectories. However, these glial cells accumulated at the frontonasal mesenchyme between the cribriform plate and the olfactory bulb in the Sox 10 mutants, and neither accompanied the olfactory axon projections in the peripheral nerve fascicles nor entered the olfactory bulb to form the olfactory nerve layer. In addition, some evidences for a role of Sox10 in differentiation of olfactory glia were found, as these cells express low levels of BFABP. However, the remaining olfactory glial cells in the *Sox10* mutants still express *ErbB3*, in contrast to what was observed previously in neural crest cells, in which *ErbB3* expression controlled by Sox10. Sox transcription factors constitute a large family and their DNA binding domains, HMG-boxes, are highly conserved in their structures (Pevny and Lovell-Badge, 1997; Wegner, 1999). Thus, other Sox factors might function redundantly with Sox10 to maintain *ErbB3* expression in those olfactory glia formed in the *Sox10* mutant. However, the fact that these abnormal cells expressed the mutant *Sox10* transcripts, *ErbB3*, S100 and BFABP establishes them as olfactory glia.

The phenotype observed in *Sox10* mutants was compatible with a function of Sox10 in terminal differentiation of olfactory glia. Sox10 would then control the expression of unknown genes that enable the olfactory glia to distribute evenly along the olfactory axon tracts and to enter the olfactory bulb. It has been reported that the olfactory nerve layer comprises distinct subpopulations of glial cells, which differ in morphology, differentiation timing and immunocytochemical profiles (Doucette, 1989; Pixley, 1992; Franceschini and Barnett, 1996; Astic et al., 1998; Au et al., 2002). An alternative possibility is that the *Sox10* mutation affects only one of these subpopulations of glial lineages.

4.4. Aberrant olfactory axon projections in *NRG1/ErbB* and *Sox10* mutants

The axon projections of olfactory sensory neurons were aberrant in *NRG1/ErbB* mutant embryos. At E18.5, olfactory axons entered the olfactory bulb ventromedially, but did not reach the dorsal portion of the olfactory bulb. OMP-positive axons projected to deep layers of the olfactory bulb, where olfactory axons in control litters are never observed.

Analysis of the olfactory axon projections of *P2*- and *mOR37A*-expressing neurons by using *P2-IRES-tau-lacZ* and *mOR37A-IRES-tau-lacZ* alleles indicated that these axons could still converge in *NRG1β/β* and *ErbB3* mutant embryos, although one of two *P2*- glomeruli and the *mOR37A*-glomerulus were frequently absent. However, the glomerulus-like axon aggregates formed in these mutants were aberrant, i.e. they were smaller, usually located at incorrect positions. The exact alterations observed were not entirely identical in different individuals and or even between the two halves of the olfactory bulb of the same embryo. It should be noted that the axons of *P2*- and *mOR37A*-expressing neurons converge only in the ventral bulb. The major alteration in axon projections in the *NRG1β/β* and *ErbB3* mutants were observed in the dorsal bulb when anti-OMP antibodies that label all olfactory axon projections were used. Thus, the *NRG1β/β* and *ErbB3* mutations appeared to affect distinct olfactory axon projections in a differential manner. Those that form glomeruli in the dorsal portion were unable to reach their target domains, but those that form glomeruli in the ventral bulb could perhaps reach their target region and were less severely affected. *P2*- and *mOR37A*-expressing neurons in the *NRG1β/β* or *ErbB3* mutants project rarely into deep layers of the olfactory bulb, indicating that such OMP-positive axons aberrantly projected into the deep layers of the olfactory bulb were formed by other olfactory sensory neurons.

Aberrant axon projections of olfactory neurons were also present in *Sox10* mutants, and resembled those observed in embryos with mutations in the Neuregulin-1 signaling system. Again, the most severely affected axon projections were found in the dorsal olfactory bulb, and OMP-positive axon projections reached the deep layers of the olfactory bulb were also observed in these mutants.

4.5. Interactions between olfactory glial cells and olfactory sensory neurons

What causes the similar alterations in olfactory axon projection of *NRG1/ErbB* or *Sox10* mutants? Not only *NRG1β* and *ErbB2*, but also *ErbB3* mutants displayed these aberrant axon projections. *NRG1* and *ErbB2* are expressed in many cell types of the developing olfactory nervous system. In contrast, *ErbB3* expression is restricted and observed only in the support cells, olfactory glia and oligodendrocytes. Oligodendrocytes express *ErbB3* at low levels and just start to invade the olfactory bulb at the stage that the phenotype is analyzed. *ErbB3* is not required cell autonomously in the olfactory neurons in order to project correctly and indirect effects account thus for the aberrant axon projections in *ErbB3* mutants. Olfactory glia were dramatically reduced in numbers by the *NRG1β*, *ErbB2* or *ErbB3* mutations, and it could be therefore postulated that the severe deficits in olfactory glia caused the changes in the topology of the olfactory axon projections. Independent support for this conclusion came from the analysis of *Sox10* mutants. In such mutants, olfactory glia did not accompany olfactory axons in the olfactory nerve layer, but remain outside of the olfactory bulb. Severe alterations in olfactory axon projections were present in these mutants, which resemble those observed in *NRG1β*, *ErbB2* or *ErbB3* mutants.

Olfactory sensory neurons are renowned for their ability to regenerate throughout life, and it has been suggested that olfactory glia provide factors that can allow or enhance this regeneration (Ramon-Cueto and Avila, 1998). In *NRG1/ErbB* mutants, an increase in the apoptosis frequency in the olfactory epithelium and a decrease in the number of OMP-positive neurons were observed. Moreover, the turnover of olfactory sensory neurons was also increased in these mutants. Therefore, as was observed previously for sensory or motoneurons in the absence of Schwann cells (Woldeyesus et al., 1999; Britsch et al., 2001), the lack of olfactory glia appear to influence also the survival of olfactory sensory neurons.

4.6. The possible roles of olfactory glial cells in olfactory axon projections

Little is known about how olfactory axons navigate from the developing olfactory placode and initiate the first connection with the developing olfactory bulb. Studies in zebrafish indicated that

a precocious transient class of pioneer neurons provides the first connection between the developing olfactory epithelium and olfactory bulb (Whitlock and Westerfield, 1998). These pioneer neurons, which are distinct from olfactory sensory neurons, prefigure the primary olfactory pathway before outgrowth of olfactory sensory axons or expression of olfactory receptor genes. They establish an axon scaffold for the later-arriving olfactory sensory neuron axons and then undergo apoptotic cell death after the axons of the sensory neurons grow into the olfactory primordium. Ablating these pioneer neurons before axonogenesis, resulted in severe misrouting of the following sensory axons. Studies in the rat also suggested that a subpopulation of early olfactory axons, the pioneer axons, follows a special pathway to reach the developing telencephalon. These pioneer axons regulate proliferation and differentiation of CNS precursor cells and thus may induce the morphogenesis of the olfactory bulb (Gong and Shipley, 1995). In *NRG1/ErbB* and *Sox10* mutants, the initial development of olfactory axon projections appeared normal although these mutants suffered severe changes in the development of olfactory glial cells. Olfactory sensory neurons residing in the olfactory epithelium developed and extended their axons to the olfactory bulb primordium. The proliferation and differentiation of CNS precursor cells took place and so did the morphogenesis of the olfactory bulb. Therefore, olfactory sensory neurons do not require olfactory glial cells for their initial axon projections.

The co-existence of olfactory glial cells in both the peripheral and central nervous systems is unique. In spinal or cranial nerves, the type of glia that accompanies the nerve changes when the axons enter the central nervous system. In the periphery, nerves are accompanied by Schwann cells, and once they enter the central nervous system, by astrocytes and oligodendrocytes. However, olfactory glial cells enfold olfactory axons along the entire path and in addition, contribute exclusively to form the glia limitans at the olfactory axon entry zone. Thus, these olfactory glial cells appear to be important for the entry of growing olfactory axons to the olfactory bulb (Doucette, 1991; reviewed by Ramon-Cueto and Valverde, 1995; Ramon-Cueto and Avila, 1998).

Olfactory axons and accompanying glial progenitors first contact the telencephalic vesicle at about E11.5 in the mouse. Very soon after this, the meningeal membrane of the developing bulb begins to break down near the midpoint of the contact between axons and telencephalic vesicle. The breaks in the meningeal membrane become progressively larger as increasingly olfactory axons and glia cell progenitors contact and enter the bulb primordium. In *NRG1/ErbB* mutants, the meningeal membrane was broken, but the axon entry zone remained small. The meningeal membrane retained intact in medial and lateral aspects of the mutant olfactory bulb, and appeared as an intact boundary that separates the olfactory bulb from the frontonasal mesenchyme. It is thus possible that olfactory glia took over a function in forming a broad entry zone for olfactory axons, for instance by producing some proteases that might be important in this process. A role of olfactory glia in penetrating the meningeal membrane was also supported by electron microscope observations (Tennent and Chuah, 1996). It should be noted that the entry zone in *Sox10* mutants was larger than in *NRG1/ErbB* mutants; possibly, the remaining olfactory glia in *Sox10* mutants could participate in partial degradation of the meningeal membrane.

In *NRG1/ErbB* and *Sox10* mutants, the olfactory glial cells were not only diminished along the peripheral olfactory nerve but were also absent in the superficial layer of the olfactory bulb, the olfactory nerve layer. The subpopulation of glial cells remaining in *Sox10* mutants accumulated in the frontonasal mesenchyme, ventromedially to the olfactory bulb, and failed to migrate around the olfactory bulb. As a consequence of this glial cell deficiency, the olfactory nerve layer that normally comprises glial cells and olfactory axons was not properly formed in either *NRG1/ErbB* or *Sox10* mutants. The olfactory axons in these mutants reached and penetrated the olfactory bulb ventromedially but did not extend to dorsal positions of the bulb. Glial cells present in the olfactory nerve layer might thus be of importance for extension of olfactory axons around the olfactory bulb. Due to the absence of olfactory glia cells, olfactory axons could not extend properly, and could not find their correct targets in *NRG1/ErbB* and *Sox10* mutants.

Glia-derived signals in insects and vertebrates do not only control the survival of neurons but also have important functions in providing guidance cues for navigating axons. In *Drosophila*

for instance, midline glia and the retinal basal glia provide cues that guide axons at the midline and in the developing optic stalk, respectively (Rothberg et al., 1990; Mitchell et al., 1996; Hummel et al., 1999; Rangarajan et al., 1999). The ablation of peripheral glia in the *Drosophila* embryo demonstrates that these cells are required to direct motor and sensory axons at the transition zone between the central and peripheral nervous systems (Sepp et al., 2001). In the mouse, glial cells can provide guidance cues for axons that cross the midline (Serafini et al., 1996 6; Bertuzzi et al., 1999). The olfactory glial cells enfold the axons throughout their length in either the peripheral fascicles or the first parts of the CNS. These cells also provide diffusible factors and neural cell adhesion molecules, which might act as guidance cues (Miragall et al., 1989; Whitesides and LaMantia, 1996; Oland et al., 1998). For example, these cells express semaphorin 3A (sem3A), which is essential for the topographically correct projections of olfactory axons (Schwarting et al., 2000). Misexpression in the chick of a dominant negative neuropilin-1 that blocks semaphorin-mediated signaling in olfactory sensory axons induces these axons to enter the telencephalon prematurely and to overshoot (Renzi et al., 2000). Changes in the expression of guidance cues provided by olfactory glia might thus contribute to the alterations in the topology of olfactory axon projections observed in *NRG1/ErbB* and *Sox10* mutant embryos.

4.7. Conclusions

By the analysis of different mutant mouse strains, an essential role of NRG1, ErbB3 and ErbB2 in the development of olfactory glia was demonstrated in this thesis. In mouse embryos homozygous for mutation in the *NRG1*, *ErbB3* or *ErbB2* genes, the numbers of olfactory glial cells were severely reduced. Further analysis indicated that the Neuregulin-1 signaling system provides important growth and survival signals for olfactory glia. Neuregulin-1, the ligand, is produced by olfactory sensory neurons and presented by the axon membrane to olfactory glial cells that express ErbB2/ErbB3 heteromer as the receptor. This is similar to the previously observed function of the Neuregulin-1 signaling system in the development of the Schwann cell lineage. In contrast, in *Sox10* mutants, olfactory glial cells were formed, but distributed in an abnormal manner, the changes observed consistent with a function of *Sox10* in a differentiation

step in this cell lineage. Sox10 has been previously described to be essential for the early differentiation of Schwann cell precursors from neural crest cells, and for terminal differentiation of oligodendrocytes, i.e. the expression of myelin proteins. Sox10 emerges thus as a transcription factor of general importance for the development of glia, although the exact Sox10 target genes appear to differ in distinct glial subpopulations. It is noteworthy that in *NRG1/ErbB* and also in *Sox10* mutants, olfactory axon projections were impaired and the general features of this impairment were somewhat similar in both types of mutants. For instance, in contrast to control littermates, olfactory axons in mutants were absent in the dorsal aspect of the olfactory bulb, and were observed in deep layers of the olfactory bulb. Thus, this finding indicates that olfactory glial cells produce factors that are of importance for the correct axon projections, for example, the trophic factors that allow olfactory axons to extend to particular sites.

5. Summary

The *Neuregulin-1 (NRG1)* gene encodes a group of EGF-like ligands that signal via ErbB receptor tyrosine kinases. Multiple isoforms of Neuregulin-1 (NRG1) are produced by usage of different promoters and alternative splicing. The different isoforms of Neuregulin-1 are expressed in distinct spatial and temporal patterns and take over diverse biological functions *in vivo*.

In this thesis, α- and β-isoform specific knockout mouse strains of the *Neuregulin-1* gene (*NRG1α* and *NRG1β*) were generated and isoform-specific functions of Neuregulin-1 were analyzed. The β-isoforms of Neuregulin-1 are essential for the development of Schwann cells and olfactory glial cells, i.e. severe reductions in the numbers of these two glial cell types were observed in *NRG1β* mutants. The comparison of the *NRG1β* and the corresponding ErbB receptor mutants (*ErbB2R* and *ErbB3*) revealed similar phenotypes, indicating that these glial cells receive a neuronally produced Neuregulin-1 signal using the ErbB2/ErbB3 heteromeric receptors. Olfactory glial and Schwann cells have distinct developmental origins: the former are generated from the olfactory placode and the latter derived from the neural crest. Nevertheless, the Neuregulin-1 signaling system takes over similar roles in the development of both glial lineages. In contrast, the function of the transcription factor Sox10 is distinct in these two glial lineages. In particular, Sox10 controls *ErbB3* expression in Schwann cell precursors, but not in olfactory glial cells. Whereas Schwann cell precursors did not differentiate, olfactory glial cells were generated in *Sox10* mutants. However, these glia neither developed correctly nor accompanied the olfactory axons over their entire length. Olfactory axon projections in the olfactory bulb were aberrant in *NRG1/ErbB* and also in *Sox10* mutants, indicating that olfactory glial cells are essential for correct olfactory axon projection. In addition, the participation of the α-isoform of Neuregulin-1 in heart development, and its role as an important factor in the epithelial morphogenesis of the mammary gland during pregnancy and early lactation were demonstrated.

Zusammenfassung

Das Neuregulin-1 Gen (NRG1) kodiert für eine Gruppe von EGF-ähnlichen Liganden, die an ErbB Tyrosin-Kinase-Rezeptoren binden. Diese Neuregulin-1 Isoformen entstehen durch Verwendung unterschiedlicher Promotoren und durch alternatives Spleißen. Sie werden in verschiedenen zeitlichen und räumlichen Mustern exprimiert und übernehmen unterschiedliche biologische Funktionen *in vivo*.

In dieser Dissertation wurden gezielt die Neuregulin-1 Allele in der Maus ausgeschaltet und analysiert, die spezifisch für die α- bzw. β-Isoform von Neuregulin-1 sind (*NRG1α* und *NRG1β*). Die β-Isoformen von Neuregulin-1 sind von essentieller Bedeutung für die Entwicklung von Schwannzellen und olfaktorischer Glia: In den *NRG1β* Mutanten wurde eine massive Abnahme der Anzahl dieser beiden Zelltypen beobachtet. Der Vergleich von *NRG1β* und den korrespondierenden ErbB Rezeptor Mutanten (*ErbB2R* und *ErbB3*) zeigte ähnliche Phänotypen. Dies ist ein Hinweis darauf, daß diese Gliazellen ein neuronal erzeugtes Neuregulin-1 Signal über einen heteromeren ErbB2/ErbB3 Rezeptor-Komplex empfangen. Olfaktorische Glia und Schwannzellen haben eine entwicklungsbiologisch unterschiedliche Herkunft: Die olfaktorischen Glia entstammen der olfaktorischen Plakode, während Schwannzellen aus der Neuralleiste hervorgehen. Dessen ungeachtet übernimmt das Neuregulin-1 Signaltransduktionssystem in der Entwicklung dieser beiden Gliazellinien eine ähnliche Funktion. Die Rolle des Transkriptionsfaktors Sox10 ist dagegen in den beiden Gliazellinien verschieden. Sox10 reguliert die Expression von ErbB3 in Vorläuferzellen der Schwannzellen, jedoch nicht in olfaktorischen Gliazellen. In *Sox10* Mutanten differenzierten die Vorläuferzellen nicht zu Schwannzellen, während olfaktorische Gliazellen gebildet wurden. Diese Gliazellen entwickelten sich jedoch nicht korrekt, und sie begleiteten die olfaktorischen Axone auch nicht über deren gesamte Länge. Die Projektionen der olfaktorischen Axone in den olfaktorischen Bulbus waren in den *NRG1/ErbB* und *Sox10* Mutanten fehlerhaft, was auf eine essentielle Rolle der olfaktorischen Glia für die Projektion olfaktorischer Axone hindeutet.
Zusätzlich konnte in dieser Arbeit die Bedeutung der α-Isoform von Neuregulin-1 in der Entwicklung des Herzens und als ein wichtiger Faktor für die Morphogenese des Brustdrüsenepithels im Verlauf der Schwangerschaft und in der frühen Laktationsphase gezeigt werden.

6. References

Anderson, D.J. (1997). Cellular and molecular biology of neural crest cell lineage determination. *Trends Genet* **13**: 276-80.

Astic, L., Pellier-Monnin, V., and Godinot, F. (1998). Spatio-temporal patterns of ensheathing cell differentiation in the rat olfactory system during development. *Neuroscience* **84**: 295-307.

Au, W.W., Treloar, H.B., and Greer, C.A. (2002). Sublaminar organization of the mouse olfactory bulb nerve layer. *J Comp Neurol* **446**: 68-80.

Baker, H., Grillo, M., and Margolis, F.L. (1989). Biochemical and immunocytochemical characterization of olfactory marker protein in the rodent central nervous system. *J Comp Neurol* **285**: 246-61.

Barber, P.C. and Lindsay, R.M. (1982). Schwann cells of the olfactory nerves contain glial fibrillary acidic protein and resemble astrocytes. *Neuroscience* **7**: 3077-90.

Beets, M.G. (1970). The molecular parameters of olfactory response. *Pharmacol Rev* **22**: 1-34.

Bermingham-McDonogh, O., Xu, Y.T., Marchionni, M.A., and Scherer, S.S. (1997). Neuregulin expression in PNS neurons: isoforms and regulation by target interactions. *Mol Cell Neurosci* **10**: 184-95.

Bertuzzi, S., Hindges, R., Mui, S.H., O'Leary, D.D., and Lemke, G. (1999). The homeodomain protein vax1 is required for axon guidance and major tract formation in the developing forebrain. *Genes Dev* **13**: 3092-105.

Britsch, S., Goerich, D.E., Riethmacher, D., Peirano, R.I., Rossner, M., Nave, K.A., Birchmeier, C., and Wegner, M. (2001). The transcription factor Sox10 is a key regulator of peripheral glial development. *Genes Dev* **15**: 66-78.

Britsch, S., Li, L., Kirchhoff, S., Theuring, F., Brinkmann, V., Birchmeier, C., and Riethmacher, D. (1998). The ErbB2 and ErbB3 receptors and their ligand, neuregulin-1, are essential for development of the sympathetic nervous system. *Genes Dev* **12**: 1825-36.

Brockes, J.P., Lemke, G.E., and Balzer, D.R., Jr. (1980). Purification and preliminary characterization of a glial growth factor from the bovine pituitary. *J Biol Chem* **255**: 8374-7.

Buck, L. and Axel, R. (1991). A novel multigene family may encode odorant receptors: a molecular basis for odor recognition. *Cell* **65**: 175-87.

Bulfone, A., Wang, F., Hevner, R., Anderson, S., Cutforth, T., Chen, S., Meneses, J., Pedersen, R., Axel, R., and Rubenstein, J.L. (1998). An olfactory sensory map develops in the absence of normal projection neurons or GABAergic interneurons. *Neuron* **21**: 1273-82.

Buonanno, A. and Fischbach, G.D. (2001). Neuregulin and ErbB receptor signaling pathways in the nervous system. *Curr Opin Neurobiol* **11**: 287-96.

Busfield, S.J., Michnick, D.A., Chickering, T.W., Revett, T.L., Ma, J., Woolf, E.A., Comrack, C.A., Dussault, B.J., Woolf, J., Goodearl, A.D., and Gearing, D.P. (1997). Characterization of a neuregulin-related gene, Don-1, that is highly expressed in restricted regions of the cerebellum and hippocampus. *Mol Cell Biol* **17**: 4007-14.

Callahan, C.A. and Thomas, J.B. (1994). Tau-beta-galactosidase, an axon-targeted fusion protein. *Proc Natl Acad Sci U S A* **91**: 5972-6.

Carraway, K.L., 3rd and Cantley, L.C. (1994). A neu acquaintance for erbB3 and erbB4: a role for receptor heterodimerization in growth signaling. *Cell* **78**: 5-8.

Carraway, K.L., 3rd, Weber, J.L., Unger, M.J., Ledesma, J., Yu, N., Gassmann, M., and Lai, C. (1997). Neuregulin-2, a new ligand of ErbB3/ErbB4-receptor tyrosine kinases. *Nature* **387**: 512-6.

Chang, H., Riese, D.J., 2nd, Gilbert, W., Stern, D.F., and McMahan, U.J. (1997). Ligands for ErbB-family receptors encoded by a neuregulin-like gene. *Nature* **387**: 509-12.

Chess, A., Simon, I., Cedar, H., and Axel, R. (1994). Allelic inactivation regulates olfactory receptor gene expression. *Cell* **78**: 823-34.

Chuah, M.I. and Au, C. (1991). Olfactory Schwann cells are derived from precursor cells in the olfactory epithelium. *J Neurosci Res* **29**: 172-80.

Clark, G. (1981). Staining Procedures. Williams & Wilkins, Baltimore, MD 21202, USA.

Couly, G.F. and Le Douarin, N.M. (1985). Mapping of the early neural primordium in quail-chick chimeras. I. Developmental relationships between placodes, facial ectoderm, and prosencephalon. *Dev Biol* **110**: 422-39.

Crovello, C.S., Lai, C., Cantley, L.C., and Carraway, K.L., 3rd. (1998). Differential signaling by the epidermal growth factor-like growth factors neuregulin-1 and neuregulin-2. *J Biol Chem* **273**: 26954-61.

Culbertson, M.R. (1999). RNA surveillance. Unforeseen consequences for gene expression, inherited genetic disorders and cancer. *Trends Genet* **15**: 74-80.

Dong, Z., Brennan, A., Liu, N., Yarden, Y., Lefkowitz, G., Mirsky, R., and Jessen, K.R. (1995). Neu differentiation factor is a neuron-glia signal and regulates survival, proliferation, and maturation of rat Schwann cell precursors. *Neuron* **15**: 585-96.

Doucette, R. (1989). Development of the nerve fiber layer in the olfactory bulb of mouse embryos. *J Comp Neurol* **285**: 514-27.

Doucette, R. (1991). PNS-CNS transitional zone of the first cranial nerve. *J Comp Neurol* **312**: 451-66.

Erickson, S.L., O'Shea, K.S., Ghaboosi, N., Loverro, L., Frantz, G., Bauer, M., Lu, L.H., and Moore, M.W. (1997). ErbB3 is required for normal cerebellar and cardiac development: a comparison with ErbB2-and heregulin-deficient mice. *Development* **124**: 4999-5011.

Erlich, H.A. (1989). PCR technology: Principles and applications for DNA amplification. Stockton Press, New York.

Falls, D.L., Harris, D.A., Johnson, F.A., Morgan, M.M., Corfas, G., and Fischbach, G.D. (1990). Mr 42,000 ARIA: a protein that may regulate the accumulation of acetylcholine receptors at developing chick neuromuscular junctions. *Cold Spring Harb Symp Quant Biol* **55**: 397-406.

Falls, D.L., Rosen, K.M., Corfas, G., Lane, W.S., and Fischbach, G.D. (1993). ARIA, a protein that stimulates acetylcholine receptor synthesis, is a member of the neu ligand family.

Cell **72**: 801-15.

Farbman, A.I. (1992). Cell Biology of Olfaction. Cambridge Universizy Press, Cambridge, UK.

Farbman, A.I. and Margolis, F.L. (1980). Olfactory marker protein during ontogeny: immunohistochemical localization. *Dev Biol* **74**: 205-15.

Fischbach, G.D. and Rosen, K.M. (1997). ARIA: a neuromuscular junction neuregulin. *Annu Rev Neurosci* **20**: 429-58.

Fitzpatrick, V.D., Pisacane, P.I., Vandlen, R.L., and Sliwkowski, M.X. (1998). Formation of a high affinity heregulin binding site using the soluble extracellular domains of ErbB2 with ErbB3 or ErbB4. *FEBS Lett* **431**: 102-6.

Fraher, J.P. (1982). The ultrastructure of sheath cells in developing rat vomeronasal nerve. *J Anat* **134**: 149-68.

Franceschini, I.A. and Barnett, S.C. (1996). Low-affinity NGF-receptor and E-N-CAM expression define two types of olfactory nerve ensheathing cells that share a common lineage. *Dev Biol* **173**: 327-43.

Garratt, A.N., Voiculescu, O., Topilko, P., Charnay, P., and Birchmeier, C. (2000). A dual role of erbB2 in myelination and in expansion of the schwann cell precursor pool. *J Cell Biol* **148**: 1035-46.

Gassmann, M., Casagranda, F., Orioli, D., Simon, H., Lai, C., Klein, R., and Lemke, G. (1995). Aberrant neural and cardiac development in mice lacking the ErbB4 neuregulin receptor. *Nature* **378**: 390-4.

Gong, Q. and Shipley, M.T. (1995). Evidence that pioneer olfactory axons regulate telencephalon cell cycle kinetics to induce the formation of the olfactory bulb. *Neuron* **14**: 91-101.

Granderath, S. and Klambt, C. (1999). Glia development in the embryonic CNS of Drosophila. *Curr Opin Neurobiol* **9**: 531-6.

Graus-Porta, D., Beerli, R.R., Daly, J.M., and Hynes, N.E. (1997). ErbB-2, the preferred heterodimerization partner of all ErbB receptors, is a mediator of lateral signaling. *Embo J* **16**: 1647-55.

Graus-Porta, D., Beerli, R.R., and Hynes, N.E. (1995). Single-chain antibody-mediated intracellular retention of ErbB-2 impairs Neu differentiation factor and epidermal growth factor signaling. *Mol Cell Biol* **15**: 1182-91.

Grinspan, J.B., Marchionni, M.A., Reeves, M., Coulaloglou, M., and Scherer, S.S. (1996). Axonal interactions regulate Schwann cell apoptosis in developing peripheral nerve: neuregulin receptors and the role of neuregulins. *J Neurosci* **16**: 6107-18.

Guy, P.M., Platko, J.V., Cantley, L.C., Cerione, R.A., and Carraway, K.L., 3rd. (1994). Insect cell-expressed p180erbB3 possesses an impaired tyrosine kinase activity. *Proc Natl Acad Sci U S A* **91**: 8132-6.

Harari, D., Tzahar, E., Romano, J., Shelly, M., Pierce, J.H., Andrews, G.C., and Yarden, Y. (1999). Neuregulin-4: a novel growth factor that acts through the ErbB-4 receptor tyrosine kinase. *Oncogene* **18**: 2681-9.

Harris, A., Adler, M., Brink, J., Lin, R., Foehr, M., Ferrer, M., Langton-Webster, B.C., Harkins, R.N., and Thompson, S.A. (1998). Homologue scanning mutagenesis of heregulin reveals receptor specific binding epitopes. *Biochem Biophys Res Commun* **251**: 220-4.

Hentze, M.W. and Kulozik, A.E. (1999). A perfect message: RNA surveillance and nonsense-mediated decay. *Cell* **96**: 307-10.

Herbarth, B., Pingault, V., Bondurand, N., Kuhlbrodt, K., Hermans-Borgmeyer, I., Puliti, A., Lemort, N., Goossens, M., and Wegner, M. (1998). Mutation of the Sry-related Sox10 gene in Dominant megacolon, a mouse model for human Hirschsprung disease. *Proc Natl Acad Sci U S A* **95**: 5161-5.

Hidalgo, A. and Booth, G.E. (2000). Glia dictate pioneer axon trajectories in the Drosophila embryonic CNS. *Development* **127**: 393-402.

Higashiyama, S., Abraham, J.A., Miller, J., Fiddes, J.C., and Klagsbrun, M. (1991). A heparin-binding growth factor secreted by macrophage-like cells that is related to EGF. *Science* **251**: 936-9.

Hinds, J.W. (1968a). Autoradiographic study of histogenesis in the mouse olfactory bulb. I. Time of origin of neurons and neuroglia. *J Comp Neurol* **134**: 287-304.

Hinds, J.W. (1968b). Autoradiographic study of histogenesis in the mouse olfactory bulb. II. Cell proliferation and migration. *J Comp Neurol* **134**: 305-22.

Ho, W.H., Armanini, M.P., Nuijens, A., Phillips, H.S., and Osheroff, P.L. (1995). Sensory and motor neuron-derived factor. A novel heregulin variant highly expressed in sensory and motor neurons. *J Biol Chem* **270**: 14523-32.

Holmes, W.E., Sliwkowski, M.X., Akita, R.W., Henzel, W.J., Lee, J., Park, J.W., Yansura, D., Abadi, N., Raab, H., Lewis, G.D., and et al. (1992). Identification of heregulin, a specific activator of p185erbB2. *Science* **256**: 1205-10.

Hooper, M., Hardy, K., Handyside, A., Hunter, S., and Monk, M. (1987). HPRT-deficient (Lesch-Nyhan) mouse embryos derived from germline colonization by cultured cells. *Nature* **326**: 292-5.

Hummel, T., Schimmelpfeng, K., and Klambt, C. (1999). Commissure formation in the embryonic CNS of Drosophila. *Development* **126**: 771-9.

Jerpseth, B., Greener, A., Short, J.M., Viola, J., and Kretz, P. (1992). XL1-Blue MRF' E. coli cells: McrA-, McrCB-, McrF-, Mrr-, HsdR- derivative of XL1-Blue cells. *Stratagies* **5**: 81-83.

Jessell, T.M., Siegel, R.E., and Fischbach, G.D. (1979). Induction of acetylcholine receptors on cultured skeletal muscle by a factor extracted from brain and spinal cord. *Proc Natl Acad Sci U S A* **76**: 5397-401.

Jessen, K.R. and Mirsky, R. (1997). Embryonic Schwann cell development: the biology of Schwann cell precursors and early Schwann cells. *J Anat* **191**: 501-5.

Jones, J.T., Akita, R.W., and Sliwkowski, M.X. (1999). Binding specificities and affinities of egf domains for ErbB receptors. *FEBS Lett* **447**: 227-31.

Joyner, A.L. (1999). Gene Targeting: A Practical Approach. Oxford University Press, Oxford,

UK.

Kapur, R.P. (1999). Early death of neural crest cells is responsible for total enteric aganglionosis in Sox10(Dom)/Sox10(Dom) mouse embryos. *Pediatr Dev Pathol* **2**: 559-69.

Karunagaran, D., Tzahar, E., Beerli, R.R., Chen, X., Graus-Porta, D., Ratzkin, B.J., Seger, R., Hynes, N.E., and Yarden, Y. (1996). ErbB-2 is a common auxiliary subunit of NDF and EGF receptors: implications for breast cancer. *Embo J* **15**: 254-64.

Klapper, L.N., Glathe, S., Vaisman, N., Hynes, N.E., Andrews, G.C., Sela, M., and Yarden, Y. (1999). The ErbB-2/HER2 oncoprotein of human carcinomas may function solely as a shared coreceptor for multiple stroma-derived growth factors. *Proc Natl Acad Sci U S A* **96**: 4995-5000.

Kokai, Y., Myers, J.N., Wada, T., Brown, V.I., LeVea, C.M., Davis, J.G., Dobashi, K., and Greene, M.I. (1989). Synergistic interaction of p185c-neu and the EGF receptor leads to transformation of rodent fibroblasts. *Cell* **58**: 287-92.

Kramer, R., Bucay, N., Kane, D.J., Martin, L.E., Tarpley, J.E., and Theill, L.E. (1996). Neuregulins with an Ig-like domain are essential for mouse myocardial and neuronal development. *Proc Natl Acad Sci U S A* **93**: 4833-8.

Kuhlbrodt, K., Herbarth, B., Sock, E., Enderich, J., Hermans-Borgmeyer, I., and Wegner, M. (1998a). Cooperative function of POU proteins and SOX proteins in glial cells. *J Biol Chem* **273**: 16050-7.

Kuhlbrodt, K., Herbarth, B., Sock, E., Hermans-Borgmeyer, I., and Wegner, M. (1998b). Sox10, a novel transcriptional modulator in glial cells. *J Neurosci* **18**: 237-50.

Kühn, R., Rajewsky, K., and Müller, W. (1991). Generation and analysis of interleukin-4 deficient mice. *Science* **254**: 707-10.

Kumar, V., Bustin, S.A., and McKay, I.A. (1995). Transforming growth factor alpha. *Cell Biol Int* **19**: 373-88.

Lancet, D., Ben-Arie, N., Cohen, S., Gat, U., Gross-Isseroff, R., Horn-Saban, S., Khen, M., Lehrach, H., Natochin, M., North, M., and et al. (1993). Olfactory receptors: transduction, diversity, human psychophysics and genome analysis. *Ciba Found Symp* **179**: 131-41.

Le Douarin, N.M. and Kalcheim, C. (1999). The neural crest. Cambrige University Press, Cambridge, UK.

Lee, K.F., Simon, H., Chen, H., Bates, B., Hung, M.C., and Hauser, C. (1995). Requirement for neuregulin receptor erbB2 in neural and cardiac development. *Nature* **378**: 394-8.

Lemke, G. (1996). Neuregulins in development. *Mol Cell Neurosci* **7**: 247-62.

Lemke, G.E. and Brockes, J.P. (1984). Identification and purification of glial growth factor. *J Neurosci* **4**: 75-83.

Levy, N.S., Bakalyar, H.A., and Reed, R.R. (1991). Signal transduction in olfactory neurons. *J Steroid Biochem Mol Biol* **39**: 633-7.

Li, L., Cleary, S., Mandarano, M.A., Long, W., Birchmeier, C., and Jones, F.E. (2002).

The breast proto-oncogene, HRGalpha regulates epithelial proliferation and lobuloalveolar development in the mouse mammary gland. *Oncogene* **21**: 4900-7.

Mahanthappa, N.K., Anton, E.S., and Matthew, W.D. (1996). Glial growth factor 2, a soluble neuregulin, directly increases Schwann cell motility and indirectly promotes neurite outgrowth. *J Neurosci* **16**: 4673-83.

Malnic, B., Hirono, J., Sato, T., and Buck, L.B. (1999). Combinatorial receptor codes for odors. *Cell* **96**: 713-23.

Marchionni, M.A., Goodearl, A.D., Chen, M.S., Bermingham-McDonogh, O., Kirk, C., Hendricks, M., Danehy, F., Misumi, D., Sudhalter, J., Kobayashi, K., and et al. (1993). Glial growth factors are alternatively spliced erbB2 ligands expressed in the nervous system. *Nature* **362**: 312-8.

Marin-Padilla, M. and Amieva, M.R. (1989). Early neurogenesis of the mouse olfactory nerve: Golgi and electron microscopic studies. *J Comp Neurol* **288**: 339-52.

Meyer, D. and Birchmeier, C. (1994). Distinct isoforms of neuregulin are expressed in mesenchymal and neuronal cells during mouse development. *Proc Natl Acad Sci U S A* **91**: 1064-8.

Meyer, D. and Birchmeier, C. (1995). Multiple essential functions of neuregulin in development. *Nature* **378**: 386-90.

Meyer, D., Yamaai, T., Garratt, A., Riethmacher-Sonnenberg, E., Kane, D., Theill, L.E., and Birchmeier, C. (1997). Isoform-specific expression and function of neuregulin. *Development* **124**: 3575-86.

Miragall, F., Kadmon, G., and Schachner, M. (1989). Expression of L1 and N-CAM cell adhesion molecules during development of the mouse olfactory system. *Dev Biol* **135**: 272-86.

Mitchell, K.J., Doyle, J.L., Serafini, T., Kennedy, T.E., Tessier-Lavigne, M., Goodman, C.S., and Dickson, B.J. (1996). Genetic analysis of Netrin genes in Drosophila: Netrins guide CNS commissural axons and peripheral motor axons. *Neuron* **17**: 203-15.

Mombaerts, P. (1999). Molecular biology of odorant receptors in vertebrates. *Annu Rev Neurosci* **22**: 487-509.

Mombaerts, P., Wang, F., Dulac, C., Chao, S.K., Nemes, A., Mendelsohn, M., Edmondson, J., and Axel, R. (1996). Visualizing an olfactory sensory map. *Cell* **87**: 675-86.

Morris, J.K., Lin, W., Hauser, C., Marchuk, Y., Getman, D., and Lee, K.F. (1999). Rescue of the cardiac defect in ErbB2 mutant mice reveals essential roles of ErbB2 in peripheral nervous system development. *Neuron* **23**: 273-83.

Morrissey, T.K., Levi, A.D., Nuijens, A., Sliwkowski, M.X., and Bunge, R.P. (1995). Axon-induced mitogenesis of human Schwann cells involves heregulin and p185erbB2. *Proc Natl Acad Sci U S A* **92**: 1431-5.

Nef, P., Hermans-Borgmeyer, I., Artieres-Pin, H., Beasley, L., Dionne, V.E., and Heinemann, S.F. (1992). Spatial pattern of receptor expression in the olfactory epithelium. *Proc Natl Acad Sci U S A* **89**: 8948-52.

Ngai, J., Dowling, M.M., Buck, L., Axel, R., and Chess, A. (1993). The family of genes encoding odorant receptors in the channel catfish. *Cell* **72**: 657-66.

O'Leary, D.D., Yates, P.A., and McLaughlin, T. (1999). Molecular development of sensory maps: representing sights and smells in the brain. *Cell* **96**: 255-69.

Oland, L.A., Pott, W.M., Higgins, M.R., and Tolbert, L.P. (1998). Targeted ingrowth and glial relationships of olfactory receptor axons in the primary olfactory pathway of an insect. *J Comp Neurol* **398**: 119-38.

Peles, E., Bacus, S.S., Koski, R.A., Lu, H.S., Wen, D., Ogden, S.G., Levy, R.B., and Yarden, Y. (1992). Isolation of the neu/HER-2 stimulatory ligand: a 44 kd glycoprotein that induces differentiation of mammary tumor cells. *Cell* **69**: 205-16.

Perroteau, I., Oberto, M., Ieraci, A., Bovolin, P., and Fasolo, A. (1998). ErbB-3 and ErbB-4 expression in the mouse olfactory system. *Ann N Y Acad Sci* **855**: 255-9.

Perroteau, I., Oberto, M., Soncin, I., Voyron, S., De Bortoli, M., Bovolin, P., and Fasolo, A. (1999). Transregulation of erbB expression in the mouse olfactory bulb. *Cell Mol Biol (Noisy-le-grand)* **45**: 293-301.

Pevny, L.H. and Lovell-Badge, R. (1997). Sox genes find their feet. *Curr Opin Genet Dev* **7**: 338-44.

Pingault, V., Bondurand, N., Kuhlbrodt, K., Goerich, D.E., Prehu, M.O., Puliti, A., Herbarth, B., Hermans-Borgmeyer, I., Legius, E., Matthijs, G., Amiel, J., Lyonnet, S., Ceccherini, I., Romeo, G., Smith, J.C., Read, A.P., Wegner, M., and Goossens, M. (1998). SOX10 mutations in patients with Waardenburg-Hirschsprung disease. *Nat Genet* **18**: 171-3.

Pinkas-Kramarski, R., Shelly, M., Guarino, B.C., Wang, L.M., Lyass, L., Alroy, I., Alimandi, M., Kuo, A., Moyer, J.D., Lavi, S., Eisenstein, M., Ratzkin, B.J., Seger, R., Bacus, S.S., Pierce, J.H., Andrews, G.C., Yarden, Y., and Alamandi, M. (1998). ErbB tyrosine kinases and the two neuregulin families constitute a ligand-receptor network. *Mol Cell Biol* **18**: 6090-101.

Pinkas-Kramarski, R., Soussan, L., Waterman, H., Levkowitz, G., Alroy, I., Klapper, L., Lavi, S., Seger, R., Ratzkin, B.J., Sela, M., and Yarden, Y. (1996). Diversification of Neu differentiation factor and epidermal growth factor signaling by combinatorial receptor interactions. *Embo J* **15**: 2452-67.

Pixley, S.K. (1992). The olfactory nerve contains two populations of glia, identified both in vivo and in vitro. *Glia* **5**: 269-84.

Plowman, G.D., Green, J.M., Culouscou, J.M., Carlton, G.W., Rothwell, V.M., and Buckley, S. (1993). Heregulin induces tyrosine phosphorylation of HER4/p180erbB4. *Nature* **366**: 473-5.

Pollock, G.S., Franceschini, I.A., Graham, G., Marchionni, M.A., and Barnett, S.C. (1999). Neuregulin is a mitogen and survival factor for olfactory bulb ensheathing cells and an isoform is produced by astrocytes. *Eur J Neurosci* **11**: 769-80.

Raff, M.C., Abney, E., Brockes, J.P., and Hornby-Smith, A. (1978). Schwann cell growth factors. *Cell* **15**: 813-22.

Ramirez-Solis, R., Rivera-Perez, J., Wallace, J.D., Wims, M., Zheng, H., and Bradley,

A. (1992). Genomic DNA microextraction: a method to screen numerous samples. *Anal Biochem* **201**: 331-5.

Ramon-Cueto, A. and Avila, J. (1998). Olfactory ensheathing glia: properties and function. *Brain Res Bull* **46**: 175-87.

Ramon-Cueto, A. and Valverde, F. (1995). Olfactory bulb ensheathing glia: a unique cell type with axonal growth- promoting properties. *Glia* **14**: 163-73.

Rangarajan, R., Gong, Q., and Gaul, U. (1999). Migration and function of glia in the developing Drosophila eye. *Development* **126**: 3285-92.

Renzi, M.J., Wexler, T.L., and Raper, J.A. (2000). Olfactory sensory axons expressing a dominant-negative semaphorin receptor enter the CNS early and overshoot their target. *Neuron* **28**: 437-47.

Ressler, K.J., Sullivan, S.L., and Buck, L.B. (1993). A zonal organization of odorant receptor gene expression in the olfactory epithelium. *Cell* **73**: 597-609.

Ressler, K.J., Sullivan, S.L., and Buck, L.B. (1994). Information coding in the olfactory system: evidence for a stereotyped and highly organized epitope map in the olfactory bulb. *Cell* **79**: 1245-55.

Riese, D.J., 2nd, Bermingham, Y., van Raaij, T.M., Buckley, S., Plowman, G.D., and Stern, D.F. (1996a). Betacellulin activates the epidermal growth factor receptor and erbB-4, and induces cellular response patterns distinct from those stimulated by epidermal growth factor or neuregulin-beta. *Oncogene* **12**: 345-53.

Riese, D.J., 2nd, van Raaij, T.M., Plowman, G.D., Andrews, G.C., and Stern, D.F. (1995). The cellular response to neuregulins is governed by complex interactions of the erbB receptor family. *Mol Cell Biol* **15**: 5770-6.

Riese, D.J., Kim, E.D., Elenius, K., Buckley, S., Klagsbrun, M., Plowman, G.D., and Stern, D.F. (1996b). The epidermal growth factor receptor couples transforming growth factor- alpha, heparin-binding epidermal growth factor-like factor, and amphiregulin to Neu, ErbB-3, and ErbB-4. *J Biol Chem* **271**: 20047-52.

Riethmacher, D., Sonnenberg-Riethmacher, E., Brinkmann, V., Yamaai, T., Lewin, G.R., and Birchmeier, C. (1997). Severe neuropathies in mice with targeted mutations in the ErbB3 receptor. *Nature* **389**: 725-30.

Rothberg, J.M., Jacobs, J.R., Goodman, C.S., and Artavanis-Tsakonas, S. (1990). slit: an extracellular protein necessary for development of midline glia and commissural axon pathways contains both EGF and LRR domains. *Genes Dev* **4**: 2169-87.

Royal, S.J. and Key, B. (1999). Development of P2 olfactory glomeruli in P2-internal ribosome entry site-tau-LacZ transgenic mice. *J Neurosci* **19**: 9856-64.

Sambrook, J. and Russell, D.W. (2001). Molecular Cloning: A Laboratory Manual. Cold Spring Harbor Laboratory Press, Cold Spring Harbor, New York 11803-2500, USA.

Schaefer, M.L., Finger, T.E., and Restrepo, D. (2001). Variability of position of the P2 glomerulus within a map of the mouse olfactory bulb. *J Comp Neurol* **436**: 351-62.

Schwarting, G.A., Kostek, C., Ahmad, N., Dibble, C., Pays, L., and Puschel, A.W. (2000). Semaphorin 3A is required for guidance of olfactory axons in mice. *J Neurosci* **20**:

7691-7.

Sepp, K.J., Schulte, J., and Auld, V.J. (2001). Peripheral glia direct axon guidance across the CNS/PNS transition zone. *Dev Biol* **238**: 47-63.

Serafini, T., Colamarino, S.A., Leonardo, E.D., Wang, H., Beddington, R., Skarnes, W.C., and Tessier-Lavigne, M. (1996). Netrin-1 is required for commissural axon guidance in the developing vertebrate nervous system. *Cell* **87**: 1001-14.

Shepherd, G.M. (1994). Neurobiology. Oxford University Press, Oxford, UK.

Shing, Y., Christofori, G., Hanahan, D., Ono, Y., Sasada, R., Igarashi, K., and Folkman, J. (1993). Betacellulin: a mitogen from pancreatic beta cell tumors. *Science* **259**: 1604-7.

Shoyab, M., Plowman, G.D., McDonald, V.L., Bradley, J.G., and Todaro, G.J. (1989). Structure and function of human amphiregulin: a member of the epidermal growth factor family. *Science* **243**: 1074-6.

Sliwkowski, M.X., Schaefer, G., Akita, R.W., Lofgren, J.A., Fitzpatrick, V.D., Nuijens, A., Fendly, B.M., Cerione, R.A., Vandlen, R.L., and Carraway, K.L., 3rd. (1994). Coexpression of erbB2 and erbB3 proteins reconstitutes a high affinity receptor for heregulin. *J Biol Chem* **269**: 14661-5.

Sorge, J.A. (1988). Bacteriophage lambda cloning vectors. *Biotechnology* **10**: 43-60.

Southard-Smith, E.M., Angrist, M., Ellison, J.S., Agarwala, R., Baxevanis, A.D., Chakravarti, A., and Pavan, W.J. (1999). The Sox10(Dom) mouse: modeling the genetic variation of Waardenburg- Shah (WS4) syndrome. *Genome Res* **9**: 215-25.

Southard-Smith, E.M., Kos, L., and Pavan, W.J. (1998). Sox10 mutation disrupts neural crest development in Dom Hirschsprung mouse model. *Nat Genet* **18**: 60-4.

Stolt, C.C., Rehberg, S., Ader, M., Lommes, P., Riethmacher, D., Schachner, M., Bartsch, U., and Wegner, M. (2002). Terminal differentiation of myelin-forming oligodendrocytes depends on the transcription factor Sox10. *Genes Dev* **16**: 165-70.

Strotmann, J., Conzelmann, S., Beck, A., Feinstein, P., Breer, H., and Mombaerts, P. (2000). Local permutations in the glomerular array of the mouse olfactory bulb. *J Neurosci* **20**: 6927-38.

Strotmann, J., Wanner, I., Krieger, J., Raming, K., and Breer, H. (1992). Expression of odorant receptors in spatially restricted subsets of chemosensory neurones. *Neuroreport* **3**: 1053-6.

Sullivan, S.L., Adamson, M.C., Ressler, K.J., Kozak, C.A., and Buck, L.B. (1996). The chromosomal distribution of mouse odorant receptor genes. *Proc Natl Acad Sci U S A* **93**: 884-8.

Syroid, D.E., Maycox, P.R., Burrola, P.G., Liu, N., Wen, D., Lee, K.F., Lemke, G., and Kilpatrick, T.J. (1996). Cell death in the Schwann cell lineage and its regulation by neuregulin. *Proc Natl Acad Sci U S A* **93**: 9229-34.

Tennent, R. and Chuah, M.I. (1996). Ultrastructural study of ensheathing cells in early development of olfactory axons. *Brain Res Dev Brain Res* **95**: 135-9.

Toyoda, H., Komurasaki, T., Uchida, D., Takayama, Y., Isobe, T., Okuyama, T., and Hanada, K. (1995). Epiregulin. A novel epidermal growth factor with mitogenic activity for rat primary hepatocytes. *J Biol Chem* **270**: 7495-500.

Tzahar, E., Levkowitz, G., Karunagaran, D., Yi, L., Peles, E., Lavi, S., Chang, D., Liu, N., Yayon, A., Wen, D., and et al. (1994). ErbB-3 and ErbB-4 function as the respective low and high affinity receptors of all Neu differentiation factor/heregulin isoforms. *J Biol Chem* **269**: 25226-33.

Tzahar, E., Pinkas-Kramarski, R., Moyer, J.D., Klapper, L.N., Alroy, I., Levkowitz, G., Shelly, M., Henis, S., Eisenstein, M., Ratzkin, B.J., Sela, M., Andrews, G.C., and Yarden, Y. (1997). Bivalence of EGF-like ligands drives the ErbB signaling network. *Embo J* **16**: 4938-50.

Tzahar, E., Waterman, H., Chen, X., Levkowitz, G., Karunagaran, D., Lavi, S., Ratzkin, B.J., and Yarden, Y. (1996). A hierarchical network of interreceptor interactions determines signal transduction by Neu differentiation factor/neuregulin and epidermal growth factor. *Mol Cell Biol* **16**: 5276-87.

Valverde, F., Santacana, M., and Heredia, M. (1992). Formation of an olfactory glomerulus: morphological aspects of development and organization. *Neuroscience* **49**: 255-75.

Vassar, R., Chao, S.K., Sitcheran, R., Nunez, J.M., Vosshall, L.B., and Axel, R. (1994). Topographic organization of sensory projections to the olfactory bulb. *Cell* **79**: 981-91.

Vassar, R., Ngai, J., and Axel, R. (1993). Spatial segregation of odorant receptor expression in the mammalian olfactory epithelium. *Cell* **74**: 309-18.

Wang, F., Nemes, A., Mendelsohn, M., and Axel, R. (1998). Odorant receptors govern the formation of a precise topographic map. *Cell* **93**: 47-60.

Wegner, M. (1999). From head to toes: the multiple facets of Sox proteins. *Nucleic Acids Res* **27**: 1409-20.

Wen, D., Peles, E., Cupples, R., Suggs, S.V., Bacus, S.S., Luo, Y., Trail, G., Hu, S., Silbiger, S.M., Levy, R.B., and et al. (1992). Neu differentiation factor: a transmembrane glycoprotein containing an EGF domain and an immunoglobulin homology unit. *Cell* **69**: 559-72.

Wen, D., Suggs, S.V., Karunagaran, D., Liu, N., Cupples, R.L., Luo, Y., Janssen, A.M., Ben-Baruch, N., Trollinger, D.B., Jacobsen, V.L., and et al. (1994). Structural and functional aspects of the multiplicity of Neu differentiation factors. *Mol Cell Biol* **14**: 1909-19.

Whitesides, J.G., 3rd and LaMantia, A.S. (1996). Differential adhesion and the initial assembly of the mammalian olfactory nerve. *J Comp Neurol* **373**: 240-54.

Whitlock, K.E. and Westerfield, M. (1998). A transient population of neurons pioneers the olfactory pathway in the zebrafish. *J Neurosci* **18**: 8919-27.

Woldeyesus, M.T., Britsch, S., Riethmacher, D., Xu, L., Sonnenberg-Riethmacher, E., Abou-Rebyeh, F., Harvey, R., Caroni, P., and Birchmeier, C. (1999). Peripheral nervous system defects in erbB2 mutants following genetic rescue of heart development. *Genes Dev* **13**: 2538-48.

Wolpowitz, D., Mason, T.B., Dietrich, P., Mendelsohn, M., Talmage, D.A., and Role, L.W. (2000). Cysteine-rich domain isoforms of the neuregulin-1 gene are required for maintenance of peripheral synapses. *Neuron* **25**: 79-91.

Yang, X., Arber, S., William, C., Li, L., Tanabe, Y., Jessell, T.M., Birchmeier, C., and Burden, S.J. (2001). Patterning of muscle acetylcholine receptor gene expression in the absence of motor innervation. *Neuron* **30**: 399-410.

Yang, X., Kuo, Y., Devay, P., Yu, C., and Role, L. (1998). A cysteine-rich isoform of neuregulin controls the level of expression of neuronal nicotinic receptor channels during synaptogenesis. *Neuron* **20**: 255-70.

Yang, Y., Spitzer, E., Meyer, D., Sachs, M., Niemann, C., Hartmann, G., Weidner, K.M., Birchmeier, C., and Birchmeier, W. (1995). Sequential requirement of hepatocyte growth factor and neuregulin in the morphogenesis and differentiation of the mammary gland. *J Cell Biol* **131**: 215-26.

Zhang, D., Sliwkowski, M.X., Mark, M., Frantz, G., Akita, R., Sun, Y., Hillan, K., Crowley, C., Brush, J., and Godowski, P.J. (1997). Neuregulin-3 (NRG3): a novel neural tissue-enriched protein that binds and activates ErbB4. *Proc Natl Acad Sci U S A* **94**: 9562-7.

Declaration

Ich versichere, daß ich die von mir vorgelegte Dissertation selbständig angefertigt, die benutzten Quellen und Hilfsmittel vollständig angegeben und die Stellen der Arbeit einschließlich Tabellen, Karten und Abbildungen, die anderen Werken im Wortlaut oder dem Sinn nach entnommen sind, in jedem Einzelfall als Entlehnung kenntlich gemacht habe; daß diese Dissertation noch keiner anderen Fakultät oder Universität zur Prüfung vorgelegen hat; daß sie abgesehen von unten angegebenen Teilpublikationen noch nicht veröffentlicht worden ist sowie, daß ich eine solche Veröffentlichung vor Abschluß des Promotionsverfahrens nicht vornehmen werde. Die Bestimmungen dieser Promotionsordnung sind mir bekannt. Die von mir vorgelegte Dissertation ist von Prof. Dr. Walter Dörfler und von Prof. Dr. Carmen Birchmeier betreut worden.

Li Li

Teile dieser Dissertation sind bereits in folgenden Publikationen veröffentlicht worden:

Li, L., Müller, T., Strehle, M., Gaio, U., Strotmann, J., Breer, H., Britsch, S. & Birchmeier, C. (2002). Neuregulin-1 and Sox10 are essential for the development of olfactory glia and for correct projections of olfactory neuron. *In preparation.*

Li, L., Cleary, S., Mandarano, M.A., Long, W., Birchmeier, C., and Jones, F.E. (2002). The breast proto-oncogene, HRGalpha regulates epithelial proliferation and lobuloalveolar development in the mouse mammary gland. *Oncogene* **21**: 4900-7.

Yang, X., Arber, S., William, C., Li, L., Tanabe, Y., Jessell, T.M., Birchmeier, C., and Burden, S.J. (2001). Patterning of muscle acetylcholine receptor gene expression in the absence of motor innervation. *Neuron* **30**: 399-410.

Britsch, S., Li, L., Kirchhoff, S., Theuring, F., Brinkmann, V., Birchmeier, C., and Riethmacher, D. (1998). The ErbB2 and ErbB3 receptors and their ligand, neuregulin-1, are essential for development of the sympathetic nervous system. *Genes Dev* **12**: 1825-36